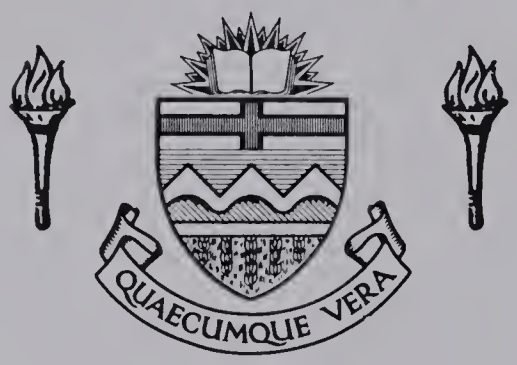

THE UNIVERSITY OF ALBERTA

RELEASE FORM

NAME OF AUTHOR OSKAR VALDIMARSSON

TITLE OF THESIS MINIMUM REINFORCEMENT IN CONCRETE MEMBERS

DEGREE FOR WHICH THESIS WAS PRESENTED MASTER OF SCIENCE

YEAR THIS DEGREE GRANTED FALL, 1981

THE UNIVERSITY OF ALBERTA

MINIMUM REINFORCEMENT IN CONCRETE MEMBERS

by

© OSKAR VALDIMARSSON

A THESIS

SUBMITTED TO THE FACULTY OF GRADUATE STUDIES AND RESEARCH

IN PARTIAL FULFILMENT OF THE REQUIREMENTS FOR THE DEGREE

OF MASTER OF SCIENCE

IN

CIVIL ENGINEERING

DEPARTMENT OF CIVIL ENGINEERING

EDMONTON, ALBERTA

FALL, 1981

THE UNIVERSITY OF ALBERTA

FACULTY OF GRADUATE STUDIES AND RESEARCH

The undersigned certify that they have read, and recommend to the Faculty of Graduate Studies and Research, for acceptance, a thesis entitled MINIMUM REINFORCEMENT IN CONCRETE MEMBERS submitted by OSKAR VALDIMARSSON in partial fulfilment of the requirements for the degree of MASTER OF SCIENCE in CIVIL ENGINEERING.

1 0 1 1

TO BRYNJA

Abstract

Twenty-six beams and slabs, with reinforcement ratios ranging from 0.08% to 0.59%, were tested to study the minimum amount of flexural reinforcement required in concrete beams. The major variables considered were: concrete strength, steel percentage, steel properties and cross-section shape. Slabs and rectangular, T- and inverted T-beams were tested.

Four of the beams failed in a brittle or nearly brittle manner; the remaining 22 members having a ductile failure. Based on the test data it is proposed that the minimum reinforcement ratio be expressed as a function of both the compressive strength of concrete and the yield strength of the reinforcing steel.

The T-beams and the inverted T-beams (flange in tension) required about 1.4 times and 2.8 times, respectively, as much reinforcement as the rectangular shapes.

Acknowledgements

The author wishes to express his sincere appreciation to the following persons and organizations for their various contributions to this thesis:

Professor J. G. MacGregor for his supervision and interest in the subject,

L. Burden and R. Helfrich for their technical assistance and practical suggestions regarding the fabrication and testing of the specimens,

A. K. Dunbar for setting up and operating the computerized part of the tests,

T. A. Casey for valuable advice and assistance in using the computer for data reduction,

The department of Civil Engineering for the use of the facilities of the I. F. Morrison Structural Laboratory.

Table of Contents

List of Tables

List of Figures

Notation

The notation used here complies, in most respects, with the ISO Standard 3898 (International Organization for Standardization, 1976).

Subscripts:

b : indicates "balanced condition"

c : indicates "concrete"

f : indicates "beam flange"

g : indicates "gross"

k : indicates "characteristic"

n : indicates "nominal"

s : indicates "steel"

t : indicates "tension in general"

u : indicates "ultimate"

w : indicates "beam web"

y : indicates "yield"

cr : indicates "cracking"

ef : indicates "effective"

tr : indicates "transformed"

ave : indicates "average value (mean)"

cal : indicates "calculated"

max : indicates "maximum"

mod : indicates "modified"

min : indicates "minimum"

obs : indicates "observed"

shr : indicates "shrinkage"

(15) : indicates stressing rate

Roman letter symbols:

a : distance or thickness; mm

b : width of a member; mm

b_f : width of the flange of T-beams and I-beams; mm

b_t : width of concrete zone in tension; mm

b_w : width of the web of T-beams and I-beams; mm

d : distance from extreme compression fibre in concrete to the centroid of reinforcing steel in tension; mm

f : strength of material; MPa

f_c : compressive strength of concrete; MPa

f_{ct} : flexural tensile strength (modulus of rupture) of concrete; MPa

f_{ck} : characteristic compressive strength of concrete (CEB), see Eqn. (2.22); MPa

f_{yk} : characteristic or specified yield strength of reinforcing steel; MPa

f'_c : specified compressive strength of concrete (ACI), see Eqn. (2.21); MPa

f_y : yield strength of reinforcing steel; MPa

f_{su} : ultimate tensile strength of reinforcing steel; MPa

h : height or thickness of a member; mm

ℓ_o : length of " almost lost bond ", see Eqn. (2.15); mm

m : bending moment per unit width; kN·m/m - or mass per unit volume; kg/m^3

s : standard deviation of a sample

t : time in days

w : dead load per unit length of member; kN/m

A_c : cross-sectional area of concrete; mm^2

A_{ct} : cross-sectional area of concrete tension zone only; mm^2

$A_{ct.ef}$: area of "effective embedment zone", see Fig. 2.2; mm^2

A_n : nominal area of welded wire fabric, see Eqn. (2.16); mm^2

A_s : cross-sectional area of reinforcing steel; mm^2

E_c : modulus of elasticity of concrete in compression; MPa

E_{ct} : modulus of elasticity of concrete in tension; MPa

E_s : longitudinal modulus of elasticity of reinforcing steel; MPa

I_g : moment of inertia of gross section about the centroidal axis, neglecting the the reinforcement; mm^4

I_{tr} : moment of inertia of transformed concrete section; mm^4

L : span length; mm

M_{cr} : moment applied on a member at the time of cracking of concrete; $kN \cdot m$

M_y : moment applied on a member at the time of yielding of reinforcing steel; $kN \cdot m$

M_u : ultimate moment capacity of a member; $kN \cdot m$

N_c : tensile normal force carried by the concrete; kN

P_{cr} : total load applied by loading machine at the time of cracking of concrete; kN

P_y : total load applied by loading machine at the time of yielding of reinforcement; kN

P_u : maximum load that can be applied before failure; kN

R : stressing rate of concrete; psi/sec or MPa/min

T : temperature in ^0C

V : volume of concrete under stress; mm^3

V_0 : volume of a 100mmx100mmx100mm cube; mm^3

X : strength of concrete; MPa

X_0 : strength of a 100mmx100mmx100mm cube; mm^3

W : section modulus; mm^3

Greek letter symbols:

α : ratio $\leq$ 1.0; see Eqns. (3.1) and (3.5)

β : ratio $\leq$ 1.0; see Eqn. (3.7)

γ : weight density; kN/m^3

δ : coefficient of variation

ε_{cu} : ultimate strain in concrete; m/m

ε_{su} : ultimate strain in reinforcing steel; m/m

ν : Poisson's ratio

ρ : reinforcement ratio; see Eqn. (2.3)

ρ_t : reinforcement ratio based on the area of the tension zone only; see Eqn. (2.1)

ρ_w : reinforcement ratio based on the web thickness of T- and I-beams;

ρ_b : reinforcement ratio producing balanced conditions; see Fig. 2.3

σ_s : normal stress in reinforcing steel; MPa

Mathematical symbols:

$\geq$: greater than or equal to

$\leq$: less than or equal to

$\cong$: approximately equal to

Σ : sum

Δ : deflection; mm - increment - or difference

ϕ : diameter of reinforcing bar; mm

Π : 3.14159

Units

The units used here are those in the SI–system of units, based on the decimal system with 7 basic units.

The units recommended for the presentation of data and results are as follows:

- for load and forces, localized or distributed : kN, kN/m, kN/m^2 (= kPa)
- for density : mass per unit volume – kg/m^3
- for weight per unit volume : kN/m^3
- for stresses and strength : MPa (= N/mm^2 = MN/m^2)
- for moments : kN·m

1. INTRODUCTION

1.1 General remarks

If the moment capacity of a concrete member after cracking is less than the cracking moment, as may be the case for extremely lightly reinforced members, a brittle fracture can occur when the concrete cracks. There is no agreement, however, on how much reinforcement is needed to avoid this, and in some cases published recommendations differ substantially. It will be the task of this study to verify experimentally the analytical results obtained by different investigators.

1.2 Object and scope

The aim of this investigation is the development of equations that define the minimum reinforcement ratio that should be allowed in concrete flexural members subjected to static loading. This minimum allowable reinforcement ratio will be based on the condition that the member should fail in a ductile manner, giving some warning before failure. Since the greatest part of the energy absorbed by a ductile member is absorbed after the member has yielded, the load-deformation characteristics in the plastic range are of particular interest.

Although many variables must be taken into accout in a complete study of the flexural load-deformation characteristics of reinforced concrete members, it was not considered practical to introduce all of them in this study. Previous investigators indicate that the most important variables are the concrete strength, steel percentage and steel properties. These and cross-section shape have been chosen as the principal variables to be studied.

Some of the previous investigations in this field are studied in Chapter 2, and compared to different code requirements. The theoretical equations for calculating moment capacities are given in Chapter 3. An attempt to estimate the effect of shrinkage on the tensile strength of concrete is also made in this chapter. Chapter 4 explains the experimental program.

The test results are presented and discussed in Chapter 5, and the last section in this chapter gives the design rules recommended. Chapter 6 is conclusions and Appendix A gives the test results in a form of graphs.

2. REVIEW OF PREVIOUS INVESTIGATIONS

2.1 Minimum reinforcement

In this section, recent literature on minimum reinforcement will be reviewed and some of the recommendations given therein will be restated in forms of tables.

In 1961, Fritz Leonhardt (1961) reported extensive tests to determine minimum allowable reinforcement in rectangular beams. Using a pneumatic pressure system and a large (300 litres) "pressure equalizer", the drop in pressure and hence load at the time of cracking, was limited to about 0.4 per cent. As a result, the loading approximated a dead load. In this series of experiments 21 beams of dimensions 200x500x2200 mm were tested, using concrete strength of 18 MPa to 50 MPa. Two different kinds of deformed rebars were used, the diameter either 6 mm or 8 mm and the yield strength ranging from 450 MPa. to 525 MPa. The ultimate tensile strength of the steel, f_{su} , was in all cases close to 560 MPa. Cubes for compressive strength tests and prisms for tensile strength tests (modulus of rupture) were also made. Leonhardt divided his results into 3 categories:

1. brittle fracture; when reinforcement does not provide a moment capacity larger than the cracking moment; i.e. $M_u = M_{cr}$.
2. borderline case; $M_{cr} < M_u < 1.05\ M_{cr}$.
3. ductile failure; $M_u \geq 1.05\ M_{cr}$.

In the test series, the reinforcement ratio was based on the area of the concrete tension zone only, i.e.

$$\rho_t = \frac{A_s}{b \cdot h/2} = \frac{A_s}{A_{ct}} \qquad (2.1)$$

(neglecting the effects of the reinforcement). Using this notation, ρ_t ranged from 0.176 to 0.423 .

Plotting ρ_t against the ratio f_c(cube) /f_{su} , and fitting a straight line to the boundary between brittle and ductile failures, Leonhardt developed the equation:

$$\rho_t = 0.12 + 2.2 \frac{f_c\,(\text{cube})}{f_{su}} \qquad (\text{in \% of } A_{ct}) \tag{2.2}$$

If the reinforcement ratio ρ_t is changed to the more commonly used

$$\rho = \frac{A_s}{b \cdot d} \tag{2.3}$$

using d = 0.9h as was the case in this test series, one gets:

$$\rho = \frac{\rho_t}{1.8} \tag{2.4}$$

and using cylinder strength rather than cube strength (assuming f_c(cyl) = 0.83 f_c(cube)), the test results can be plotted as shown in Fig. 2.1. Equation (2.2) now becomes:

$$\rho = 0.067 + 1.47 \frac{f_{c.obs}}{f_{su.obs}} \tag{2.5}$$

Finally, applying a safety factor of about 1.2, Leonhardt gave recommendations for minimum reinforcement ratio for normal, deformed bars. These ratios, expressed in terms of ρ (not ρ_t) and using concrete strength in MPa, are given in Table 2.1.

It should be noted in Table 2.1 that the compressive strength of concrete given is the specified cylinder strength, f_{ck} , not the observed strength, $f_{c.obs}$.

Some years later, Leonhardt and Mönning (1973) published new recommendations for minimum reinforcement ratio for members in flexure, this

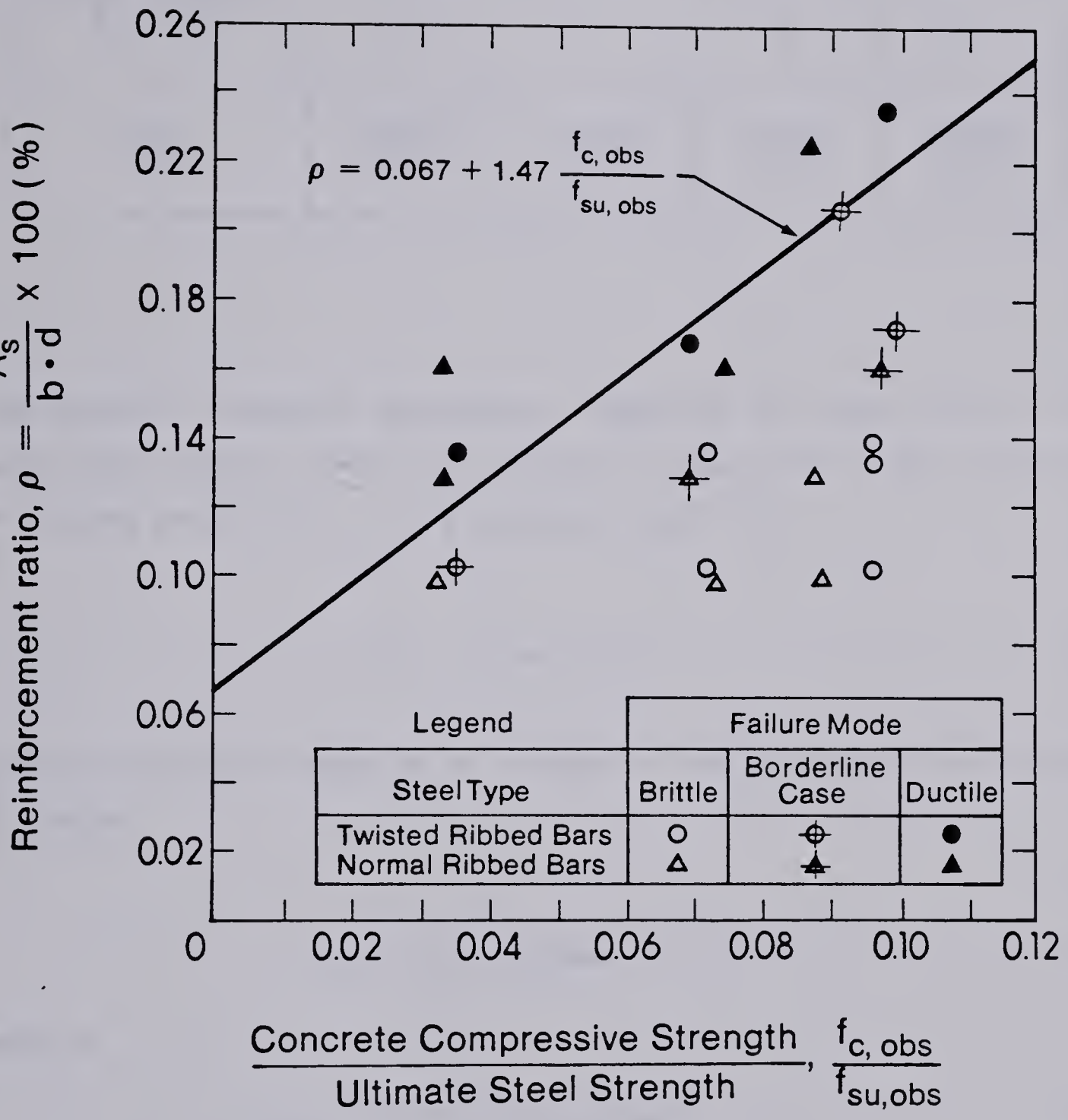

Figure 2.1 – Minimum reinforcement ratio for ductile failure. Test results taken from Leonhardt (1961).

Table 2.1 — Recommendations for minimum reinforcement ratio for rectangular members (Leonhardt, 1961).

Steel strength f_{yk} (MPa)	Concrete compressive strength, f_{ck} (MPa)			
	18	25	35	50
≤ 220	0.0017	0.0020	0.0026	0.0032
≤ 450	0.0014	0.0016	0.0020	0.0024

time based on theoretical observations. Neglecting the tensile force in the reinforcement before cracking of concrete, and using the straight line theory the cracking moment, M_{cr} , of a rectangular section is:

$$M_{cr} = \frac{}{6} b \cdot h^2 \cdot f_{ct} \qquad (2.6)$$

Assuming the tensile strength to be one-tenth of the compressive cube strength of concrete:

$$f_{ct} \cong \frac{1}{10} f_{ck}\,(\text{cube}) \qquad (2.7)$$

results in:

$$M_{cr} = 0.0167 \cdot b \cdot h^2 \cdot f_{ck}\,(\text{cube}) \qquad (2.8)$$

Taking the moment-arm as 0.95d for the reinforcement, the ultimate moment capacity after cracking is:

$$M_u = A_s \cdot f_{yk} \cdot 0.95 \cdot d \qquad (2.9)$$

Realizing that for a ductile failure $M_u \geq M_{cr}$, and using $d = 0.9h$ gives (again using $f_c(\text{cyl}) = 0.83\ f_c(\text{cube})$):

$$A_s \cdot f_{yk} \cdot 0.95 \cdot d \qquad 0.0167 \cdot b \cdot \frac{d^2}{(0.9)^2} \cdot 0.83 \cdot f_{ck} \tag{2.10}$$

thus giving the minimum amount of reinforcement necessary for a ductile behaviour:

$$\rho_{min} = \frac{A_s}{b \cdot d} = 0.0180 \cdot \frac{f_{ck}}{f_{yk}} \tag{2.11}$$

For shapes other than rectangular ρ must be expressed in terms of the concrete tension zone area (A_{ct}). Referring to the tests Leonhardt did in 1961, Leonhardt and Mönning state that for I-shaped beams, the following relation is valid:

$$\rho_{t,min} = \frac{A_s}{A_{ct}} = 1.8 \cdot \rho_{min} \tag{2.12}$$

and that in some cases eqn. (2.11) overestimates the necessary reinforcement ratio for rectangular beams. Table 2.2 summarizes their conclusions for normal deformed rebars.

Table 2.2 — Recommendations for minimum reinforcement ratio for both rectangular and I-shaped members (Leonhardt and Mönning, 1973).

Concrete compressive strength, f_{ck} MPa	ρ_{min} Rectangular members		$\rho_{t,min}$ I - beams	
	f_{yk} =220MPa	f_{yk} =450MPa	f_{yk} =220MPa	f_{yk} =450MPa
≤ 20	0.0015	0.0010	0.0027	0.0018
≤ 35	0.0020	0.0014	0.0036	0.0025
≤ 45	0.0025	0.0018	0.0045	0.0032

Leonhardt (1977) studied the amount of reinforcement required to prevent excessively wide cracks in concrete members. When a concrete member under axial tension cracks, the tensile force which was carried by the concrete, $N_c = A_{ct} \cdot f_{ct}$, must suddenly be taken over by the reinforcing bars. This causes a *jump of stress* in the steel at the crack. The steel stress in the cracked section, at the cracking load, can easily be calculated as:

$$\sigma_s = \frac{f_{ct}}{\rho_t} \quad \left(\text{where } \rho_t = \frac{A_s}{A_{ct}} \right) \tag{2.13}$$

The sudden jump of steel stress is then:

$$\Delta\sigma_s = \sigma_s - \frac{E_s}{E_c} \cdot f_{ct} = f_{ct} \cdot \left(\frac{1}{\rho_t} - \frac{E_s}{E_c} \right) \tag{2.14}$$

Thus a small ρ_t gives rise to a high jump of steel stress, a large ρ_t to a low jump.

A high steel stress jump leads to bond stresses beyond the bond-strength between rebars and concrete and tends to destroy the bond on a short length adjacent to the crack. Leonhardt estimates the length, ℓ_o, of "almost lost bond" (for standard ribbed rebars) as:

$$\ell_o = \frac{\sigma_s}{45} \cdot \phi \qquad \begin{pmatrix} \sigma_s \text{ in MPa} \\ \phi \text{ in mm} \end{pmatrix} \tag{2.15}$$

If the steel stress jumps up to the yield strength of the steel, ℓ_o can be assumed $\cong 6 \cdot \phi$. The crack width is a function of the steel strain at the crack and the length of "almost lost bond". For members in flexure instead of axial tension, the sudden jump of steel stress is considerably smaller, only about 40% of above mentioned values if ρ_t is used or 20% if ρ is used.

In crack width calculations the concept "effective embedment area" is often used. This is the part of the concrete tension zone area where the

rebars are assumed to be effective in controling the crack width and spacing. Leonhardt's definition of effective embedment area is defined in Figure 2.2.

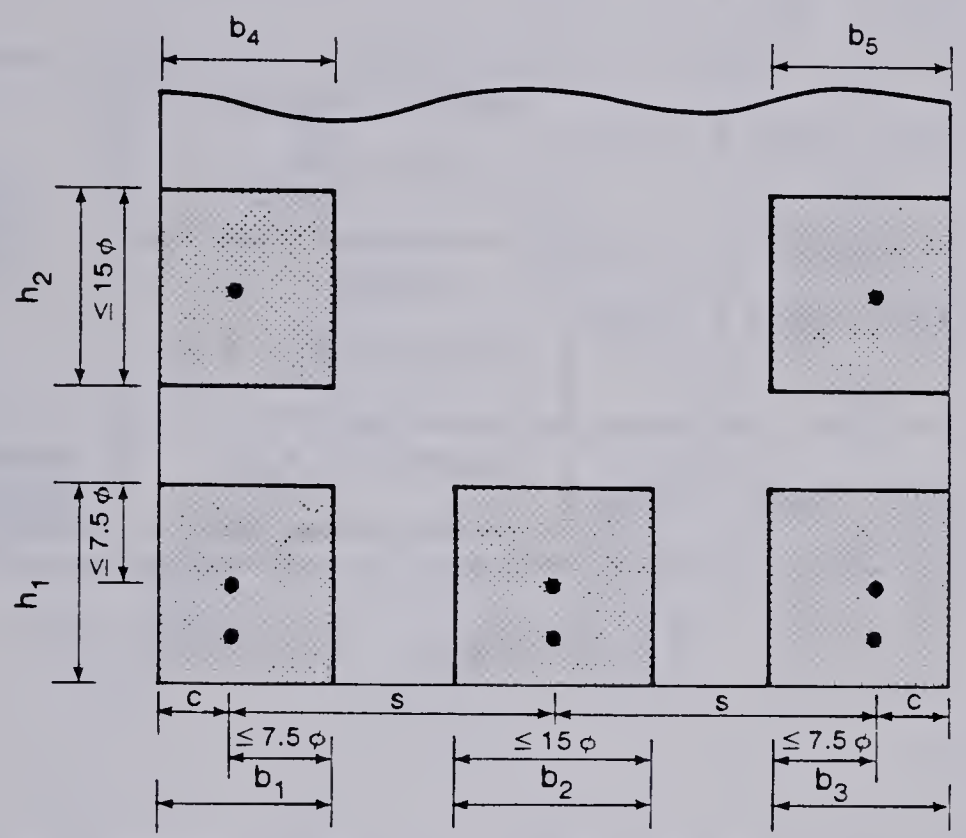

$$\rho_{t,ef} = \frac{A_s}{A_{ct,ef}} \qquad A_{ct,ef} = \text{Shaded Area}$$

Figure 2.2 - Definition of "effective embedment area", $A_{ct,ef}$ (CEB, 1977)

This concept is used in Table 2.3.

Based on this study the values in Table 2.3 are recommended for minimum ratios of reinforcement to satisfy limit states of crack width and ultimate load requirements (for members in flexure).

In 1969, ACI Committee 439 (ACI 439, 1969) reported on the "Effect of steel strength and of reinforcement ratio on the mode of failure and strain energy capacity of reinforced concrete beams". The report is a theoretical study based on idealized stress-strain curves for steel, and the tensile strength of the concrete is neglected, both in computing reinforcement ratios and strain

Table 2.3 — Recommendations for minimum ratios of reinforcement to satisfy limit states of crack width and/or ultimate load requirements (Leonhardt, 1977).

Minimum reinforcement ratio, based on:		Concrete compressive strength, f_{ck} (MPa)				
		10	20	30	40	50
ultimate load (failure)	Rectangular beams $\rho = \frac{A_s}{b \cdot d} \cdot 100$ (%)	0.10	0.10	0.12	0.14	0.16
	I - beams $\rho_t = \frac{A_s}{A_{ct}} \cdot 100$ (%)	0.20	0.26	0.31	0.36	0.40
Limit states of cracking (σ_s = 200MPa)	$\rho_{t,ef}$* for mean crack width 0.4mm	0.62	0.65	0.68	0.72	0.77

*for definition of $\rho_{t,ef}$ see Fig. 2.2

energy. The minimum values of ρ given earlier in this section are therefore not directly comparable to the ratios suggested by ACI 439. In all calculations the concrete strength was assumed to be f'_c = 4000 psi (≅ 28 MPa); with steel strengths varying from f_y = 40 ksi (≅ 280 MPa) to f_y = 75 ksi (≅ 530 MPa). To present their results, the committee plotted the strain energy capacity of concrete members against the reinforcement ratio ρ , as shown in Fig. 2.3. Although Fig. 2.3 is taken from another paper (Mirza and MacGregor, 1981), it is essentially the same as the plot published by Committee 439.

Figure 2.3 has three types of lines. The first (from left to right) represents the situation where rebars fail before the concrete crushes at the top. The second line shows the case where reinforcement yields, but does not break, before concrete crushes at the top. The third line gives the situation where the area of the steel is so large that concrete crushes before the steel yields.

The main conclusions of this paper are:

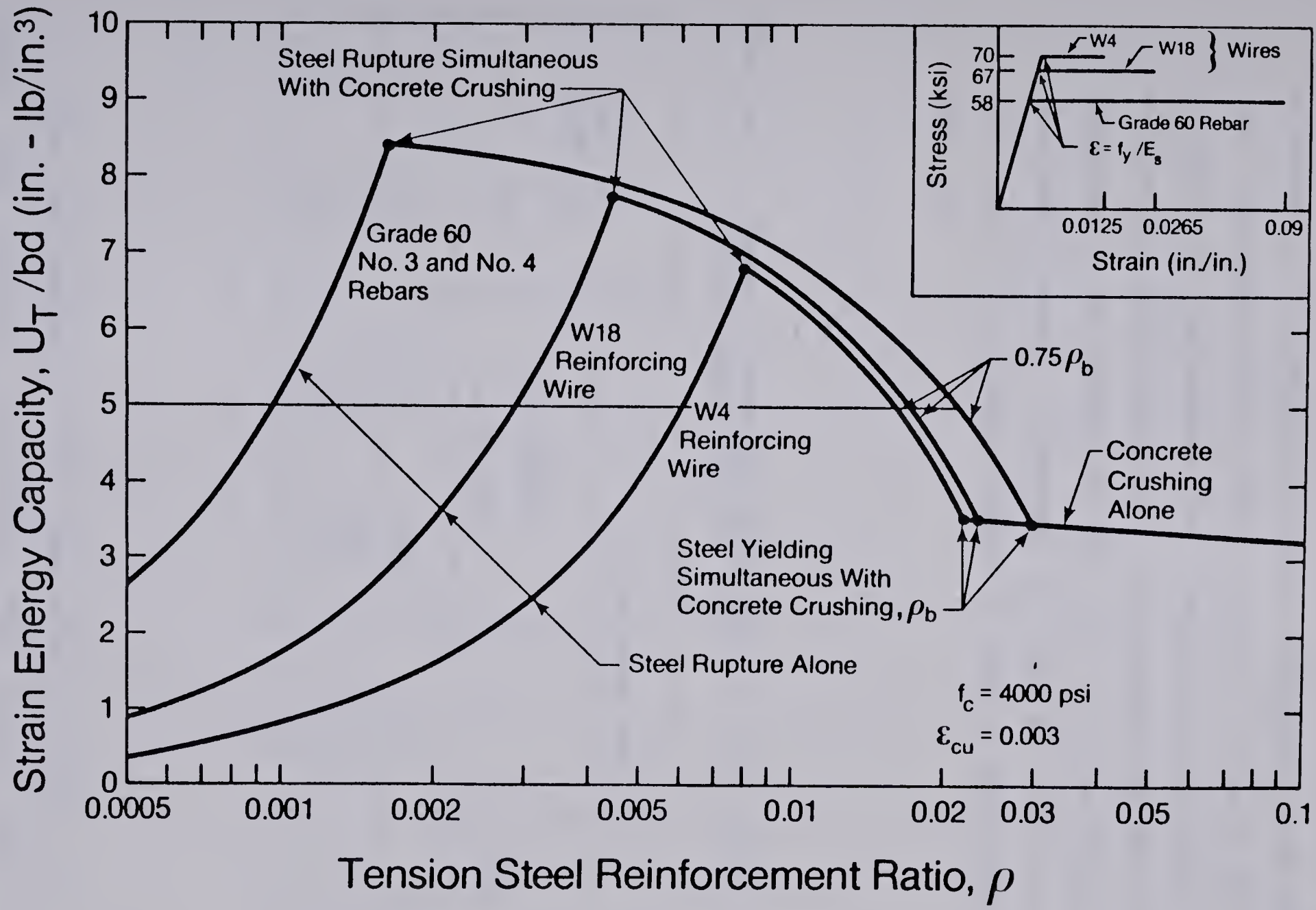

Figure 2.3 — Strain energy capacity of rectangular concrete members (loaded in flexure) with tension reinforcement only (Mirza and MacGregor, 1981).

1. In order to obtain a ductile failure in dynamically loaded structures, it is suggested that the reinforcing steel ratio should be limited to a value of ρ between $\rho = 1.4/f_y$ (MPa) as given in the Canadian code (CSA A23.3, 1977), (see section 2.2) and $0.75\,\rho_2$, where ρ_2 is given in Table 2.4. In addition they recommended that ρ should be at least 0.005. It should be noted that 0.005 exceeds $1.4/f_y$ if f_y exceeds 280 MPa (40 ksi).
2. Regardless of the strength of steel used in the reinforcing bars, the strain-energy capacity is maximized by using an amount of reinforcing steel close to the minimum required to cause a ductile failure (ρ_{min} in Table 2.4).

Table 2.4 — Range of reinforcing steel ratio to insure ductile failure in concrete beams (ACI 439, 1969).

Steel yield strength, f_{yk}		Reinforcement ratio, ρ			
(ksi)	(MPa)	$\rho_{min} = \frac{1.4}{f_y\ (MPa)}$ but ≥ 0.005		ρ_2	$\rho_{max} = 0.75\,\rho_2$
40	~280	(0.0050)	0.005	0.034	0.025
60	~420	(0.0033)	0.005	0.018	0.013
75	~530	(0.0027)	0.005	0.013	0.010

Mirza and MacGregor (1981) made similar calculations for one way concrete slabs, comparing the different strain energy capacity of slabs reinforced with welded wire fabric and conventional rebars. As a part of this study they plotted the strain energy capacity of slabs containing different types

and amount of reinforcement against the reinforcement ratio, ρ , as shown in Fig. 2.3.

Figure 2.3 suggests that the strain energy capacity of rectangular sections having the maximum allowable reinforcement ratio of $\rho_{max} = 0.75 \cdot \rho_b$ (in North-American codes) is approximately 5 in-lbs/in . Based on the assumption that this is the minimum tolerable ductility, Mirza and MacGregor recommend the corresponding minimum reinforcement ratios for rectangular slabs as (see horizontal line at 5 in-lbs/in in Fig. 2.3):

Grade 60 rebars.... $\rho_{min} = 0.001$

W4 wires..... $\rho_{min} = 0.006$

W18 wires..... $\rho_{min} = 0.003$

For the welded wire fabric, they give the following equation:

$$\rho_{min} = \frac{0.0012}{\sqrt{A_n}} \qquad (2.16)$$

where A_n is the nominal area of one wire in in^2 (to convert to SI-units, multiply Eqn. 2.16 by 25.4).

Only 4000 psi concrete was considered in the Mirza and MacGregor study. Both this study and the ACI 439 report neglect the relationship between cracking moment and ultimate moment. Finally, the authors emphasize that the ductility is required only in those locations in a structure where the actual load capacity of the structure depends on the reinforcing steel yielding before the structure assumes a failure mechanism by successive formation of plastic hinges. Hence, the above mentioned ratios need only to be used for members requiring ductility.

McCollister, Siess and Newmark (1954) reported test results of three beams with small amounts of reinforcement. Beams N-1 and N-2 had the same amount of reinforcement. Beams N-2 and N-3 were moist cured and tested in moist condition, while N-1 was allowed to dry out. The concrete strengths, reinforcement ratios and steel strengths are summarized in Table 2.5.

Table 2.5 — Data for three test specimens tested for minimum reinforcement (McCollister, Siess and Newmark, 1954).

Member	Concrete strength, $f'_{c,obs}$ (psi)	Steel yield strength, $f_{y,obs}$ (psi)	Reinforcement ratio, $\rho = A_s/b \cdot d$
N-1	6138	47600	0.0017
N-2	5649	49100	0.0017
N-3	6407	41600	0.0031

Because of higher degree of hydration and the lack of shrinkage stresses due to being cured and tested in the moist condition, beams N-2 and N-3 had a cracking load appreciably higher than beam N-1. The companion beams N-1 and N-2 both failed at a deflection of about 75 mm (3 inches). In the case of N-1 which had a low cracking load, the steel was just able to resist that load after strain hardening had taken place. N-1 would thus be regarded as a boundary case between brittle and ductile failures.

Beam N-2 failed in a brittle manner since its moment capacity after cracking was less than at cracking. Beam N-3, although badly damaged by cracks, was able to withstand a load about 10% higher than the cracking load and will therefore be considered ductile. It should be noted that the concrete compressive strength given in Table 2.5 is $f_{c,obs}$, that is the actual strength when tested.

2.2 Present design code requirements for minimum reinforcement

2.2.1 North American codes

The codes referred to here are CAN3-A23.3-M77 (CSA A23.3, 1977), the Canadian code, and ACI 318-77 (ACI 318, 1977), widely used in the United States of America. These two codes are in most respects identical, but since the Canadian code uses the SI-units, it will be used as the main reference here.

The requirements are as follows:

Non-prestressed members.

"At any section of a flexural member (except slabs of uniform thickness) where tension (*positive*[1]) reinforcement is required by analysis, the ratio ρ supplied shall not be less than that given by:

$$\rho_{min} = \frac{1.4}{f_y} \quad (f_y \text{ in MPa}) \tag{2.17}$$

unless the area of reinforcement provided at every section, positive and negative, is at least one third greater than that required by analysis. In T-beams and joists where the web is in tension the ratio shall be computed for this purpose using the width of the web".

For structural slabs of uniform thickness the area of reinforcement in the direction of the span shall provide at least the following ratios of reinforcement area to gross concrete area, but not less than 0.0014:

For plain bars	0.0025
Slabs where deformed bars having a yield strength less than 400 MPa are used	0.0020
Slabs where deformed bars having a yield strength of 400 MPa or weldel wire fabric, deformed or plane, are used	0.0018

---

[1] The ACI code uses the word "positive" where the Canadian code uses "tension".

Slabs where reinforcement with yield strength exceeding 400 MPa measured at a yield strain of 0.35 per cent is used . . . . . $\frac{0.0018 \times 400}{f_y}$

The reason for different rules for slabs and other members is given in the ACI 318 Commentary (ACI 318, 1977b) which says that the minimum reinforcement required for slabs is somewhat less than that required for beams since an overload would be distributed laterally and a sudden failure would be less likely.

Prestressed members.

"The total amount of all types of reinforcement shall be such that the ultimate capacity of the member is at least 1.2 times the cracking moment where cracking moment is defined as that which induces a tensile stress in the concrete equal to the modulus of rupture defined as:

$$f_{ct} = 0.6\sqrt{f'_c} \qquad (2.18)$$

Minimum bonded reinforcement shall be provided in the pre-compressed tension zone of ..flexural members in which the prestressing steel is unbonded. Such bonded reinforcement shall be distributed uniformly over the tension zone near the extreme tension fibre.

The minimum amount of bonded reinforcement, A_s , in beams and one-way slabs shall be:

$$A_s = \frac{N_c}{0.5 \cdot f_y} \quad \text{or} \quad A_s = 0.004 \cdot A_{ct} \qquad (2.19)$$

whichever is larger, where A_{ct} = area of the tension zone and N_c = tensile force in the concrete under load of D + 1.2L and f_y shall not exceed 400 MPa".

2.2.2 Euro-International concrete committee model code (CEB, 1977)

The minimum reinforcement requirements in the CEB Model Code are as follows:

1. "A minimum area of longitudinal reinforcement should be provided in beams and slabs to ensure that there is a sufficient reserve of strength after cracking. The area of longitudinal tensile reinforcement provided should not in general be less than:

   0.0015 b_t d for steel grades S400 or S500 or for prestressing steels.
   0.0025 b_t d for steel grade S220
   where b_t is the average width of the concrete zone in tension.

   In a T-beam, if the neutral axis is located in the flange, the width of the latter is not taken into account in evaluating b_t".

2. "A minimum amount of reinforcement should be provided in all cases for the control of cracking, even for members which had been checked for the decompression limit state. That reinforcement should be so dimensioned that:

   a) at cracking the stress in the steel remains below f_{yk}.

   b) the crack widths remain below a specified limit".

In order to satisfy condition a), one should ensure that:

$$\rho_{t,ef} = \frac{A_s}{A_{ct,ef}} \geq \frac{f_{ct}}{f_{yk}} \qquad (2.20)$$

where $A_{ct,ef}$ denotes that part of the tension zone of the concrete where the reinforcing bars can effectively influence the crack widths (effective embedment zone). The effective embedment zone is as defined in Fig. 2.2. It should be noted that in this code no distinction is made between the amount of minimum required reinforcement in non-prestressed and prestressed members.

2.3 Comparison between various minimum reinforcement requirements

In comparing different literature one must be aware of different usage of some reference values, such as concrete strength. Fig 2.1 for example, uses the actual compressive cylinder strength on the day the member was tested, while design is generally based on the specified 28 day strength. The most commonly used reference value for steel strength is the specified or characteristic yield strength, f_{yk} .

Also, since the North-American and the European definitions of specified concrete compressive strength are a little different, all comparison will be based on the North-American definition, f'_c , and other specifications will be modified to be comparable to it.

The North-American definition of specified compressive strength of concrete is:

$$f'_c = f_{c,ave} - 1.343\ s \qquad (2.21)$$

and the European definition is:

$$f_{ck} = f_{c,ave} - 1.64\ s \qquad (2.22)$$

where $f_{c,ave}$ = average strength to be used as a basis for selecting concrete proportions.
s = standard deviation of individual strength tests.

Thus, in order to compare these two, the following relationship will be used (assuming a coefficient of variation for the concrete as, $\delta_c = 0.15$) :

$$f'_c = 1.06\ f_{ck} \qquad (2.23)$$

In order to compare the code requirements and the recommendations given in Section 2.1, Fig. 2.1 must be replotted in terms of f'_c and f_{yk} . This results in a new equation for the boundary line, which now becomes:

$$\rho_{min} = 0.067 + 1.24\ \frac{f'_c}{f_{yk}} \qquad (2.24)$$

This line is compared in Fig. 2.4 to the other recommendations presented in sections 2.1 and 2.2. In this figure the concrete strength is limited to 15 MPa $\leq f'_c \leq$ 45 MPa, and the steel strength is limited to 200 MPa $\leq f_{yk} \leq$ 600 MPa, which gives lower and upper boundaries for f'_c / f_{yk} equal to 0.025 and 0.225, respectively. The lines and bands plotted in Fig. 2.4 all are for rectangular unprestressed members loaded in flexure. Three observations can be made from the data plotted in Fig. 2.4:

1. The CEB requirements are similar to most of the other requirements, including the CSA-ACI "temperature and shrinkage" reinforcement, and quite close to Leonhardt's test results.
2. The CSA-ACI recommendations for beams are much higher than the others and in no case do they cross Leonhardt's line.
3. Leonhardt's recommendations (1961, 1973 and 1977) seem to move away from his test-line as the years go by, and his 1977 proposals are well below the minimum suggested by the tests he reported in 1961.

2.4 Concrete strength in tension and compression

Although the present test program deals with specimens where tensile strength is more important than compressive strength, both of them will be discussed here since the tensile strength is often expressed as a function of the compressive strength.

2.4.1 Effect of loading rate

The observed strength of concrete is considerably affected by the rate of application of the load: the lower the rate of loading, the lower the apparent strength.

Mirza, Hatzinikolas and MacGregor (1979) recommend the following relationships for the effect of the rate of loading:

a) for compressive strength:

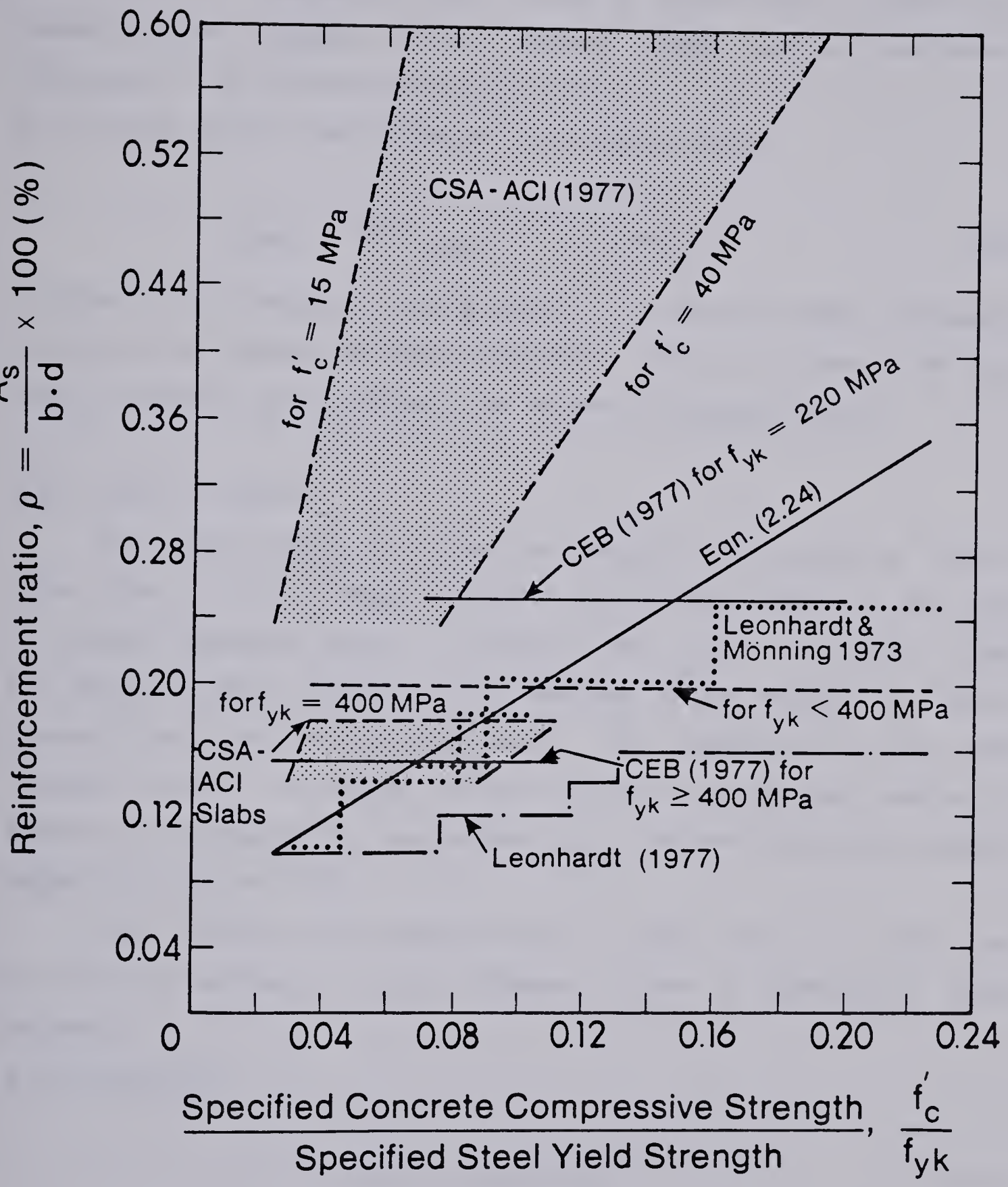

Figure 2.4 – Comparison between different recommendations for minimum reinforcement ratio in rectangular concrete members.

$$f_{C(R)} = 0.89\ f_{C(35)}\ (1 + 0.08 \cdot \log R) \qquad (2.25)$$

in which $0.1 \leq R$ psi/sec $\leq 10\ 000$, where R is the rate of stressing (the normal rate of stressing for the standard cylinder test is approximately 35 psi/sec or 15 MPa/min (CSA A23.2, 1977)).

b) for tensile strength (both in flexure and splitting tension):

$$f_{Ct(R)} = 0.96\ f_{Ct(2.5)}\ (1 + 0.11 \cdot \log R) \qquad (2.26)$$

in which $0.01 \leq R$ psi/sec ≤ 170 (2.5 psi/sec or 1 MPa/min roughly corresponds to the rate of stressing of control specimens). Mirza et al assume that $f_{C(R)}$ and $f_{Ct(R)}$ have the same coefficients of variation as $f_{C(35)}$ and $f_{Ct(2.5)}$.

2.4.2 Effect of volume

The in-situ strength of concrete is affected by the *volume of material under stress.* In 1931, Reagel and Willis reported that variations in the depth of concrete specimens caused a variation in the modulus of rupture. Linder and Sprague (1955) reported a 15% decrease in the modulus of rupture between 6 inch and 18 inch deep beams. They developed what they called "rectibolic formula", to account for the difference between the modulus of elasticity in compression, E_C, and tension, E_{Ct}. The ratio E_C/E_{Ct} they reported ranged from 1.47 to 1.85.

Bolotin (1965), using statistical theory of brittle fracture of solids, gave the following estimates for the influence of size in geometrically similar specimens:

a) in compression:

$$X = X_0\ (0.58 + 0.42\ (V_0/V)^{1/3}) \qquad (2.27)$$

in which X_0 and V_0 represent the strength and volume of an 100mmx100mmx100mm cube specimen. Eqn. (2.27) indicates that as the volume increases, the mean strength decreases. The coefficient of variation for eqn. (2.27) can be taken as:

$$\delta_x = \frac{0.147\ (V_0/V)^{1/3}}{0.58\ +\ 0.42\ (V_0/V)^{1/3}} \tag{2.28}$$

b) in tension:

$$X = X_0\ (0.43\ +\ 0.57\ (V_0/V)^{1/3}) \tag{2.29}$$

The coefficient of variation can in this case be taken as:

$$\delta_x = \frac{0.200\ (V_0/V)^{1/3}}{0.43\ +\ 0.57\ (V_0/V)^{1/3}} \tag{2.30}$$

In both tension and compression the value of the strength three standard deviations below the mean is essentially independent of volume.

2.4.3 The relationship between compressive and tensile strength

In studies of the strength of reinforced concrete elements it is a common practice to express tensile concrete strength as a function of the compressive strength. The CSA-ACI codes recommend the use of:

$$f_{ct} = 0.6\sqrt{f'_c} \tag{2.31}$$

The CEB Model Code recommends the use of:

$$f_{ct} = 0.3 \cdot (f_{ck})^{2/3} \tag{2.32}$$

Regression analysis (Mirza et al, 1979) of data from 588 sets of modulus-of-rupture beams with third point loading and standard cylinders gave the following relation (developed for square-root relationship):

$$f_{ct} = 0.69\sqrt{f_c} \tag{2.33}$$

The effect of age of concrete should also be taken into account. Neville (1970) reports that the following relationship is valid for normal Portland cement concrete:

$$f_c(t) = f_c(28) \frac{4}{3 + 28/t} \qquad (2.34)$$

where t is age of concrete in days.

Eqn. (2.34) is plotted in Fig. 2.5, for a 28 day strength of 30 MPa.

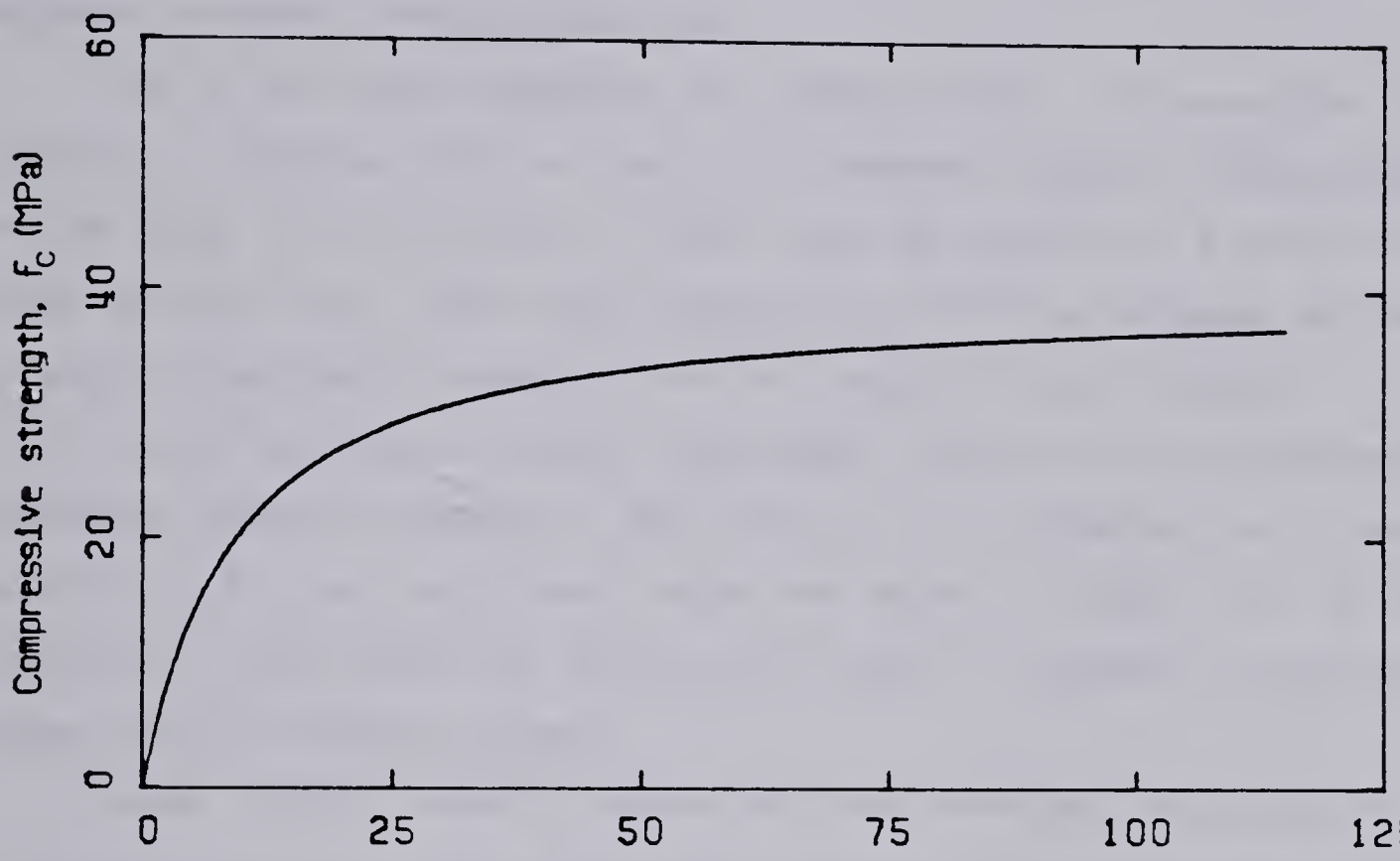

Figure 2.5 -- Assumed strength development of concrete (normal Portland cement).

2.4.4 Effect of shrinkage

Portland cement concrete has the tendency to shrink with loss of water. On exposure of a concrete member to drying conditions, moisture slowly diffuses from the interior mass of the concrete to the surface, replacing the moisture lost by surface evaporation. As a result, moisture gradients are produced, which in turn induce stresses in the concrete.

Drying shrinkage of concrete has been found to be one of the principal causes of cracking (Cady, Clear and Marshall, 1972 and ACI Committee 224,

1980). Factors such as: composition of cement, aggregate size, water content, chemical admixtures, pozzolans (fly ash), member size, and duration of moist curing all have some effect on the shrinkage of concrete members.
Although a considerable amount of work has been done on this subject, no overall agreement has been reached so far on the form that mathematical equations describing shrinkage should take.

One of the early researchers was Carlson (1937). He stated that: "The diffusion of moisture from the interior of concrete toward a drying surface can be linked to the diffusion of heat from the interior of a solid to the cooler surface," also: "...when both moisture loss and drying shrinkage are stated in terms of per cent of expected total, they should be nearly identical."
Based on his experiments, Carlson recommends values for the percentage of evaporable moisture remaining in slabs drying in an atmosphere with relative humidity of 50 per cent; these values are shown in Table 2.6. He also explains how these values for slabs can be used for members of any shape, drying from any number of sides.

Neville (1970) correctly points out that shrinkage and creep occur simultaneously and can not be separated completely. Shrinkage causes stress in the concrete, which in turn activates the creep action. This creep or relaxation reduces the effective shrinkage stresses and so on. In his book on creep Neville gives the following iterative expression for calculating actual shrinkage stresses after relaxation, based on a given initial stress:

$$\sigma_{i+\frac{1}{2}} = \sigma_{i-\frac{1}{2}} + \frac{E_i}{1+\phi_{ii}} \left[\sum_{j=1}^{i} \Delta\varepsilon_j - \sum_{j=1}^{i-1} (\sigma_{j+\frac{1}{2}} - \sigma_{j-\frac{1}{2}}) \frac{1}{E_j} (1+\phi_{ij}) \right] \qquad (2.35)$$

The notation in eqn. (2.35) is based on Fig. 2.6.
For good agreement with experimental results, the number of steps needed in Eqn. (2.35) is small, usually about five. It is advisable to choose shorter intervals in the early stages when the rates of creep and shrinkage are highest.

Table 2.6 — Percentage of evaporable moisture remaining in drying slabs at various depths from drying surface (Carlson, 1937).

Dist. from drying surface	Time of continous drying in terms of K•t/a														
	.005	.01	.02	.04	.06	.08	.10	.15	.20	.25	.30	.40	.60	.80	1.0
0.1 a	70	52	38	27	23	20	18	14	12	10	9	7	4	3	2
0.2 a	92	82	67	52	43	38	34	28	24	20	18	13	8	5	3
0.3 a	98	93	85	71	60	54	49	41	35	30	27	20	12	7	5
0.4 a	99	98	95	84	75	68	63	53	46	39	35	27	16	10	6
0.5 a	100	99	99	93	85	79	74	63	55	48	42	33	20	12	8
0.6 a	100	100	100	97	91	86	82	72	63	55	49	38	23	14	9
0.7 a	100	100	100	99	95	91	88	79	69	61	54	42	26	16	10
0.8 a	100	100	100	100	97	94	92	83	73	65	58	45	27	16	10
0.9 a	100	100	100	100	98	96	94	85	76	67	60	47	28	17	11
1.0 a	100	100	100	100	99	97	95	86	77	68	61	48	28	17	11

Notes: K = moisture diffusion constant (.0001 ft^2/day for average concrete)
t = time from beginning of drying in days
a = half-thickness of slab drying from both faces.

Cady, Clear and Marshall (1972) tested 30 standard test cylinders for the splitting tensile strength. Prior to testing the specimens were dryed at 140 ^{0}C for various time periods to produce the degree of saturation desired. Their test results are replotted in Fig. 2.7.

It is evident from Fig. 2.7 that the minimum tensile strength is obtained at a point at which about half of the total evaporable water has been removed. The maximum strength loss compared to the saturated condition is in the order of 30% to 35%. This observation confirms the observation that tensile strength of concrete is lower during the intermediate stages of drying, when steep moisture gradients exist in the specimen. It can be seen that the tensile

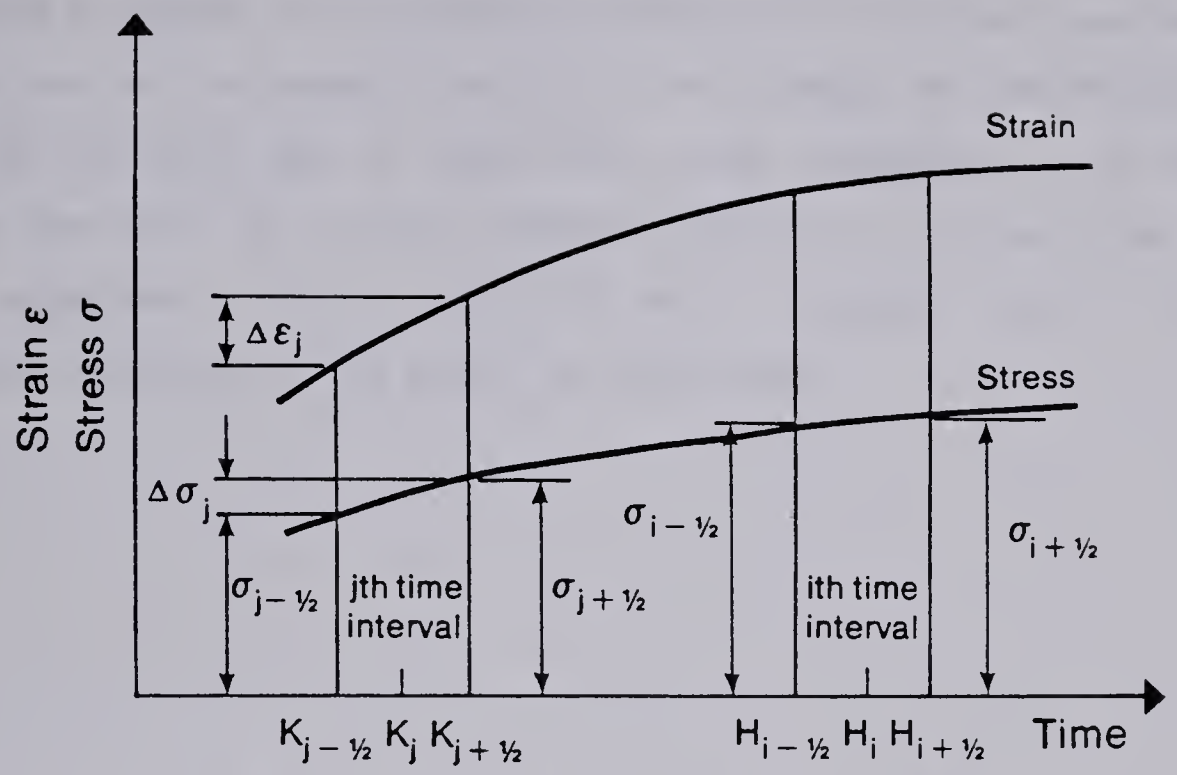

Figure 2.6 – Step-by-step procedure of eq. (2.35) (Neville, 1970)

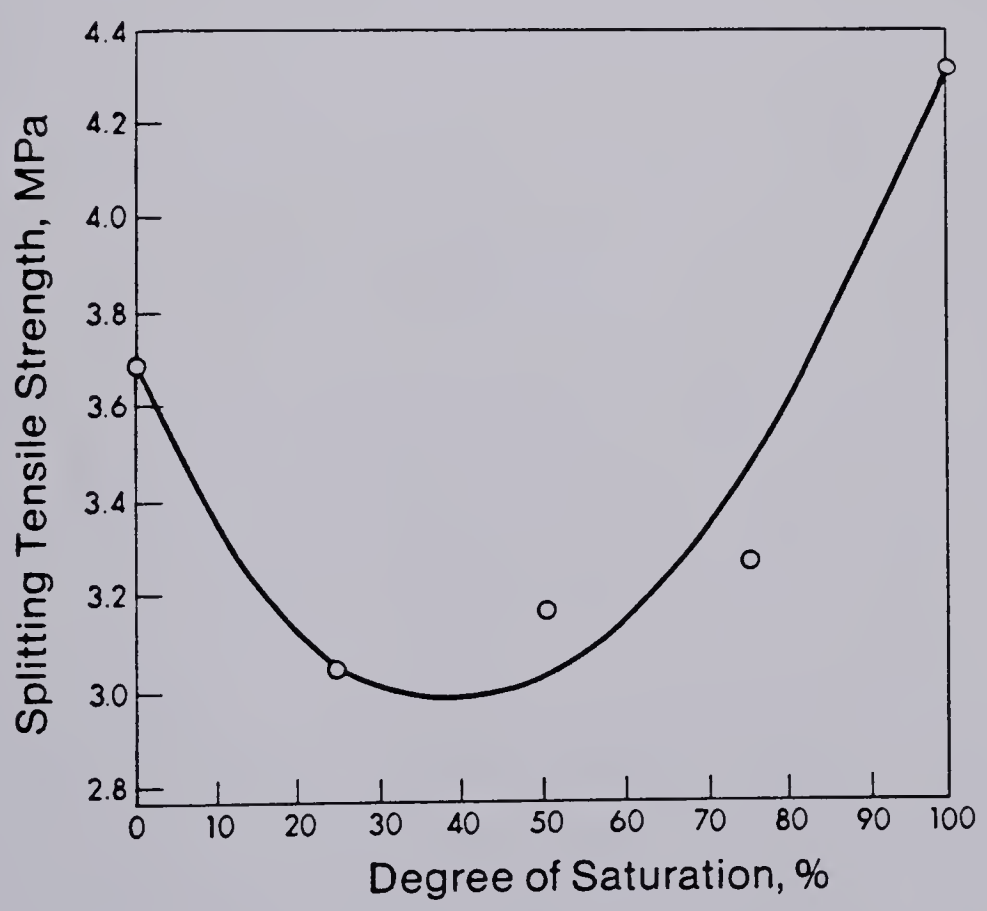

Figure 2.7 – Splitting tensile strength of concrete cylinders versus degree of saturation (Cady, et al. 1972)

strength is highest in the totally dry condition and the totally saturated condition. These are the two states in which it is not possible to have moisture gradients. It must be noted that in practise the drying temperature is, of course, much lower than 140 °C and thus moisture gradients are not nearly as steep as in this experiment. However, the 35% loss in strength serves to illustrate the possible magnitude of the effect of rapid drying.

3. THEORY

3.1 Moment capacities

3.1.1 Cracking moment

The cracking moment capacity of the test specimens will be calculated using the transformed area of the cross-section, i.e. the steel area will be transformed to an equivalent area of concrete, using the modular ratio $E_S/E_C = n$. Calling αh the distance from the extreme fibre in compresion to the neutral axis (N.A.), one gets the following equations for the rectangular shapes:

$$\alpha h = \frac{(n-1)\cdot A_S \cdot d + 1/2 \cdot b \cdot h^2}{b \cdot h + (n-1)\cdot A_S} \qquad (3.1)$$

and

$$I_{tr} = \frac{1}{3}\cdot b \cdot (\alpha h)^3 + \frac{1}{3}\cdot b \cdot (1-\alpha)^3 \cdot h^3 + (n-1)\cdot A_S \cdot (d - \alpha h)^2 \qquad (3.2)$$

which finally gives:

$$M_{cr,cal} = \frac{I_{tr} \cdot f_{ct}}{(1-\alpha)\cdot h} \qquad (3.3)$$

Similar equations can be derived for the T - shapes and the I - shapes. For comparison, the cracking moment will also be calculated using the gross concrete area, i.e. ignoring the reinforcing steel. In that case $\alpha = 0.5$.

3.1.2 Yielding moment

The yielding moment capacity will be calculated using two different approaches. First the CSA-ACI (CSA-A23.3-M77 and ACI 318-1977) code equation for nominal moment capacity (M_n) will be used:

$$M_{y,cal} = A_S \cdot f_y \cdot (d - a/2) \qquad (3.4)$$

$$\text{where: } a = \frac{A_s \cdot f_y}{0.85 \cdot f_c \cdot b}$$

Secondly, the straight line theory, which gives the equation:

$$M_{y,cal} = A_s \cdot f_y \cdot d \cdot (1 - \alpha/3) \qquad (3.5)$$

$$\text{where: } \alpha = \sqrt{2n\rho + (n\rho)^2} - n\rho$$

The values these two equations give will be compared to the yielding moment capacities observed in the tests.

3.1.3 Ultimate moment

Two different methods will be used to calculate the ultimate moment capacities of the members. First the CSA–ACI equation (3.4) will be used, substituting f_{su} for f_y :

$$M_{u,cal} = A_s \cdot f_{su} \cdot (d - a/2) \qquad (3.6)$$

$$\text{where: } a = \frac{A_s \cdot f_{su}}{0.85 \cdot f_c \cdot b}$$

Alternatively, using strain compatibility, an equation relating stress and strain in the reinforcing steel at ultimate can be derived:

$$\sigma_{su} = \frac{\beta \cdot 0.85 \cdot f_c \cdot \varepsilon_{cu}}{\rho (\varepsilon_{su} + \varepsilon_{cu})} \qquad (3.7)$$

where: $\beta = 0.85$ for $f_c \leq 30$ MPa
$\beta = 0.65$ for $f_c \geq 55$ MPa
(linear interpolation between)

By varying ε_{su} and computing σ_{su} one can compute points on a line representing Eqn. (3.7). The intersection of this line and the stress – strain curve for the reinforcing steel gives the steel stress at failure, σ_{su} . This σ_{su} is then substituted for f_{su} in Eqn. (3.6) to find the ultimate moment capacity. If the reinforcing bars fracture at the ultimate load, it is not neccesary to use Eqn. (3.7) to determine σ_{su} since it is then known that $\sigma_{su} = f_{su}$. In these

cases only Eqn. (3.6) will be used. If, on the other hand, the bars do not break the steel stress must be calculated using Eqn. (3.7) and the resulting σ_{su} used in Eqn. (3.6). Both M_{cr} /M_y and M_{cr} /M_u are of interest here and will be discussed in Chapter 5.

3.2 Moment contours in slabs

An elastic finite element program for slabs (Hrabok, unpublished) was used to find the bending moments in the slabs, especially the point loaded slabs (see section 4.4.2). The moment contours for both types of slabs (point loaded and line loaded) for a total load of P = 61.5 kN are given in Fig. 3.1.

3.3 Effect of shrinkage on the tensile strength of concrete

As mentioned earlier (section 2.4.4), drying shrinkage can considerably reduce the tensile strength of concrete.

The shrinkage effects in rectangular beams, drying from all four faces are estimated here. Two different size beams, with cross-sections 310 mm x 310 mm and 89 mm x 115 mm will be considered, representing the R series beams and the modulus of rupture beams described in section 4.2.

Table 2.6 (Carlson, 1937) will be used to find the moisture percentage remaining in the members at different times from the beginning of drying. Since both beams are drying from four sides, results from each two adjoining sides must be multiplied together to get the amount of evaporable moisture remaining in the members. Typical results from these calculations are shown in Fig. 3.2 as moisture content lines. Based on these contours, the cross-section of the member is divided into regions, each region having approximately the same shape as the contour lines. The first region (the shell) has a thickness of 1/10 a (a being half the thickness of the member) at the sides where the effects from the other sides are negligible. The second region goes from 1/10 a to 1/2 a at the sides. The third region (the core) represents the area from 1/2 a to the centre. Figure 3.3 gives the total areas and shapes of the

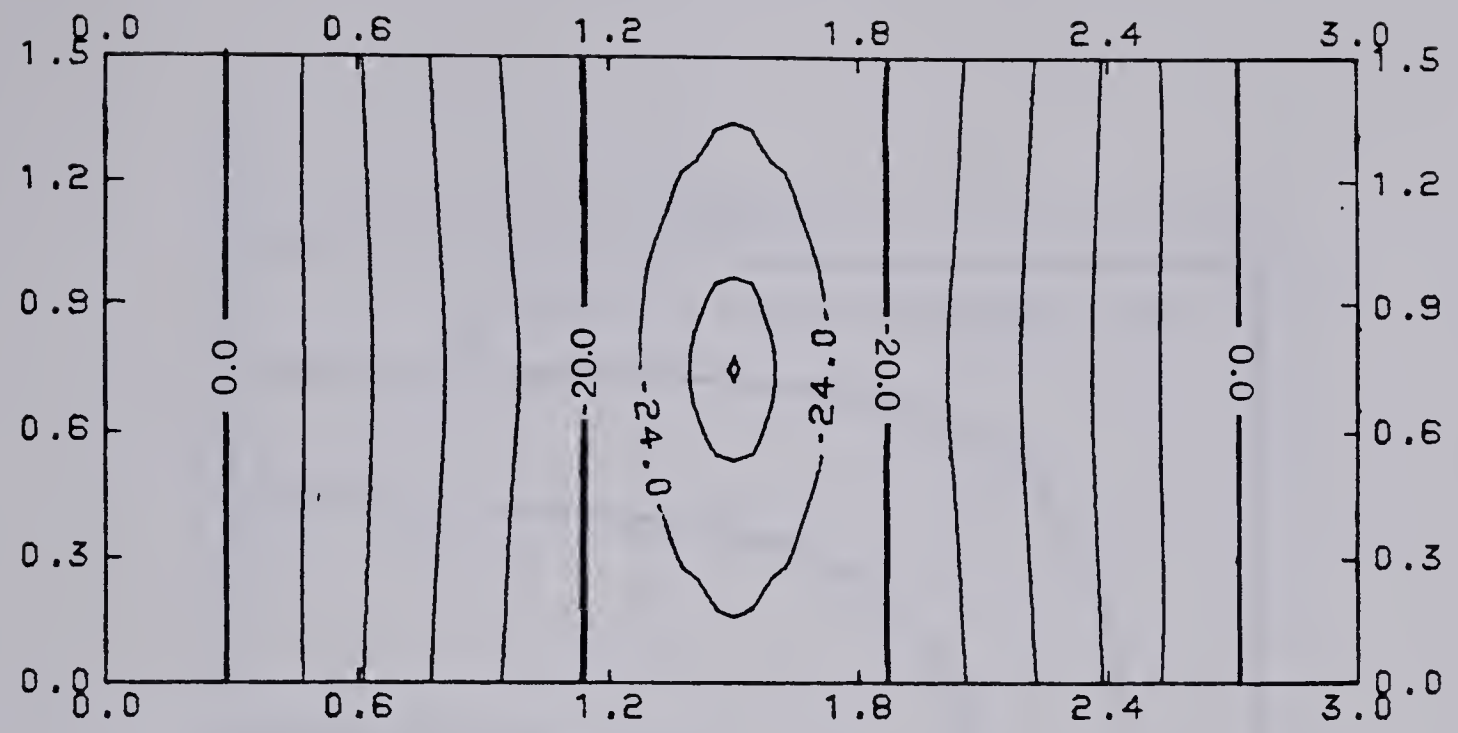

For point load at centre

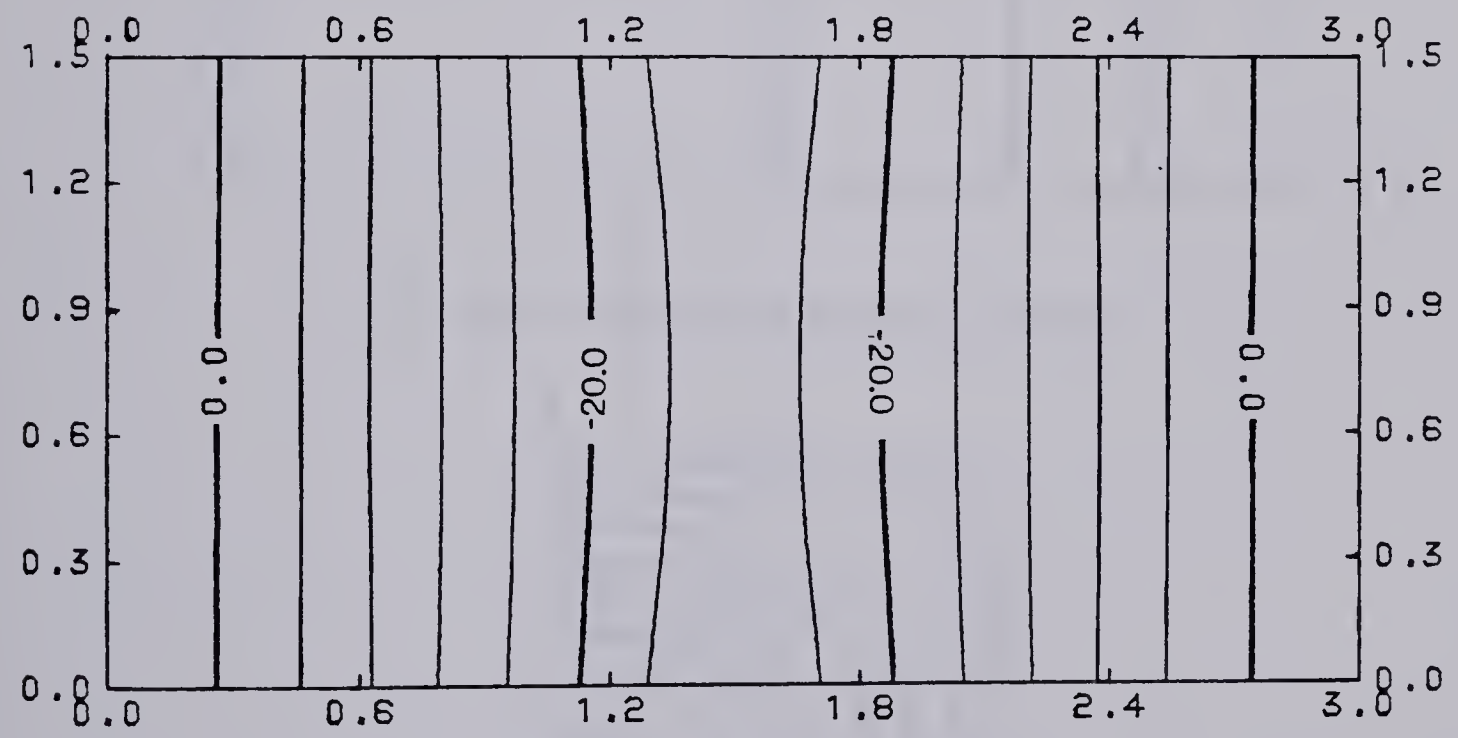

For line load across midspan

Moments in kN·m/m

Distances in m

Figure 3.1 — Bending moment contours in slabs, $\nu = \frac{1}{6}$

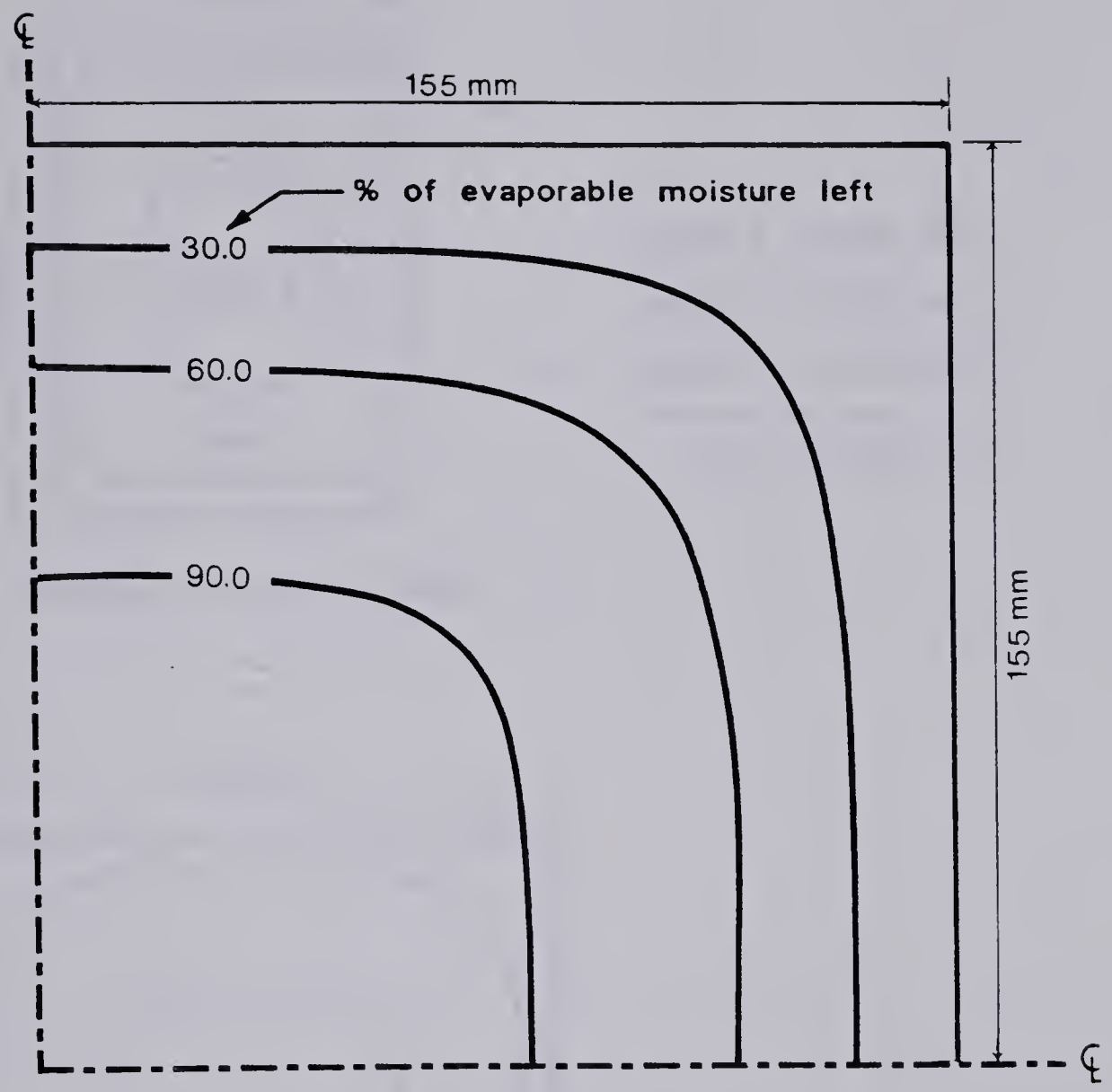

310 mm × 310 mm cross-section

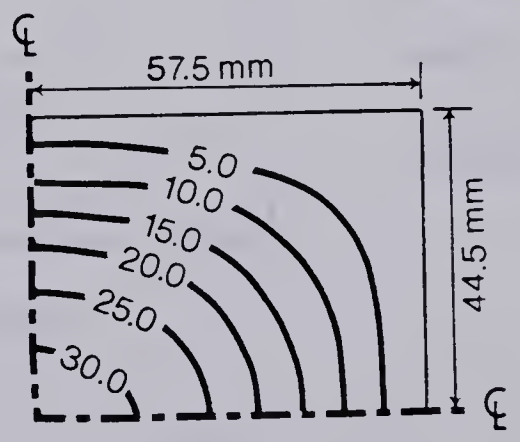

89 mm × 115 mm cross-section

Figure 3.2 — Typical moisture content contours in cross-sections of different size.

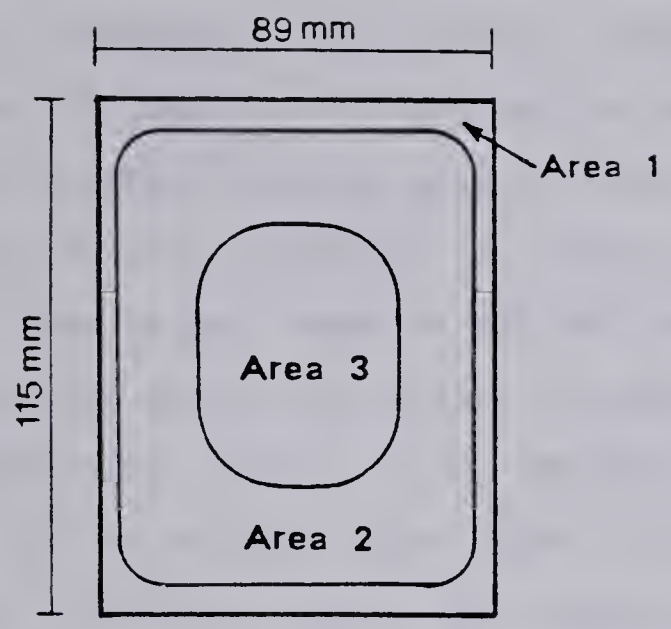

Area 1 : 2700 mm²

Area 2 : 5135 mm²

Area 3 : 2400 mm²

Total : 10235 mm²

Modulus of rupture beams

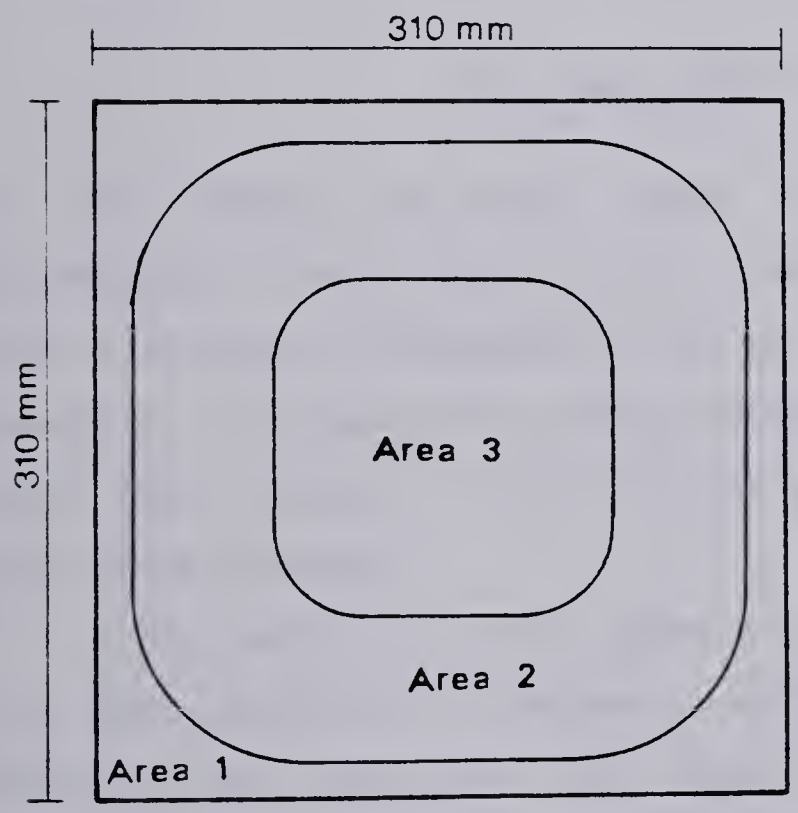

Area 1 : 20800 mm²

Area 2 : 52100 mm²

Area 3 : 23200 mm²

Total : 96100 mm²

R series beams

Figure 3.3 — Areas and shapes of regions used in shrinkage calculations.

regions for both beams.

The percentage of the moisture remaining in each region at different times from the beginning of drying can be calculated using Table 2.6. Then by assuming an ultimate shrinkage strain of 400 x 10^{-6} m/m and that shrinkage is proportional to the percentage of moisture evaporated from the specimen, values of strain in each region at different times are obtained.

Once the strain in all regions has been obtained as a function of time, the corresponding stress can be calculated, taking into account the creep occurring due to the given strain. Eqn. (2.35) will be used for this purpose. The creep coefficients used in the calculations are derived from graphs and tables in Appendix E in the CEB model code (CEB, 1978). For the development of concrete compressive strength with time, Eqn. (2.34) is used. The modulus of elasticity is taken as:

$$E_C = 5000\sqrt{f_C} \qquad (3.8)$$

The time intervals are chosen smaller in the early stages of drying as recommended by Neville (section 2.4.4). Calculations are done for two strength levels of concrete, corresponding to 28 day strengths of 20 MPa and 40 MPa, respectively. The results from these calculations are shown in Fig. 3.4 for the smaller beams (modulus of rupture beams) and in Figures 3.5 and 3.6 for the larger beams (R-beams).

In the modulus of rupture beams the shell (region 1) starts in tension at early ages, switching to compression at ages greater than about 18 days. Because of their greater size, the R series beams dry more slowly, the outside staying in tension throughout the period considered.

Since all members will be older than 18 days when tested, shrinkage stresses are clearly not going to affect the tensile strength of the modulus of rupture beams. Therefore, results are only shown for one strength level of concrete for these beams (Fig. 3.4). Figures 3.4, 3.5 and 3.6 will be used in Chapter 5 to aid in explaining differences between calculated and observed values of the cracking moment, M_{Cr}.

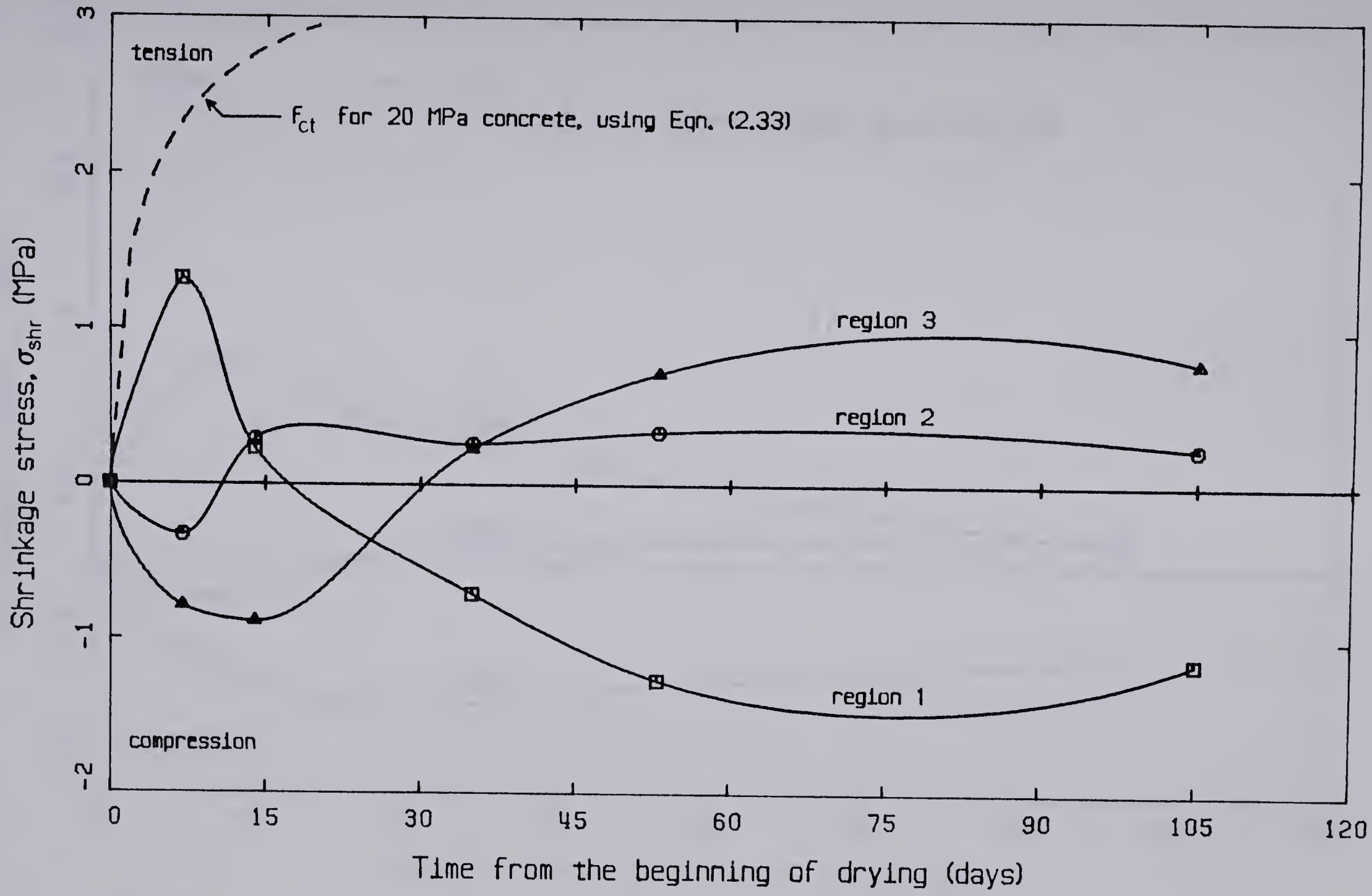

Figure 3.4 — Shrinkage stress distribution in modulus of rupture beams as a function of time; 20 MPa concrete.

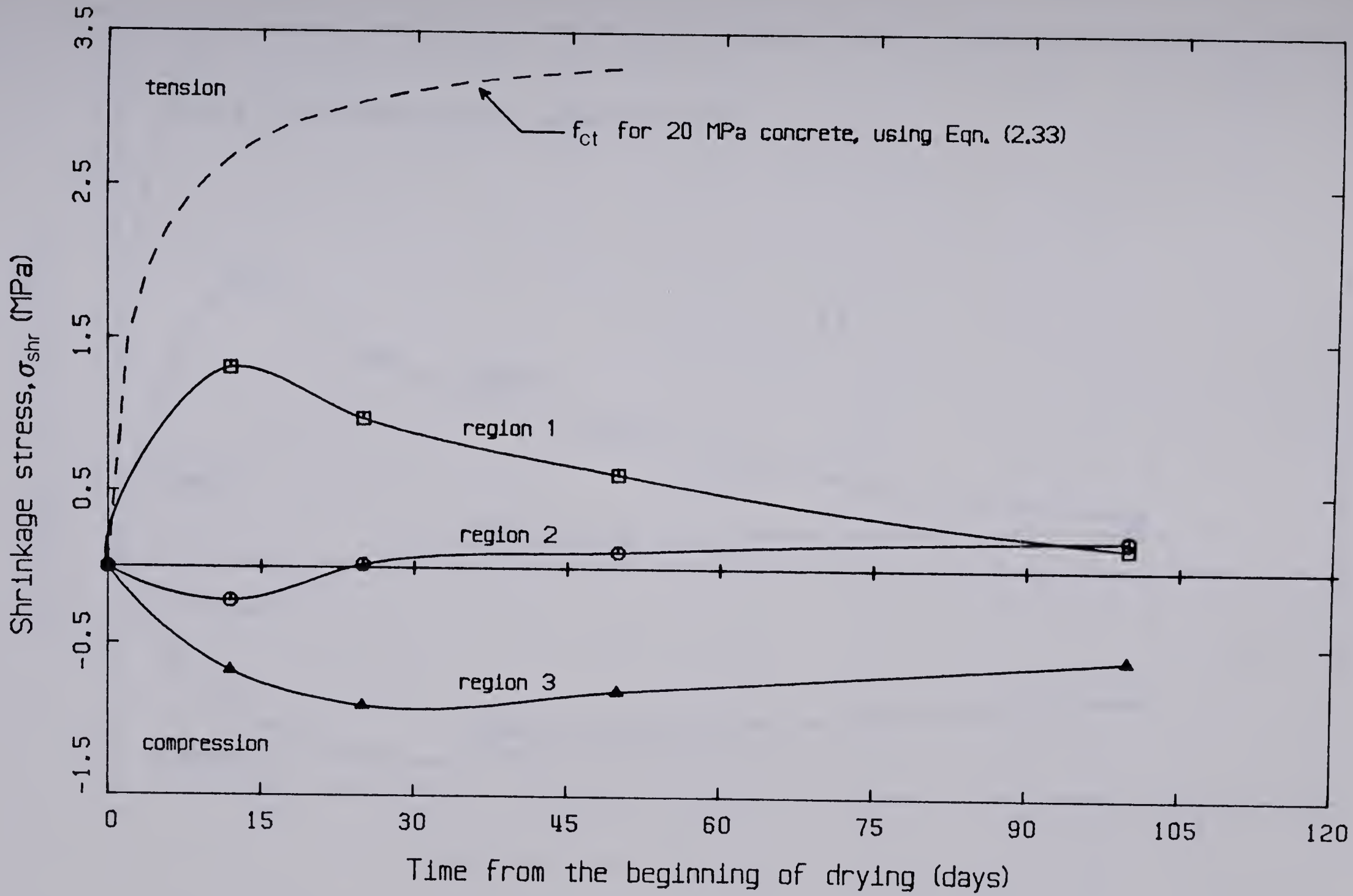

Figure 3.5 — Shrinkage stress distribution in R series beams as a function of time; 20 MPa concrete.

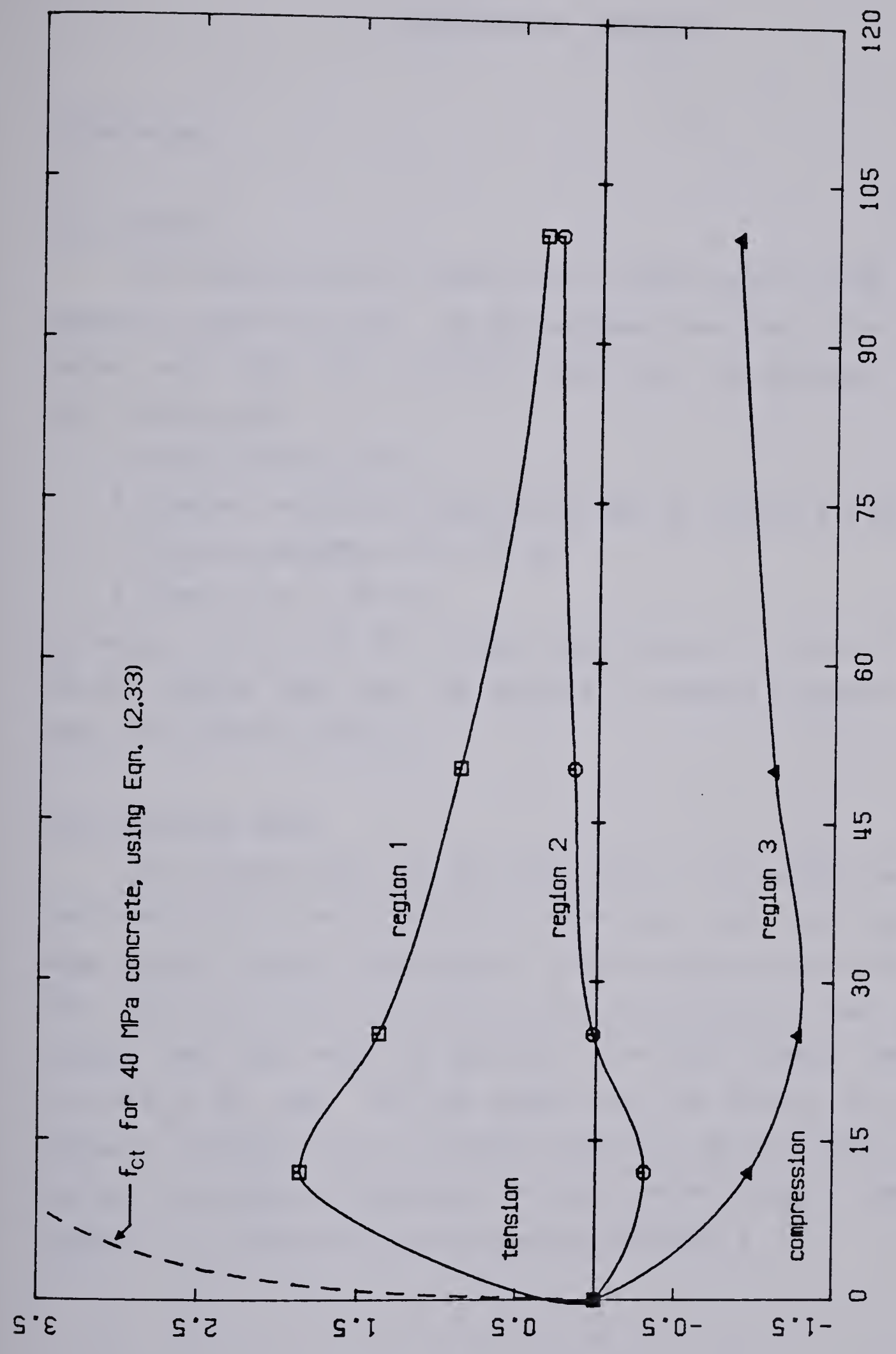

Figure 3.6 — Shrinkage stress distribution in R series beams as a function of time; 40 MPa concrete.

4. EXPERIMENTAL PROGRAM

4.1 Materials

4.1.1 Concrete

The concrete used was bought from a local concrete supplier and was delivered in ready-mix trucks. The test specimens were cast in four separate batches, each batch using a different truck load. The parameters specified when ordering were:

1. normal Portland cement
2. specified compressive strength at 28 days, f'_c, 20 MPa and 45 MPa
3. maximum aggregate size of 20 mm
4. slump of 70 - 75 mm

In batches 1 and 2, 20 MPa concrete was used, and in batches 3 and 4, 45 MPa concrete was used. The observed or measured properties of each batch are tabulated in Chapter 5.

4.1.2 Reinforcing steel

The reinforcing steel was also bought from a local supplier, except for the 6 mm diameter steel referred to as ϕ6mm steel, which was a part of a larger shipment imported from Sweden. All reinforcing bars had a well defined yield point and all bars of the same size that were supposed to have the same strength were taken from the same heat. The yield strength varied from 371 MPa to 551 MPa. The high strength steel was used in the first two batches in combination with low strength concrete and the low strength steel in the last two batches in combination with high strength concrete. Stress-strain diagrams for all reinforcing bars are presented in Chapter 5.

4.2 Test specimens

Specimens of four different cross-section shapes were tested: Rectangular beams, T-beams, inverted T-beams (i.e. with the flange in tension) and slabs. Cylinders for compressive strength and modulus of rupture beams were also tested at about the same age as the other members. Each group of specimens will be described in more details in the following sections.

4.2.1 Cylinders and modulus of rupture beams

For each batch 18 cylinders and 18 beams were cast. The cylinders were the standard 6 in by 12 in (152 mm by 304 mm) and the cross section of the modulus of rupture beams is given in Fig. 4.1. These beams had overall dimensions of 89 mm by 115 mm by 400 mm and were loaded at their third points on a 345 mm span.

4.2.2 Rectangular beams

Eight beams of this shape were cast, four using low strength concrete (20 MPa) and four using high strength concrete (45 MPa). The identification R1 to R8 will be used for these beams. The length of the beams was 3.5 m and typical cross section dimensions are given in Fig. 4.1. The properties of the individual beams are summarized in Table 5.5.

4.2.3 T-beams and inverted T-beams

Five T-beams were cast, two using 20 MPa concrete and three using 45 MPa concrete. The identification T1 to T5 will be used for these beams. A typical cross-section is shown in Fig. 4.1. The same cross-section was used for the inverted T-beams as for the T-beams, the only difference being that the reinforcement was placed in the flange part of the beam. Five inverted T-beams were cast, two using 20 MPa concrete and three using 45 MPa concrete. The identification I1 to I5 will be used for the inverted T-beams. The length of both T-beams and inverted T-beams was 4.0 m. The properties of the individual T-beams are summarized in Table 5.7, and for the

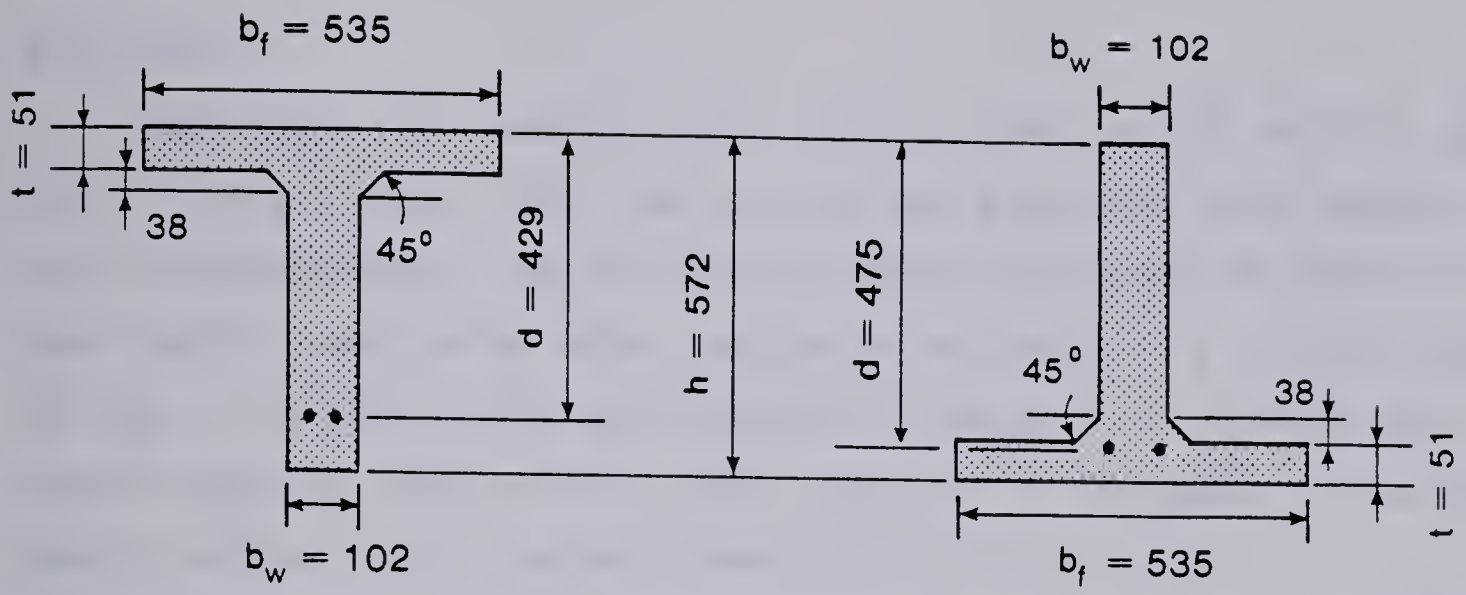

T-beam
Length = 4000 mm

I-beam
Length = 4000 mm

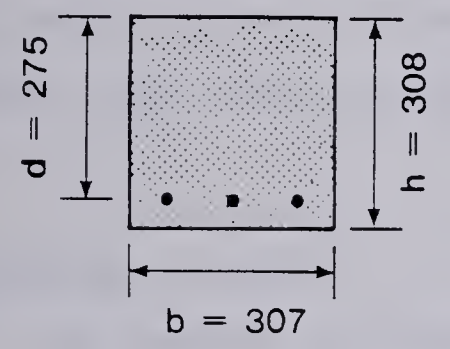

R-beam
Length = 3500 mm

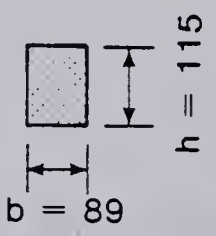

Modulus of Rupture Beam
Length = 400 mm

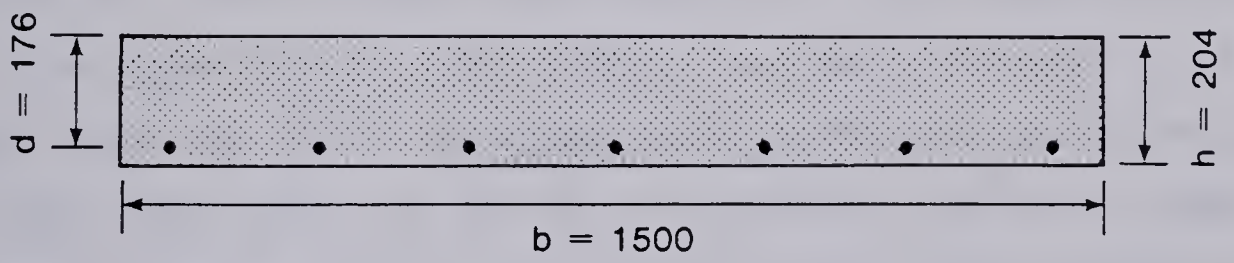

Slabs P and L
Length = 3000 mm

All Dimensions are mm
Scale 1 : 15

Figure 4.1 - Cross-section dimensions of test specimens.

I-beams in Table 5.9.

4.2.4 Slabs

Eight slabs were cast, two pairs using 20 MPa concrete and two pairs using 45 MPa concrete. Each pair of slabs had exactly the same amount and type of reinforcement. This was done in order to investigate the effect of a point load at centre on the slabs compared to the effect of a line load across the slab. The point loading case produced a distribution of moments about a section under the load that was roughly similar to the distribution of moments about a section through a spread footing adjacent to the column.

The identification P1 to P4 will be used for the slabs loaded with a point load, and L1 to L4 for the slabs loaded with a line load. The slabs were 3.0 m long and a typical cross-section is given in Fig. 4.1. The properties of the individual slabs are summarized in Table 5.11.

4.3 Curing procedures

All members were kept moist in the forms for one week. After that they were taken out of the forms and allowed to dry in the laboratory, where the relative humidity was approximately 50 per cent. The same procedure was used for the control cylinders and modulus of rupture beams for batches 1 and 2 (i.e. when the 20 MPa concrete was used). For batches 3 and 4, however, only half (9) of the cylinders and beams were cured this way, the rest were moist cured from the day of casting until the day of testing. This was done to get an indication of the effect of the short time moist-curing of the members, both on the degree of hydration and possibly also on the shrinkage stresses.

4.4 Loading apparatus and instrumentation

All members were loaded in a 1.4 million pound MTS machine (Material Testing System) under a controlled rate of loading. Loads were measured by a 25 kip capacity load cell sensitive to ±0.3% of the full rated capacity. The rate of loading was controlled using this load cell. Deflection was measured using electrical transducers (LVTD's). The maximum range for these transducers is 6 in (150 mm) and since some of the members deflected that much without breaking, the transducers had to be set to max range at the beginning of the test, losing some of the accuracy that is available at a smaller range. The minimum accuracy of the deflection readings was ±0.3 mm. Both load and deflection readings were taken automatically by a computer. In the following two sections, the test set-ups for the beams and slabs will be explained in more detail.

4.4.1 Beams

For all the beams (R, T, I) a third point loading system was used, the beams being simply supported at both ends. The deflection was measured at three points; at midspan and at the two loading points. The test set-up for the beams is shown in Fig. 4.2.

4.4.2 Slabs

Two types of loads were applied to the slabs. Half the slabs were loaded by a line load at midspan and the rest with a point load at centre. The slabs were simply supported at the ends and free at the sides. Deflections were measured on each side of the slabs at midspan. The test set-up for the slabs is shown in plan view in Fig. 4.3. To be able to investigate the order of crack formation in the slabs, several 10 mm wide by 200 mm long strips of brittle electrical conducting paint were painted on the bottom of each slab at the location shown in Fig. 4.3. A low voltage electrical current was sent through these strips. When a crack formed the current flow stopped, giving an indication of the time of crack formation.

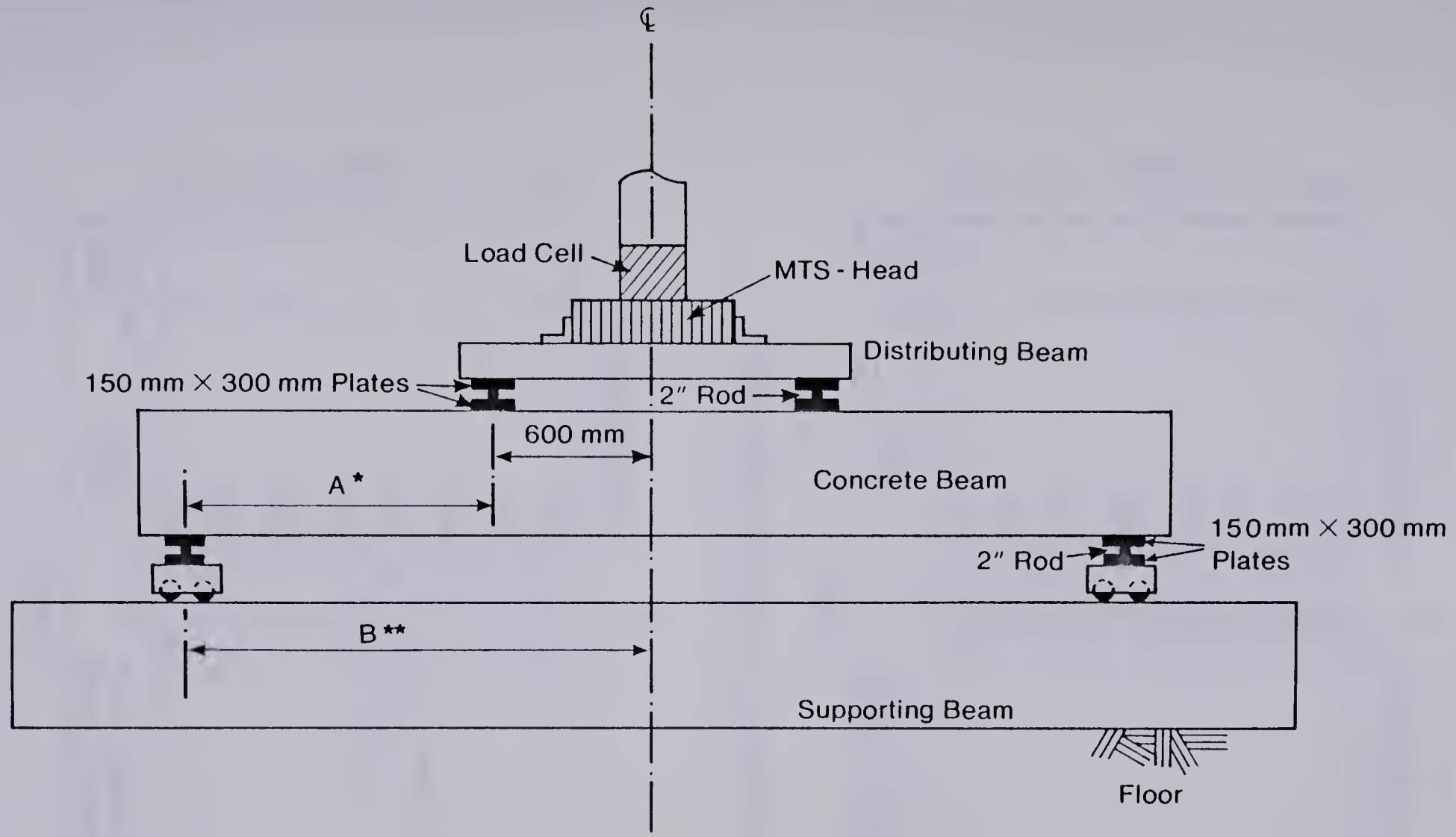

* For T and I beams A = 1200 mm
For R - beams A = 900 mm
** For T and I beams B = 1800 mm
For R - beams B = 1500 mm

Figure 4.2 – Test set-up for beams.

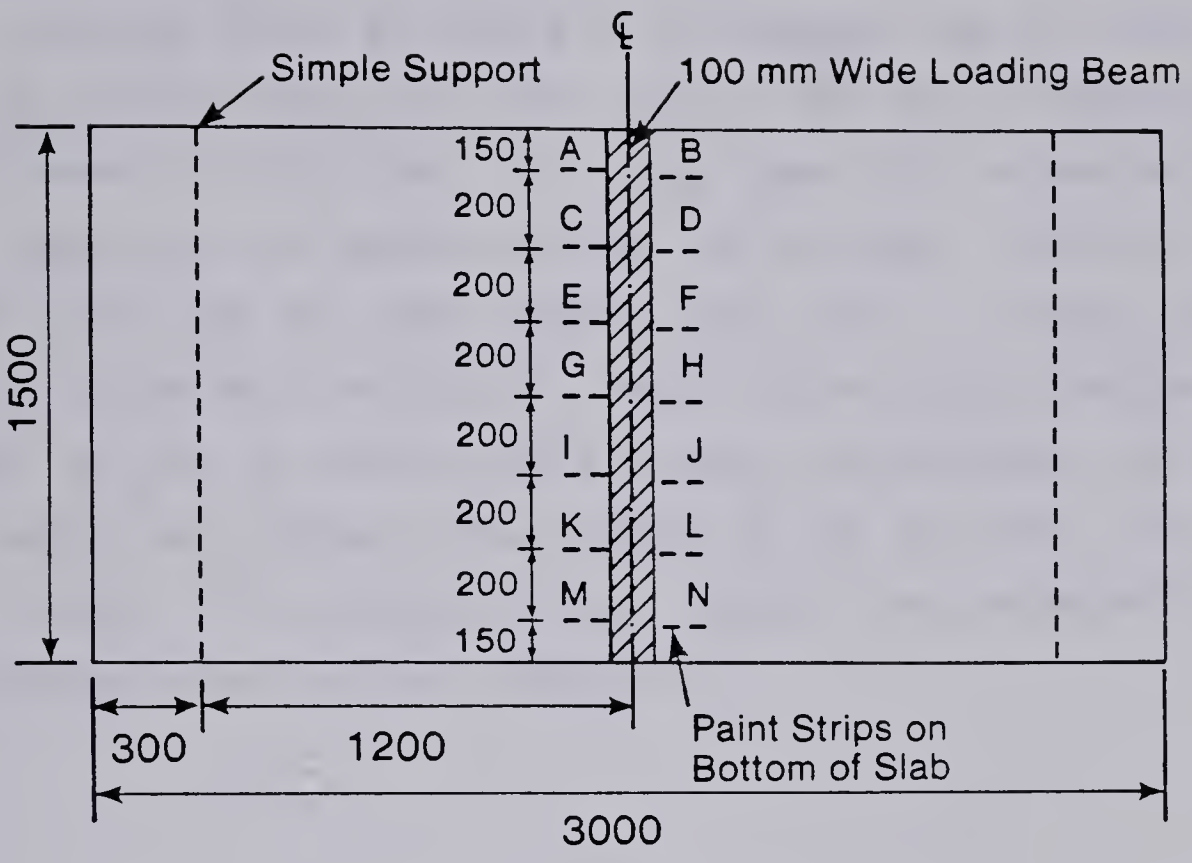

Plan View of Line Load Set-up

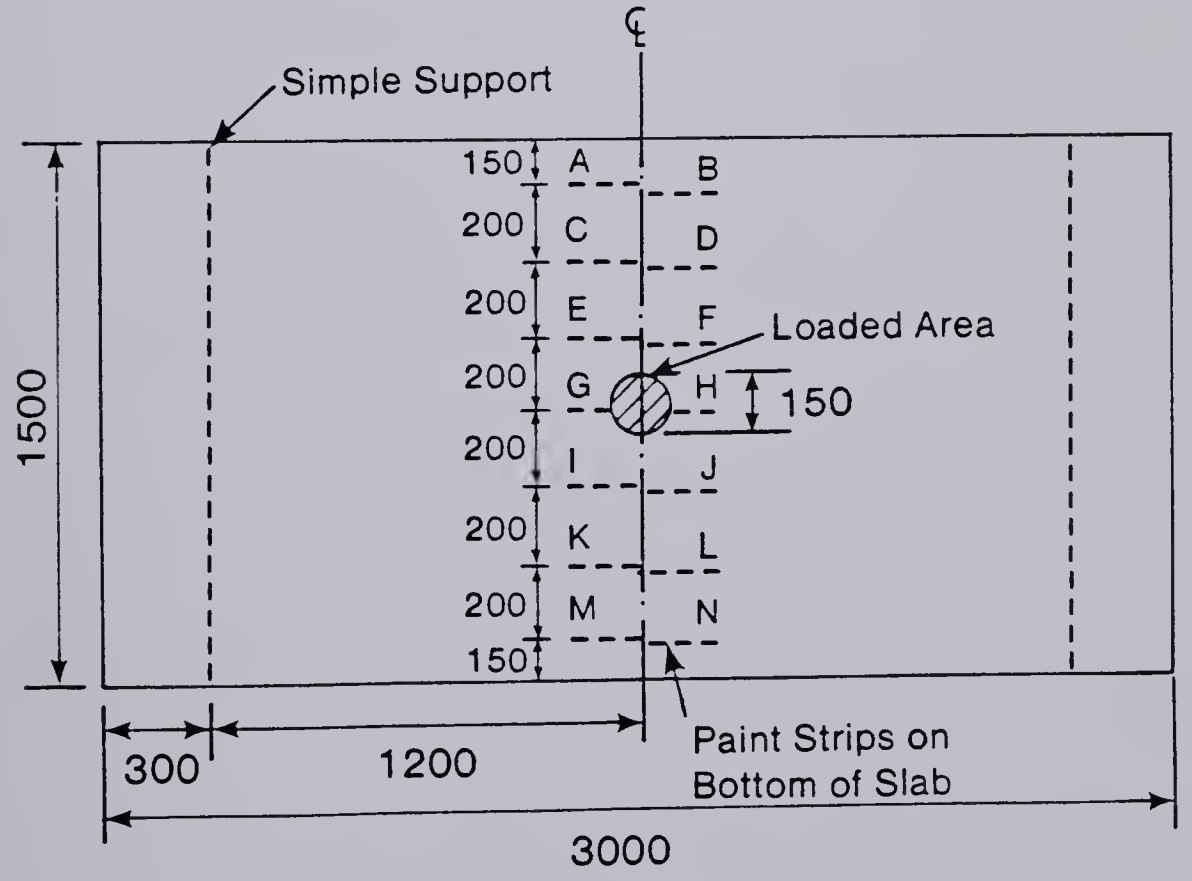

Plan View of Point Load Set-up

All dimensions are mm

Figure 4.3 – Test set-up for slabs

4.5 Testing procedures

As mentioned before, the loading of the members was at a fixed rate, controlled by the load cell in the MTS machine. The rate of loading ranged from 670 N/min to 1340 N/min. All readings were taken automatically by a computer, using up to 20 different channels for the slabs. The time of day was read every time the other readings were taken. Cracking generally occurred 30–50 min after the start of loading. Before cracking, readings were taken every 30 sec, but shortly before cracking was anticipated the interval between readings was changed to take readings as fast as possible, with about 2–3 sec intervals. This procedure closely monitored the load–deflection and load–time curves as can be seen in Appendix A.

5. TEST RESULTS

5.1 Presentation of test results

5.1.1 Reinforcing steel

Deformed (ribbed) reinforcing steel was used in all test specimens, the yield strength ranging from 371 MPa to 551 MPa. All reinforcing bars had a definite yield point. Table 5.1 gives the cross-sectional and material properties of the reinforcing bars used. Stress-strain curves for the different bars are presented in Fig. 5.1. The stress given is in all cases based on the measured bar areas, found by weighing the bars. The area of the 6 mm bar corresponded to a diameter of 6.6 mm. All the reinforcing bars were tested at a slow strain rate, giving approximately a static yield strength.

Table 5.1 — Cross-sectional and material properties of reinforcing bars.

Bar name	Nominal bar dia. (mm)	Heat No.	Area* (mm^2)	f_y (MPa)	f_{su} (MPa)	ε_{su} (%)**
ϕ6 mm	6	1	34.0	477	659	15
#4	12.7	3	124.0	488	712	17
#4	12.7	5	124.0	371	576	21
10M	11.3	2	98.0	551	765	15
10M	11.3	4	96.0	380	578	22

*The area was determined by weighing the bars.
**Approximate values.

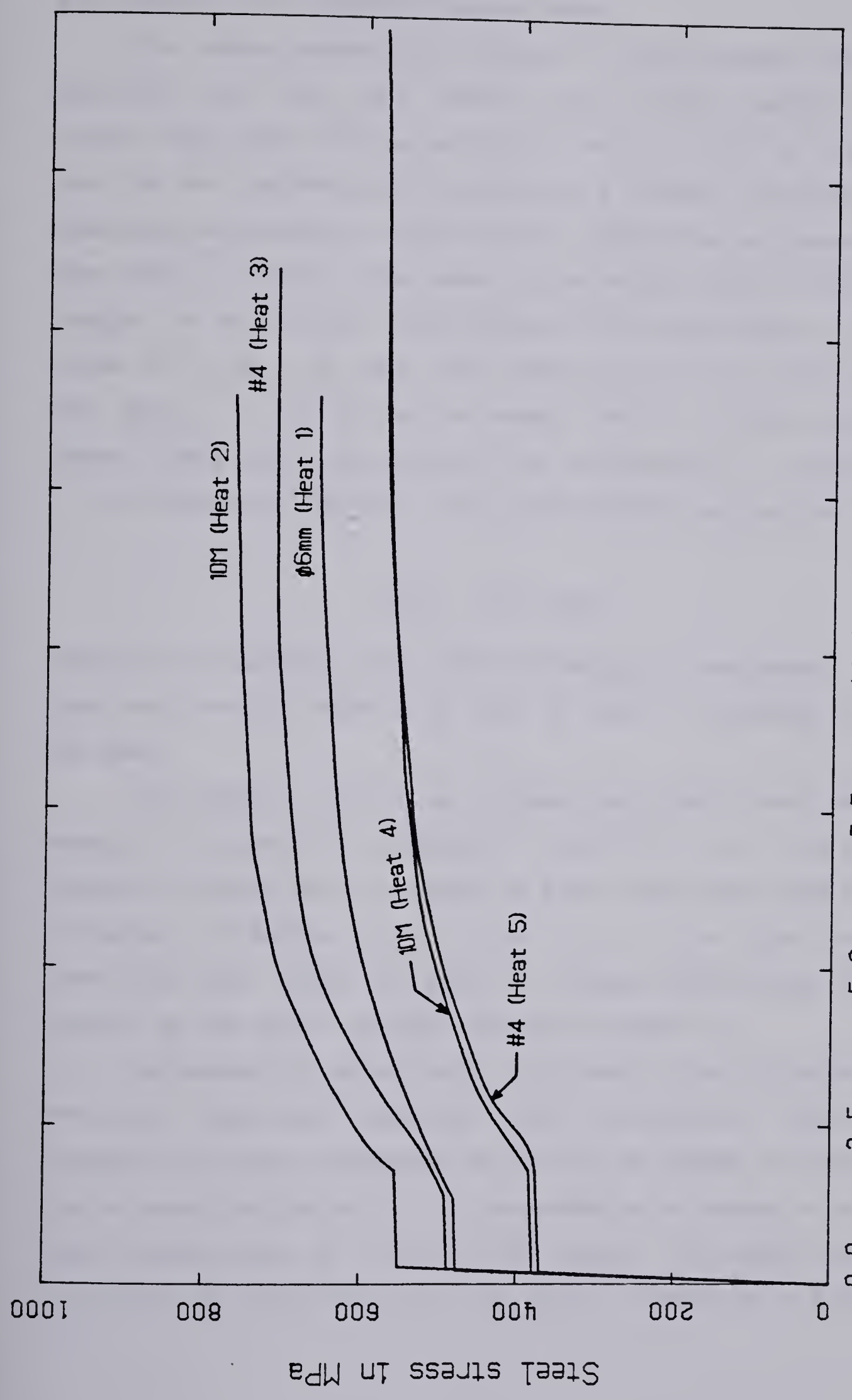

Figure 5.1 — Stress-strain curves for reinforcing bars.

5.1.2 Cylinders and modulus of rupture beams

The control cylinders and modulus of rupture beams were tested in accordance with CSA A23.2 "Methods of Test for Concrete". The data obtained from these tests was corrected in two ways: first for rate of loading, since the test specimens were stressed at a different rate than the control specimens; and second, for age at testing. Because the test specimens from a given batch of concrete were tested at ages ranging from 55 to 93 days, the strengths of the concrete were obtained from curves fitted to control tests carried out at 55 to 97 days. The loading rate for the control cylinders was 400 kN/min. To correct for the loading rate, Eqn. (2.25) was used. The applied loading rate in the cylinder tests corresponds to a stressing rate of R = 22 MPa/min (53 psi/sec). The correction factor thus becomes:

$$f_{C(15)} = 0.99 \cdot f_{C(22)} \tag{5.1}$$

where R = 15 MPa/min is the standard stressing rate (see section 2.4.1). Since the correction factor is so close to unity, no correction was made in this case.

For batches 1 and 2, six cylinders were tested each time and the average load registered. As explained in section 4.3, half of the cylinders and modulus of rupture beams in batches 3 and 4 were moist cured until the day of testing. For batches 3 and 4, three "dry" and three "moist" cylinders were tested each time. Table 5.2 gives the average ultimate loads, P_u , for the cylinders as well as the calculated compressive strength, f_c .

The modulus of rupture beams were loaded at the third points of a 345 mm span. They were loaded at a rate of 52 kN/min. Since the tensile strength of concrete is dependant on the rate of loading, a reference loading rate is chosen (see section 2.4.1) corresponding to an increase in extreme fibre stress (stressing rate) of 1 MPa/min (2.5 psi/sec). The applied loading rate in the modulus of rupture tests, ΔP = 52 kN/min, corresponds to a stressing rate of:

Table 5.2 — Compressive strength of control cylinders at different ages.

Batch 1	dry*	age (days)	76	86	97
		P_u (kN)	501.5	510.0	520.2
		f_c (MPa)	27.6	28.1	28.7
Batch 2	dry	age (days)	61	69	80
		P_u (kN)	488.7	490.8	494.9
		f_c (MPa)	26.9	27.0	27.3
Batch 3	dry	age (days)	64	70	92
		P_u (kN)	900.0	868.9	892.6
		f_c (MPa)	49.6	47.9	49.2
	moist**	P_u (kN)	973.0	962.3	993.7
		f_c (MPa)	53.6	53.0	54.8
Batch 4	dry	age (days)	55	66	78
		P_u (kN)	777.7	831.1	851.8
		f_c (MPa)	42.9	45.8	46.9
	moist	P_u (kN)	854.9	937.8	940.8
		f_c (MPa)	47.1	51.7	51.8

*dry means : cured at 50% R.H.
**moist means : cured at 100% R.H.

$$R = \frac{\Delta M}{W} = \frac{\Delta P/2 \cdot L/3}{1/6 \cdot b \cdot h^2} = 15 \text{ MPa/min (36 psi/sec)} \qquad (5.2)$$

where L = span length = 345 mm, b = 89 mm, h = 115 mm.

Using Eqn. (2.26) to correct for the difference in stressing rates, the reference strength now becomes:

$$f_{Ct(1)} = 0.89 \cdot f_{Ct(15)} \qquad (5.3)$$

where R = 1 MPa/min is the standard stressing rate.

The tensile strength, f_{ct} , (modulus of rupture) is calculated using the equation:

$$f_{ct} = \frac{M}{W} = \frac{(P_u/2)(L/3) + (1/8)\cdot w \cdot L^2}{(1/6)\, b \cdot h^2} \qquad (5.4)$$

where w is dead load per unit length of beam = 0.23 N/mm based on the specific weight of the concrete which was found to be γ_c = 22.5 kN/m³.
For batches 1 and 2, six beams were tested each time and the average strength calculated. For batches 3 and 4, three "dry" and three "moist" beams were tested each time. Table 5.3 gives the ultimate load, P_u , as well as the calculated average tensile strength of the modulus of rupture beams at different ages. The values of the tensile strength are rounded off to the nearest 0.05 MPa. The reference strength $f_{Ct(1)}$ is also given.

In Figure 5.2, the compressive strength of the concrete is plotted against age for all four batches. Using the given data-points and assuming that the development of the concrete strength follows Eqn. (2.34), a curve is fitted through each set. Although Eqn. (2.34) was probably derived for moist cured concrete only, the agreement between the test points and the computed strengths suggests that it is reasonable to assume that Eqn. (2.34) is also valid at 50% relative humidity. Using this assumption it can be seen in Fig. 5.2 that moist curing gives around 10% higher compressive strength at all ages than curing at 50% R.H. The strengths given by the curves in Fig. 5.2 were used in analyzing the test data.

In Figure 5.3, the flexural tensile strength (modulus of rupture) is plotted against age for all four batches. Assuming that the relationship

$$f_{ct} = K\cdot\sqrt{f_c} \qquad (5.5)$$

holds for all ages, where K is a constant for a given batch, curves are fitted through each data set. The constant K varies from 0.64 to 0.73 for the "dry" cured concrete, with an average of 0.69. For the moist cured concrete K is

Table 5.3 — Flexural tensile strength (modulus of rupture) of control beams at different ages.

Batch 1	dry*	age (days)	76	86	97
		P_u (N)	14290	13695	15548
		f_{ct} (MPa)	4.20	4.05	4.60
		$f_{Ct(1)}$ (MPa)	3.75	3.60	4.10
Batch 2	dry	age (days)	61	69	80
		P_u (N)	11079	13102	13878
		f_{ct} (MPa)	3.25	3.85	4.10
		$f_{Ct(1)}$ (MPa)	2.90	3.45	3.65
Batch 3	dry	age (days)	66	73	92
		P_u (N)	17031	17846	17550
		f_{ct} (MPa)	5.00	5.25	5.15
		$f_{Ct(1)}$ (MPa)	4.45	4.65	4.60
	moist**	P_u (N)	23229	21776	22110
		f_{ct} (MPa)	6.85	6.40	6.50
		$f_{Ct(1)}$ (MPa)	6.10	5.70	5.80
Batch 4	dry	age (days)	56	66	78
		P_u (N)	17105	19329	19477
		f_{ct} (MPa)	5.05	5.70	5.75
		$f_{Ct(1)}$ (MPa)	4.50	5.10	5.10
	moist	P_u (N)	22665	21627	23110
		f_{ct} (MPa)	6.65	6.35	6.80
		$f_{Ct(1)}$ (MPa)	5.90	5.65	6.05

*dry means : cured at 50% R.H.
**moist means : cured at 100% R.H.

0.80 and 0.83 respectively. The value of 0.69 corresponds with the value obtained by Mirza et al (1979), see Eqn. (2.33).

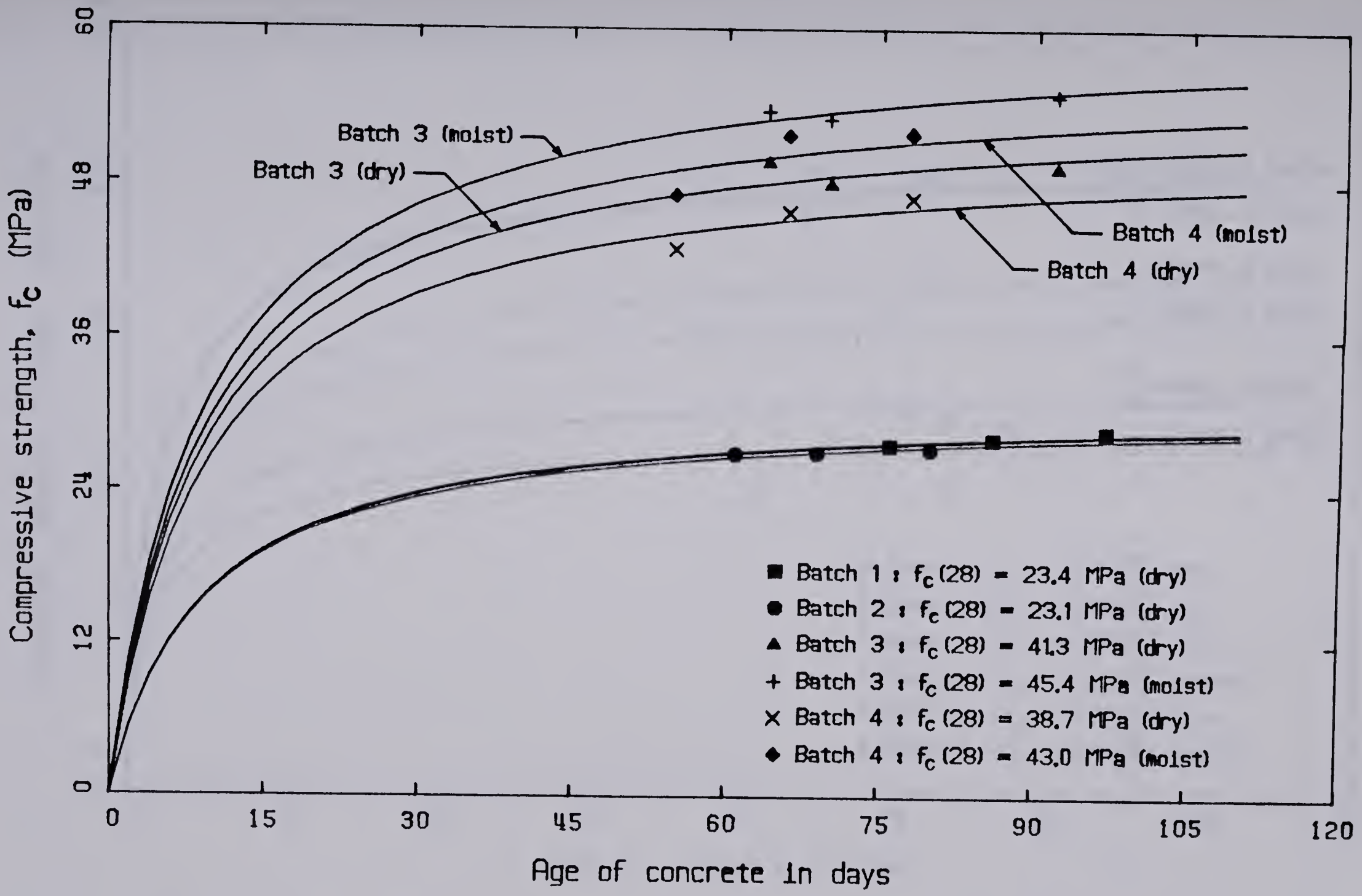

Figure 5.2 — Compressive strength of concrete at different ages.

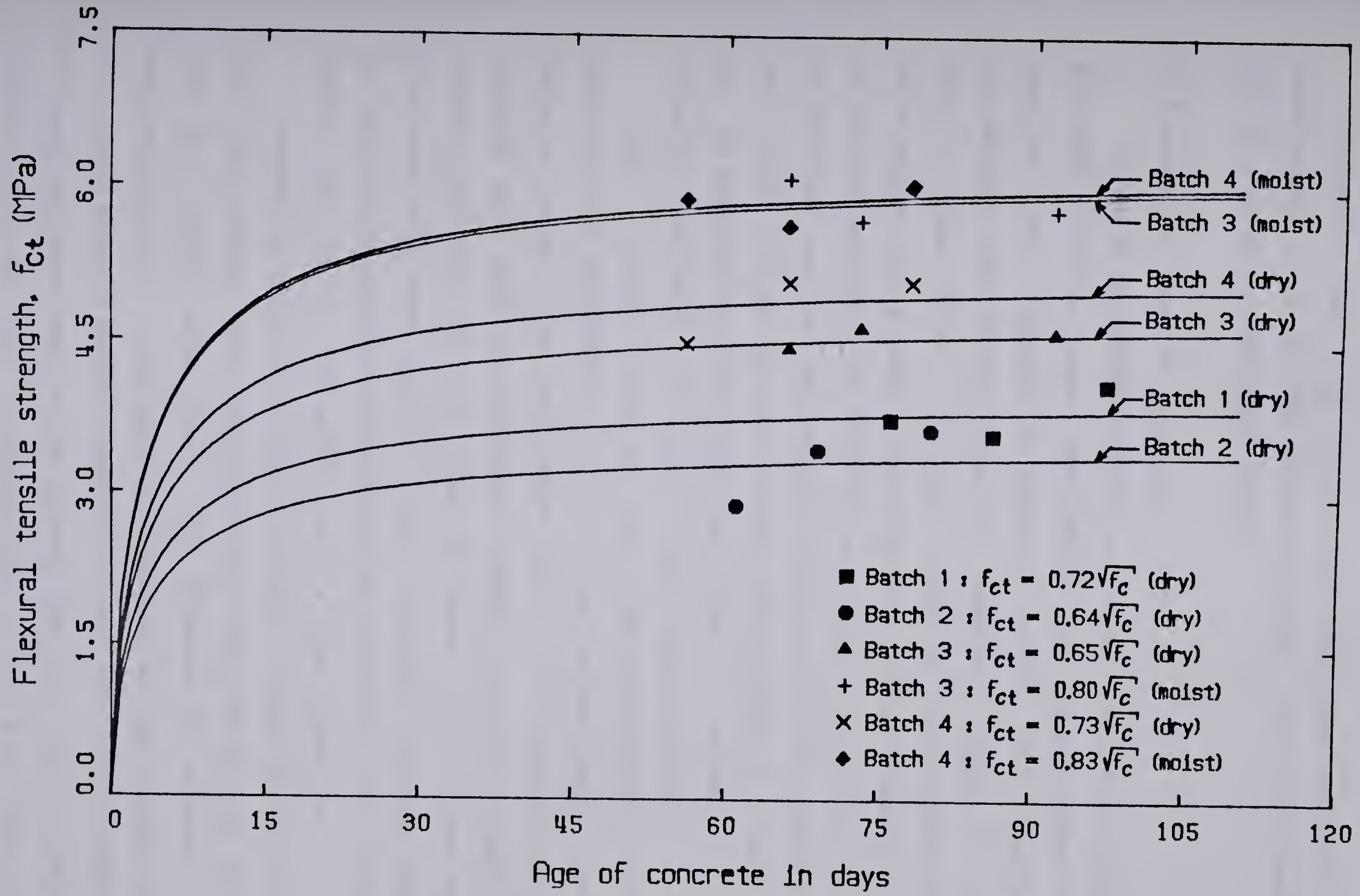

Figure 5.3 — Flexural tensile strength of concrete at different ages.

It can be seen in Fig. 5.3 that moist curing gives around 25% higher tensile strength at all ages than curing at 50% R.H. This is considerably more than the 10% gain in compressive strength.

5.1.3 Rectangular beams (R - beams)

A total of 8 rectangular beams were tested. The rate of loading was 670 N/min for these beams. Load-deflection and load-time curves for each beam are given in Appendix A, Figures A.1 to A.8. Two typical sets of load-deflection and load-time curves are presented in Figures 5.4 and 5.5. When a member fails by, for example, fracture of the reinforcing bars the failure happens very suddenly. Because of this, deflection measurements could not be taken accurately after failure and are therefore not shown on the plots. On the other hand, this load drop-off can be shown on the load-time plots. This is done in Fig. 5.4 for beam R2 which failed suddenly at a load of 41.6 kN. The loading on beam R8 (Fig.5.5) was stopped at a deflection of 125 mm without the beam failing. In this case no load drop-off occurred.

When the member cracks, the slope of the load-deflection plot changes (point A on the load-deflection plots). The next definite change in the slope occurs at yielding of the reinforcement, point B. The ultimate load is then registered, either when the reinforcement fractures, the concrete crushes or at excessive deflections (125 mm). Beam R8, shown in Fig. 5.5, had about 3 times more reinforcement than R2 (Fig. 5.4). This leads to a smaller change in the slope of the load-deflection curve for R8 than for R2 when the member cracks. It also, obviously, allows R8 to carry a higher ultimate load.

Another big difference in those two beams was that R2 was reinforced with a high strength, rather brittle reinforcing steel while R8 was reinforced with low strength ductile steel. This difference is reflected in the load-deflection plots. All the beams reinforced with the high strength steel (R1 to R4) failed before a mid-span deflection of about 100 mm was reached, but the beams reinforced with the low strength steel (R5 to R8) all reached a deflection of at least 125 mm before failing. It was also noticed that the

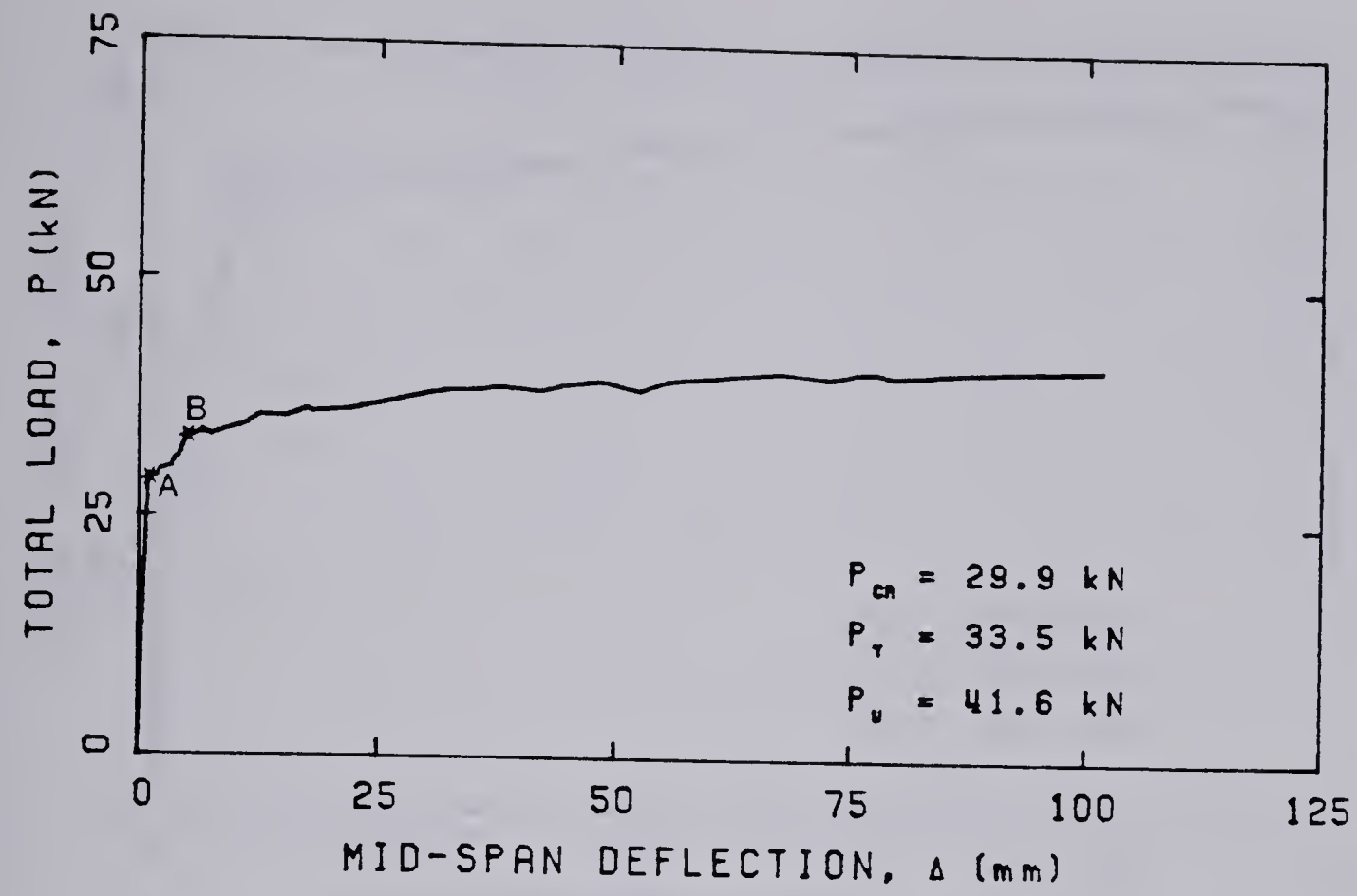

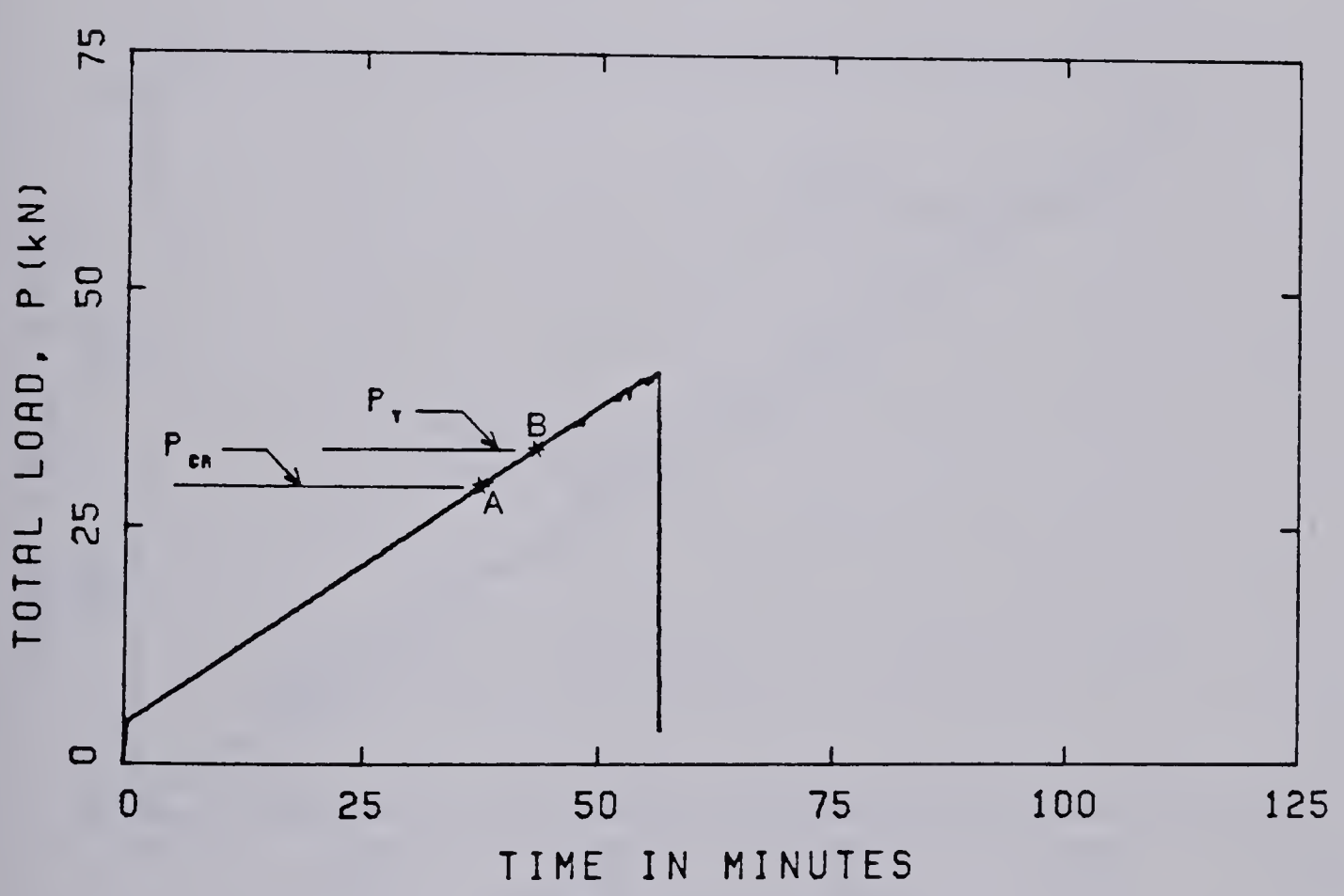

Figure 5.4 — Load-deflection and load-time curves for beam R2.

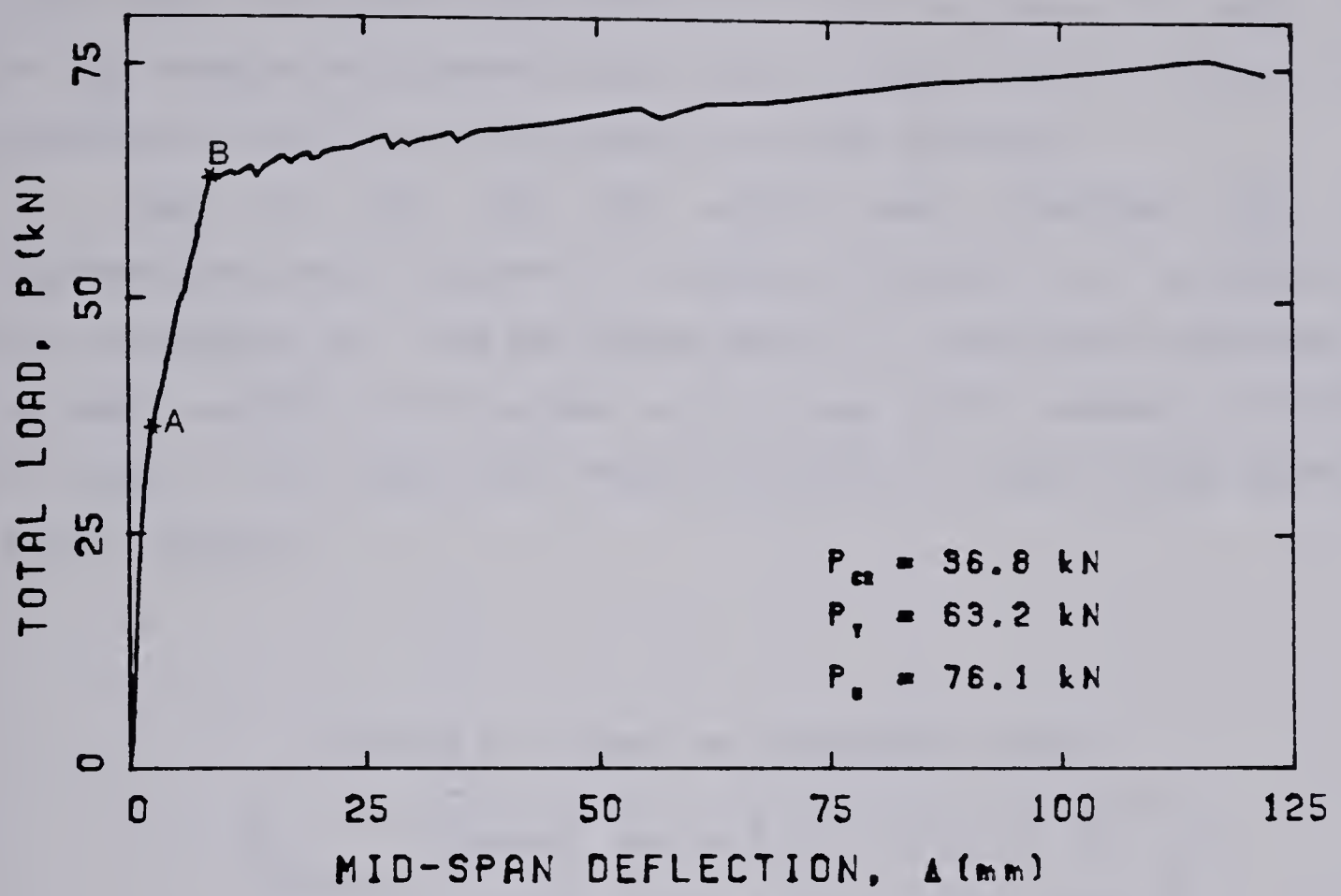

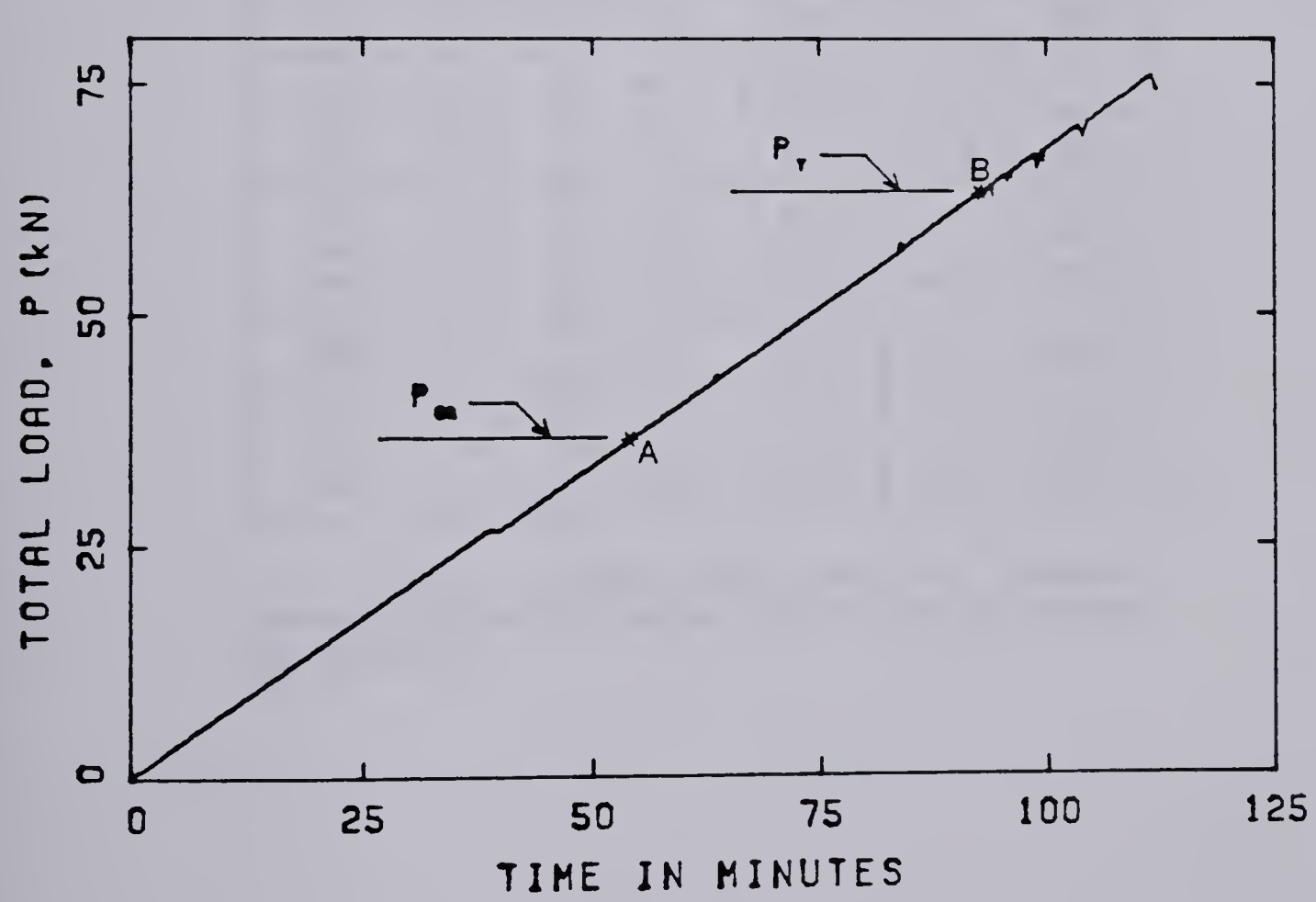

Figure 5.5 — Load-deflection and load-time curves for beam R8.

crack widths and spacing were different for these two cases; the beams with the high strength reinforcement having fewer but wider cracks. In Fig. 5.6 the approximate crack locations for beams R2 and R8 are shown.

Table 5.4 gives the total applied loads determined from the load-deflection data at the time of cracking of concrete, P_{cr} , at yielding of the reinforcement, P_y , and the ultimate load, P_u . Also given in this table are the batch numbers of the concrete and the ages of the members at the time of testing. Cross sectional and material properties for each individual beam are given in Table 5.5.

Table 5.4 — Loads on rectangular beams.

Member	Batch No.	Age in days	P_{cr} (kN)	P_y (kN)	P_u (kN)
R1	1	77	28.5	33.2	39.1
R2	2	61	29.9	33.5	41.6
R3	2	60	27.8	37.2	45.6
R4	1	76	31.5	--	31.5
R5	4	58	31.5	44.8	55.4*
R6	4	55	26.8	30.3	36.4*
R7	3	64	29.8	41.1	49.6*
R8	3	63	36.8	63.2	76.1*

*Loading stopped when mid-span deflection reached 125 mm (5 inches). Beam was still carrying the load given.

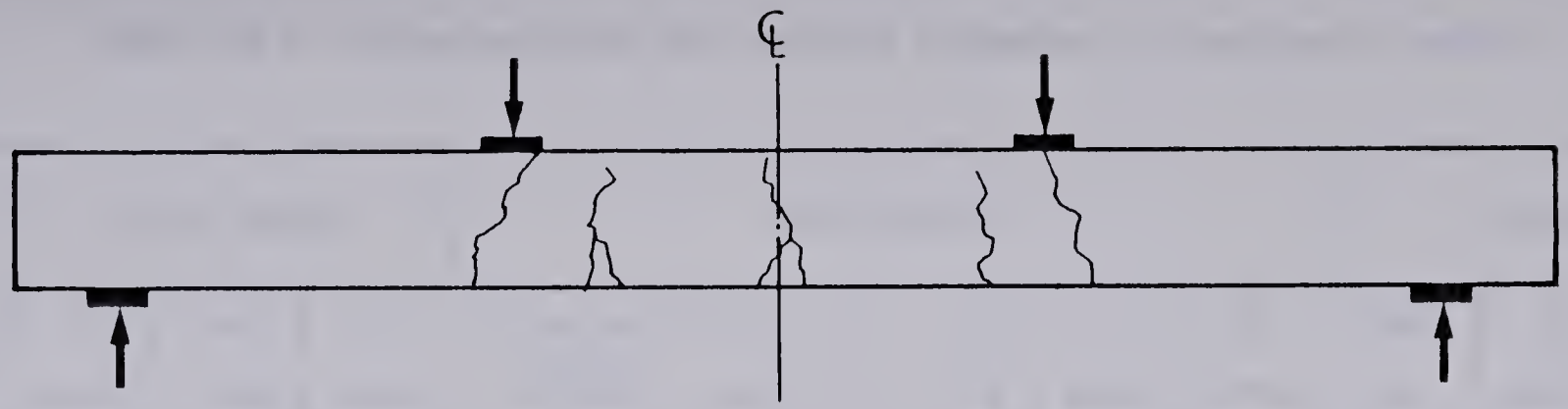

Beam R2: 1 - 10M bar (f_y = 551 MPa)

Deflection at failure ≅ 100 mm

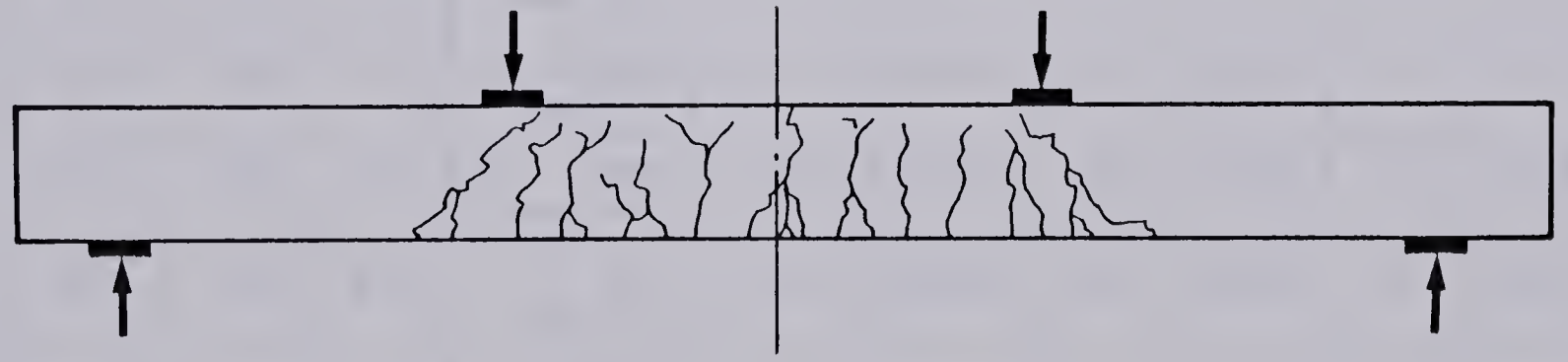

Beam R8: 3 - 10M bars (f_y = 380 MPa)

Deflection at failure > 125 mm

Figure 5.6 – Approximate locations of cracks in beams R2 and R8 at failure.

Table 5.5 — Cross-sectional and material properties of rectangular beams.

	Cross section			Reinforcement					Concrete		
Member	b (mm)	h (mm)	d (mm)	Type and number of bars	A_s (mm^2)	$\rho = \frac{A_s}{b \cdot d}$	f_y (MPa)	f_{su} (MPa)	Batch No	f_c (MPa)*	f_{ct} (MPa)*
R1	308	310	276	3 – ϕ6mm Heat 1	102	0.00120	477	659	1	27.8	3.80
R2	309	310	275	1 – 10M Heat 2	98	0.00115	551	765	2	26.7	3.31
R3	306	309	275	1 – #4 Heat 3	124	0.00147	488	712	2	26.7	3.31
R4	308	309	274	2 – ϕ6mm Heat 1	68	0.00081	477	659	1	27.8	3.80
R5	306	308	270	2 – 10M Heat 4	192	0.00232	380	578	4	44.4	4.86
R6	307	310	278	1 – #4 Heat 5	124	0.00145	371	576	4	44.1	4.85
R7	306	308	270	1 – 10M+ 2 – ϕ6mm Heats 4+1	164	0.00198	420	612	3	48.1	4.51
R8	306	307	270	3 – 10M Heat 4	288	0.00349	380	578	3	48.0	4.50

*These are from lines fitted to cylinder and modulus of rupture tests using Eqn. (2.34) and represent strengths at the age beams were tested.

5.1.4 T - beams

A total of 5 T - beams were tested. The loading rate was 670 N/min. Load-deflection and load-time curves for these beams are given in Appendix A, Figures A.9 To A.13. Beams T1 and T2 were reinforced with high strength steel and showed the same tendancy as the R-beams for few wide cracks. Beams T3 to T5 on the other hand were reinforced with lower strength steel and showed more ductility. Table 5.6 gives the total applied loads at the time of cracking of concrete, P_{cr} , at yielding of the reinforcement, P_y , and the ultimate load, P_u . It also gives the batch numbers of the concrete and the ages of the members at the time of testing. Cross sectional and material properties for each individual beam are given in Table 5.7.

Table 5.6 — Loads on T - beams.

Member	Batch No.	Age in days	P_{cr} (kN)	P_y (kN)	P_u (kN)
T1	2	68	22.1	37.3	47.4
T2	1	83	30.8	--	32.2
T3	4	63	31.0	48.6	58.2
T4	4	64	35.3	--	40.2*
T5	4	64	31.8	--	35.3*

*Loading stopped when mid-span deflection reached 125 mm (5 inches). Beam was still carrying the load given.

5.1.5 Inverted T-beams (I - beams)

A total of 5 inverted T - beams, referred to as I - beams, were tested. The loading rate was 1340 N/min for these beams. Load-deflection and load-time curves are given in Appendix A, Figures A.14 to A.18. Beams

Table 5.7 — Cross-sectional and material properties of T - beams.

	Cross section					Reinforcement					Concrete		
Member	b_w (mm)	h (mm)	b_f (mm)	t (mm)	d (mm)	Type and number of bars	A_s (mm^2)	$\rho_w = \frac{A_s}{b_w \cdot d}$	f_y (MPa)	f_{su} (MPa)	Batch No	f_c (MPa)*	f_{ct} (MPa)*
T1	101	513	532	52	430	1 - 10M Heat 2	98	0.00226	551	765	2	27.1	3.33
T2	104	512	537	50	431	2 - ϕ6mm Heat 1	68	0.00152	477	659	1	28.1	3.82
T3	102	510	532	51	427	2 - 10M Heat 4	192	0.00441	380	578	4	44.9	4.89
T4	104	514	538	53	429	1 - #4 Heat 5	124	0.00278	371	576	4	45.0	4.90
T5	103	512	535	52	429	1 - 10M Heat 4	96	0.00217	380	578	4	45.0	4.90

*These are from lines fitted to cylinder and modulus of rupture tests using Eqn. (2.34) and represent strengths at the age beams were tested.

I1 and I2 both failed by crushing of the web at about the same time as the first flexural cracks formed. In these beams the load after cracking never reached the cracking load. These must be considered as brittle failures although the deflections at failure were 80 to 120 mm. These two specimens were the only ones to fail by crushing of the concrete. Table 5.8 gives the total applied loads at the time of cracking, P_{Cr} , at the yielding of reinforcement, P_y , and the ultimate load, P_u . It also gives the batch numbers of the concrete and the ages of the members at the time of testing. Cross sectional and material properties for each individual beam are given in Table 5.9. The reinforcement ratio given is ρ_w, based on the web thickness, not the flange width.

Table 5.8 — Loads on I - beams.

Member	Batch No.	Age in days	P_{cr} (kN)	P_y (kN)	P_u (kN)
I1	1	80	56.5	--	56.5
I2	2	70	49.8	--	49.8
I3	3	77	40.7	78.2	96.3
I4	3	77	45.2	53.7	64.6*
I5	3	78	43.4	94.5	108.6*

*Loading stopped when the mid-span deflection reached 125 mm (5 inches). Beam was still carrying the load given.

5.1.6 Slabs

A total of 8 slabs were tested, 4 using a line load and 4 using a point load. The rate of loading was 1020 N/min for the slabs. Load-deflection and load-time curves for the slabs are given in Appendix A, Figures A.19 to A.26.

Table 5.9 — Cross-sectional and material properties of inverted T - beams (I - beams).

	Cross section					Reinforcement					Concrete		
Menber	b_w (mm)	h (mm)	b_f (mm)	t (mm)	d (mm)	Type and number of bars	A_s (mm^2)	$\rho_w = \frac{A_s}{b_w \cdot d}$	f_y (MPa)	f_{su} (MPa)	Batch No.	f_c (MPa)*	f_{ct} (MPa)*
I1	101	512	528	51	478	1 - #4 Heat 3	124	0.00257	488	712	1	27.9	3.80
I2	101	512	530	51	480	3 - ϕ6mm Heat 1	102	0.00210	477	659	2	27.2	3.34
I3	104	510	538	51	472	3 - 10M Heat 4	288	0.00587	380	578	3	49.1	4.56
I4	102	510	534	51	468	2 - 10M Heat 4	192	0.00402	380	578	3	49.1	4.56
I5	102	510	531	51	467	1 - 10M+ 2 - #4 Heats 4+5	344	0.00722	374	577	3	49.2	4.56

*These are from lines fitted to cylinder and modulus of rupture tests using Eqn. (2.34) and represent strengths at the age beams were tested.

In Figures 5.7 and 5.8 two typical load-deflection and load-time curves are given (slabs L4 and P4). Points A to N on the curves represent the fracture of the paint strips shown earlier (Fig. 4.3), i.e. paint strip E broke at the load shown by point E on the plots. By following the letters in Fig. 4.3 one can see the order of crack formation in the slabs. Table 5.10 gives the total applied loads at the time of cracking, P_{cr} , at yielding of the reinforcement, P_y , and the ultimate load the slabs could take, P_u . It also gives the batch numbers and the ages of the slabs at the time of testing. Cross sectional and material properties of the slabs are given in Table 5.11.

Table 5.10 — Loads on slabs.

Member	Batch No.	Age in days	P_{cr} (kN)	P_y (kN)	P_u (kN)
L1	1	91	48.2	57.7	63.3
P1	1	93	53.0	55.9	66.3
L2	2	75	45.9	48.3	52.2
P2	2	77	47.2	--	50.9
L3	3	84	53.6	80.4	109.8*
P3	3	83	52.2	87.6	103.1
L4	4	76	48.1	62.2	78.5
P4	4	77	45.5	58.9	73.9

*Loading stopped when the mid-span deflection reached 125 mm (5 inches). Slab was still carrying the load given.

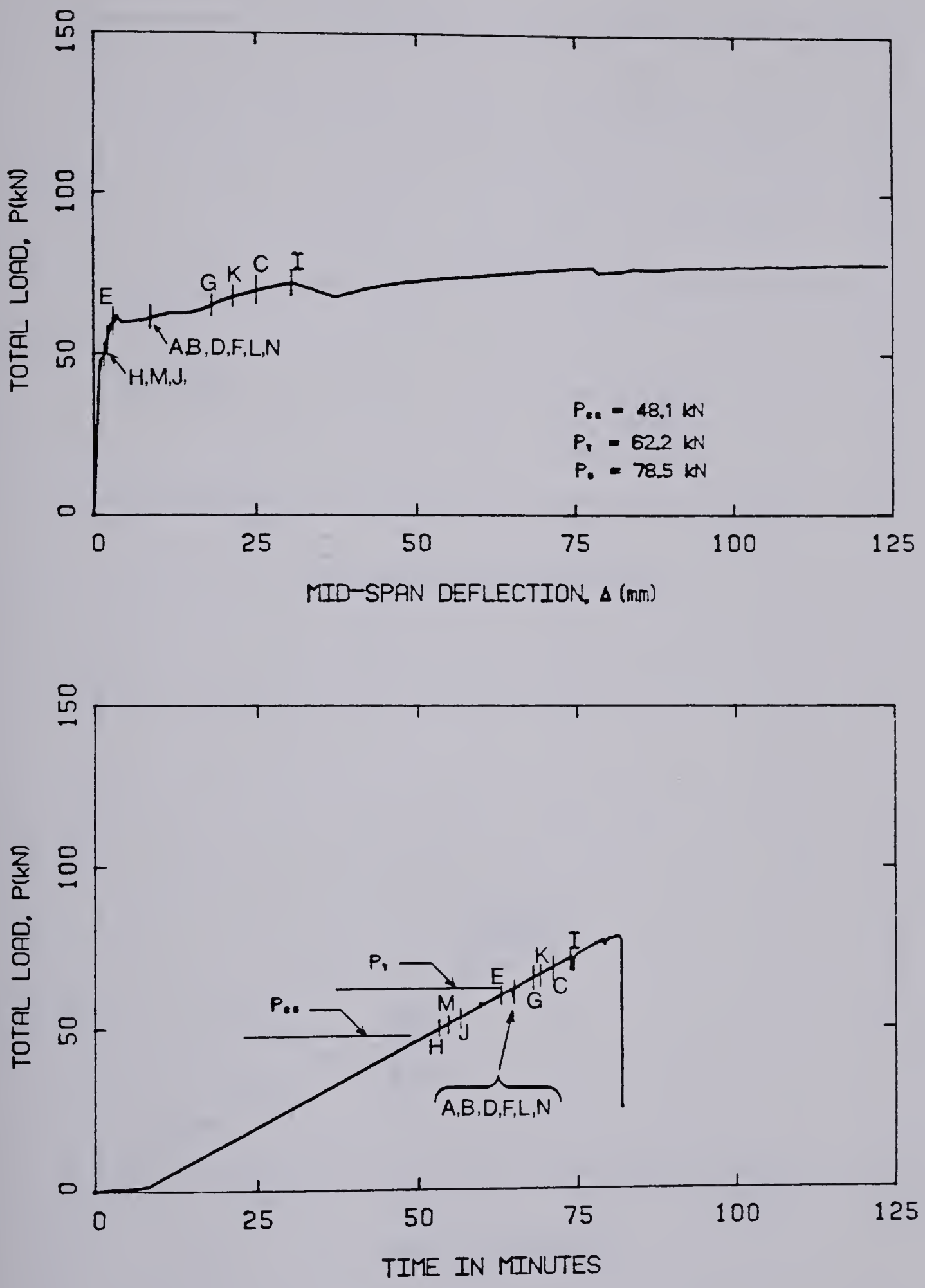

Figure 5.7 — Load-deflection and load-time curves for slab L4, showing the order of crack formation.

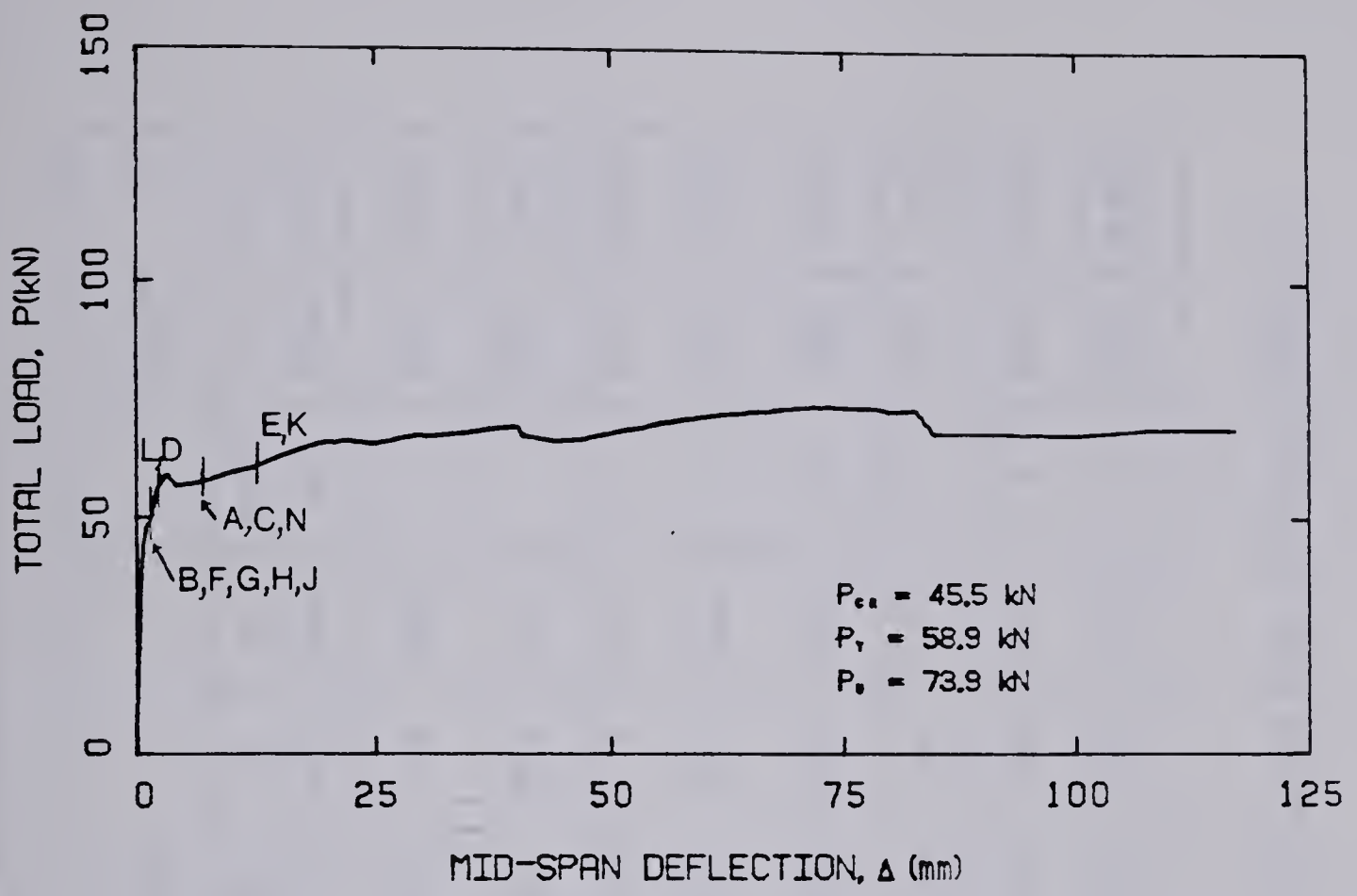

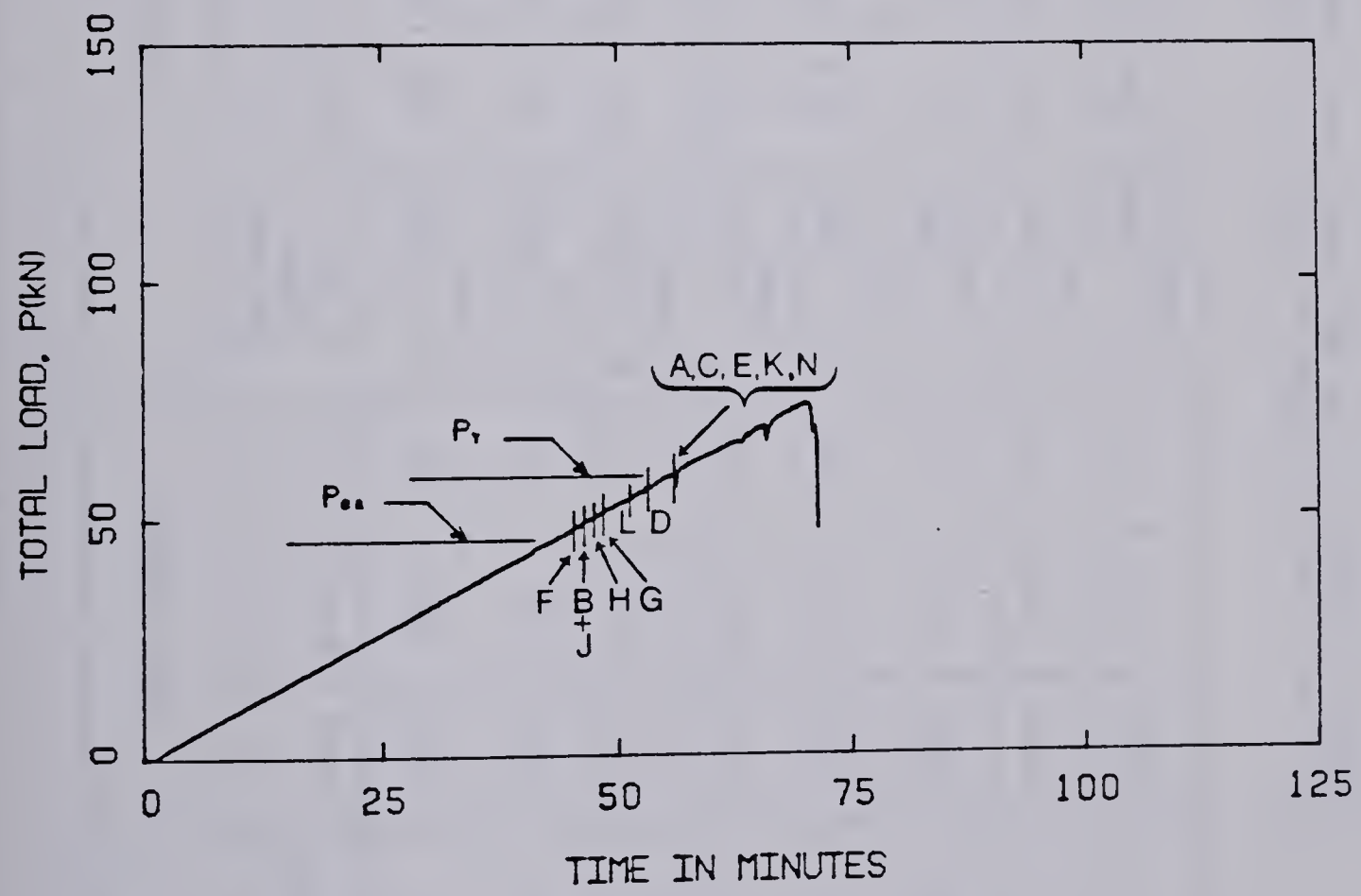

Figure 5.8 — Load-deflection and load-time curves for slab P4, showing the order of crack formation.

Table 5.11 — Cross-sectional and material properties of slabs.

	Cross section			Reinforcement					Concrete		
Member	b (mm)	h (mm)	d (mm)	Type and number of bars	A_s (mm^2)	$\rho = \frac{A_s}{b \cdot d}$	f_y (MPa)	f_{su} (MPa)	Batch No.	f_c (MPa)*	f_{ct} (MPa)*
L1	1500	202	175	10 - ϕ6mm Heat 1	340	0.00130	477	659	1	28.3	3.83
P1	1500	205	178	10 - ϕ6mm Heat 1	340	0.00127	477	659	1	28.4	3.84
L2	1502	204	177	8 - ϕ6mm Heat 1	272	0.00102	477	659	2	27.4	3.35
P2	1502	203	176	8 - ϕ6mm Heat 1	272	0.00103	477	659	2	27.5	3.36
L3	1502	200	173	7 - 10M Heat 4	672	0.00259	380	578	3	49.6	4.58
P3	1504	204	175	7 - 10M Heat 4	672	0.00255	380	578	3	49.5	4.57
L4	1503	206	178	5 - 10M Heat 4	480	0.00179	380	578	4	46.0	4.95
P4	1505	202	173	5 - 10M Heat 4	480	0.00184	380	578	4	46.0	4.95

*These are from lines fitted to cylinder and modulus of rupture tests using Eqn. (2.34) and represent strengths at the age beams were tested.

5.2 Discussion of test results

5.2.1 Comparison of calculated and observed cracking moments

In order to use the previously calculated reference tensile strength of the modulus of rupture beams, one must adjust the strength for the loading rate used on the test specimens. The load was applied on the rectangular beams at a rate of 670 N/min, which corresponds to an elastically computed increase in the extreme fibre stress of 0.06 MPa/min or 0.15 psi/sec before cracking. The correction factor for the R-beams thus becomes, using Eqn. (2.26):

$$f_{Ct(0.06)} = 0.87 \cdot f_{ct(1)} \qquad (5.6)$$

For the T-beams, the loading rate was also 670 N/min, giving a stressing rate of 0.07 MPa/min. The correction factor for the T-beams then becomes:

$$f_{Ct(0.07)} = 0.88 \cdot f_{ct(1)} \qquad (5.7)$$

The loading on the I-beams was 1340 N/min, giving a stressing rate of 0.07 MPa/min. The correction factor for the I-beams therefore is the same as for the T-beams. All the slabs, except L1 and P1, were loaded at a rate of 1020 N/min, giving a stressing rate of 0.06 MPa/min and had the same correction factor as the R-beams. For slabs LI and P1 the correction factor is:

$$f_{Ct(0.14)} = 0.91 \cdot f_{ct(1)} \qquad (5.8)$$

Using the equations in Chapter 3, the theoretical moments at cracking of concrete, yielding of reinforcement and the ultimate moments are calculated. These are compared to the observed values in Table 5.12 for the rectangular beams. Similar comparison is made for the T-beams and I-beams in Table 5.13, and for the slabs in Table 5.14. Shrinkage stresses in the rectangular beams were estimated in Chapter 3.

Table 5.12 — Calculated and observed moment capacities of rectangular beams.

	Cracking moments (kN·m)				Yielding moments (kN·m)			Ultimate moments (kN·m)		
Member	$M_{cr,cal}$			$M_{cr,obs}$	$M_{y,cal}$		$M_{y,obs}$	$M_{u,cal}$		$M_{u,obs}$
	Using I_{tr} and f_{ct}	Using I_g and f_{ct}	Using I_{tr} and $f_{ct,mod}$*		CSA–ACI (M_n)**	Str. line theory		CSA–ACI (M_n)***	Strain comp.	
R1	16.6	16.3	15.2	15.2	13.3	12.8	17.3	18.2	--	20.0
R2	14.6	14.2	12.4	15.9	14.6	14.2	17.5	20.2	--	21.1
R3	14.4	14.0	12.2	14.9	16.4	15.8	19.1	23.7	--	22.9
R4	16.4	16.1	14.9	16.6	8.8	8.6	--	12.1	--	$M_{cr,obs}$
R5	21.1	20.5	17.8	16.6	19.5	18.6	22.6	(29.4)	27.0	27.3
R6	21.2	20.7	17.7	14.5	12.7	12.2	16.0	(19.6)	18.9	18.8
R7	19.5	19.0	16.6	15.8	18.4	17.6	20.9	(26.7)	24.9	24.7
R8	19.7	18.8	16.7	19.0	29.1	27.6	30.8	(43.8)	37.3	36.6

**Based on f_y
***Based on f_{su}

*$f_{ct,mod} = f_{ct} - \sigma_{shr}$

Table 5.13 — Calculated and observed moment capacities of T-beams and inverted T-beams.

	Cracking moments (kN·m)			Yielding moments (kN·m)			Ultimate moments (kN·m)		
Member	$M_{cr,cal}$		$M_{cr,obs}$	$M_{y,cal}$		$M_{y,obs}$	$M_{u,cal}$		$M_{u,obs}$
	Using I_{tr} and f_{ct}	Using I_g and f_{ct}		CSA–ACI $(M_n)^*$	Str. line theory		CSA–ACI $(M_n)^{**}$	Strain comp.	
T1	18.3	17.7	15.9	22.6	21.8	25.0	31.0	--	31.0
T2	21.1	20.7	21.1	13.8	13.3	--	18.9	--	21.9
T3	27.2	25.9	21.2	30.5	28.9	31.8	(45.8)	37.5	37.5
T4	27.7	26.9	23.8	19.5	18.6	--	(30.0)	26.6	26.7
T5	27.1	26.5	21.7	15.5	14.8	--	(23.4)	21.7	23.8
I1	36.5	36.1	36.5	28.2	27.1	--	(40.6)	35.0	$M_{cr,obs}$
I2	31.9	32.0	32.5	22.8	22.0	--	(31.3)	27.9	$M_{cr,obs}$
I3	45.1	42.7	27.0	50.3	47.0	49.5	(75.4)	58.6	60.4
I4	44.0	44.9	29.7	33.5	31.7	34.8	(50.5)	42.6	41.4
I5	44.6	43.8	28.6	58.1	54.6	59.3	(88.1)	65.0	67.8

*Based on f_y
**Based on f_{su}

Table 5.14 — Calculated and observed moment capacities of slabs.

Member	Cracking moments (kN·m/m)			Yielding moments (kN·m/m)			Ultimate moments (kN·m/m)		
	$M_{cr,cal}$		$M_{cr,obs}$	$M_{y,cal}$		$M_{y,obs}$	$M_{u,cal}$		$M_{u,obs}$
	Using I_{tr} and f_{ct}	Using I_g and f_{ct}		CSA–ACI (M_n)**	Str. line theory		CSA–ACI (M_n)***	Strain comp.	
L1	24.1	23.7	22.5	18.7	18.0	26.3	25.7	--	28.6
P1	24.9	24.5	27.6*	19.0	18.3	25.6	26.1	--	29.8
L2	20.5	20.2	21.6	15.1	14.6	22.6	20.8	--	24.1
P2	20.3	20.1	24.6*	15.0	14.6	--	20.7	--	23.6
L3	27.4	26.6	24.7	29.1	27.7	35.4	(43.9)	40.3	47.1
P3	28.4	27.6	27.2*	29.4	28.0	38.2	44.4	--	44.4
L4	31.2	30.5	22.5	21.4	20.5	28.1	32.4	--	34.6
P4	30.0	29.3	23.7*	20.8	19.9	26.7	31.5	--	32.7

**Based on f_y
***Based on f_{su}

*Based on elastically computed maximum moment (at centre)

To be able to carry out the strain compatibility calculations explained in Chapter 3, the stress-strain curves for the rebars must be used. Figure 5.1 has been replotted in Fig. 5.9 where the intersection points are indicated for the different members.

In Fig. 5.10 the calculated cracking moments for the R series beams, using transformed moment of inertia with and without the shrinkage reduction are compared graphically to the observed values. Also given on the same plot are values obtained by using the gross moment of inertia. Similar comparison is made in Fig. 5.11 for the T series and I series beams and in Fig. 5.12 for the slabs, except that shrinkage stresses were not estimated for these members.

The difference between the cracking moments computed using the transformed moment of inertia, I_{tr} , and the gross moment, I_g , is very small for all members as would be expected because of the low steel percentages (Figures 5.10 to 5.12). In the case of R, T and I beams, the calculated cracking moments are about the same as the observed values for the beams cast in the first two batches (20 MPa concrete). For the beams cast in batches 3 and 4 (45 MPa concrete) the calculated values seem to be consistently on the high side. This is not as obvious for the slabs.

On the other hand, the "shrinkage reduced" values tend to be on the low side for beams made of the low strength concrete.

A comparison of the measured and computed values suggests that there is little advantage to using the transformed moment of inertia. On the other hand, the calculation of cracking moments appears to be improved by inclusion of the shrinkage stresses. It appears, however, that the calculations overestimated the shrinkage stresses for 20 MPa concrete and underestimated them for the 45 MPa concrete. In the shrinkage calculations, the ultimate shrinkage strain of both 20 MPa and 45 MPa concrete was assumed to be 400×10^{-6} m/m. The beam data suggests that the actual shrinkage was less than this amount for the 20 MPa concrete and more for the 45 MPa concrete. Because of the lack of shrinkage data on the concrete, shrinkage stresses were only calculated for the rectangular beams.

A correction in tensile concrete strength for volume differences was not found to give satisfactoy results and was not used.

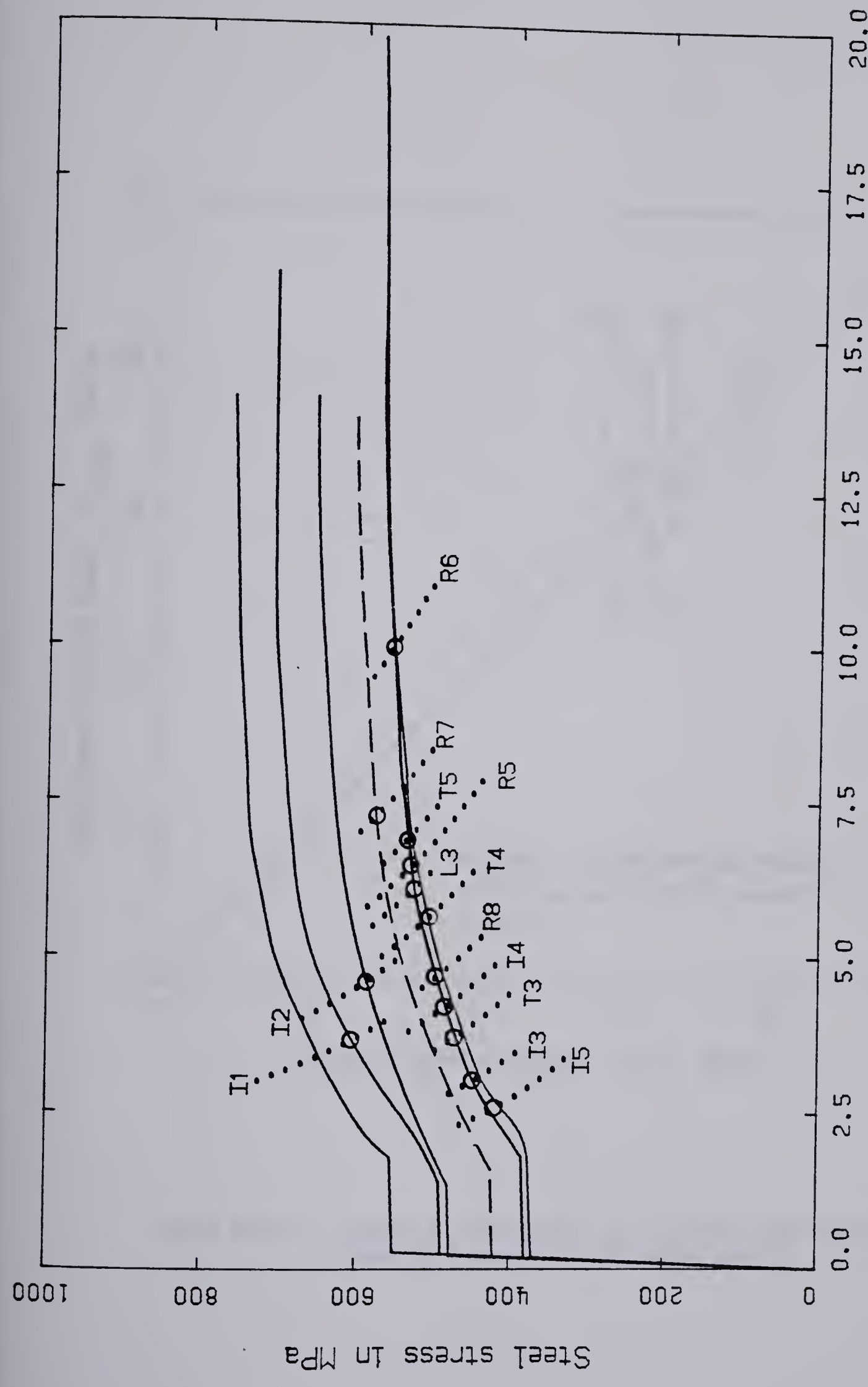

Figure 5.9 — Stress-strain curves for reinforcing bars, including lines used in strain compatibility calculations.

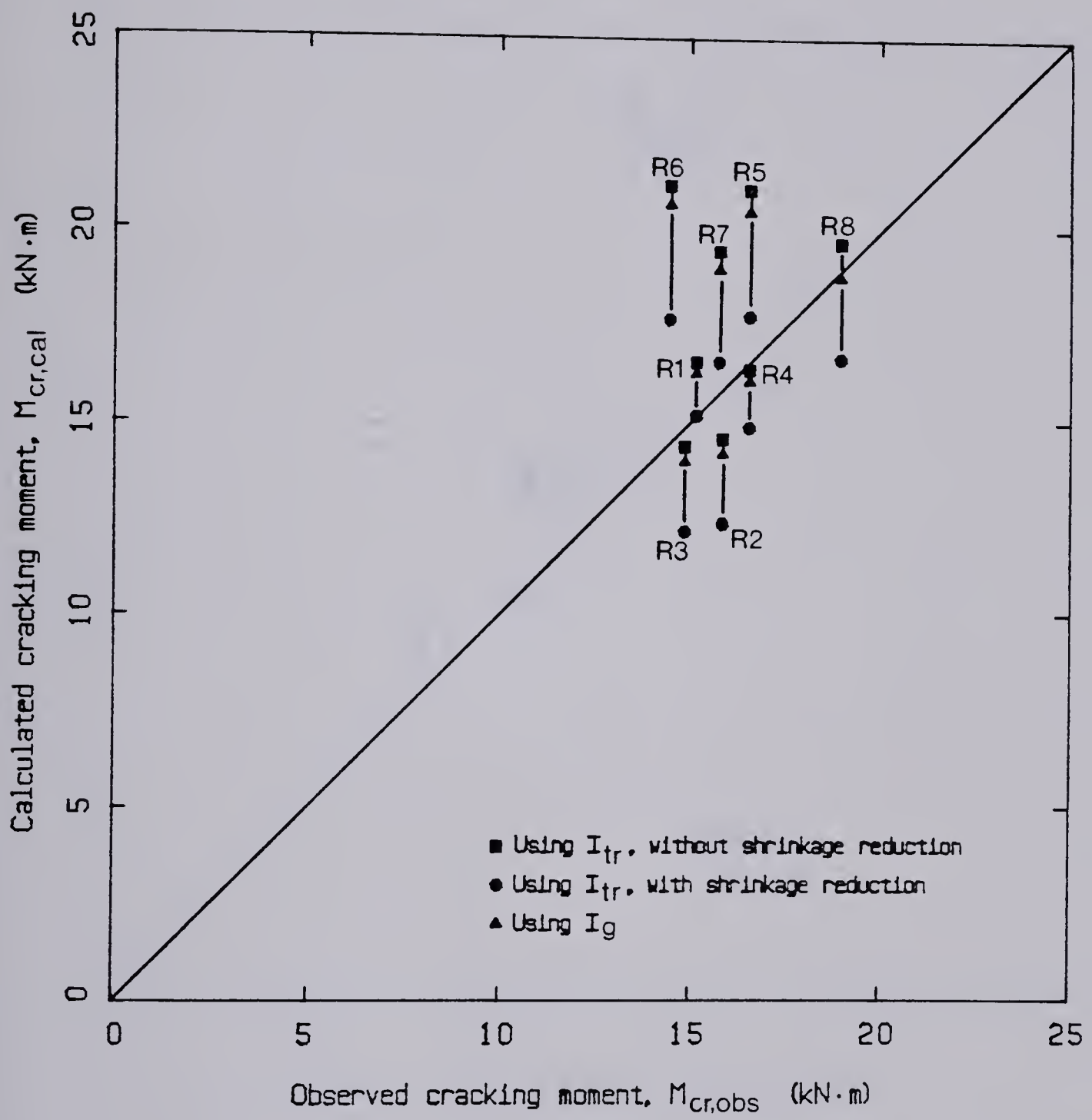

Figure 5.10 — Graphical comparison of calculated and observed cracking moments for R series beams.

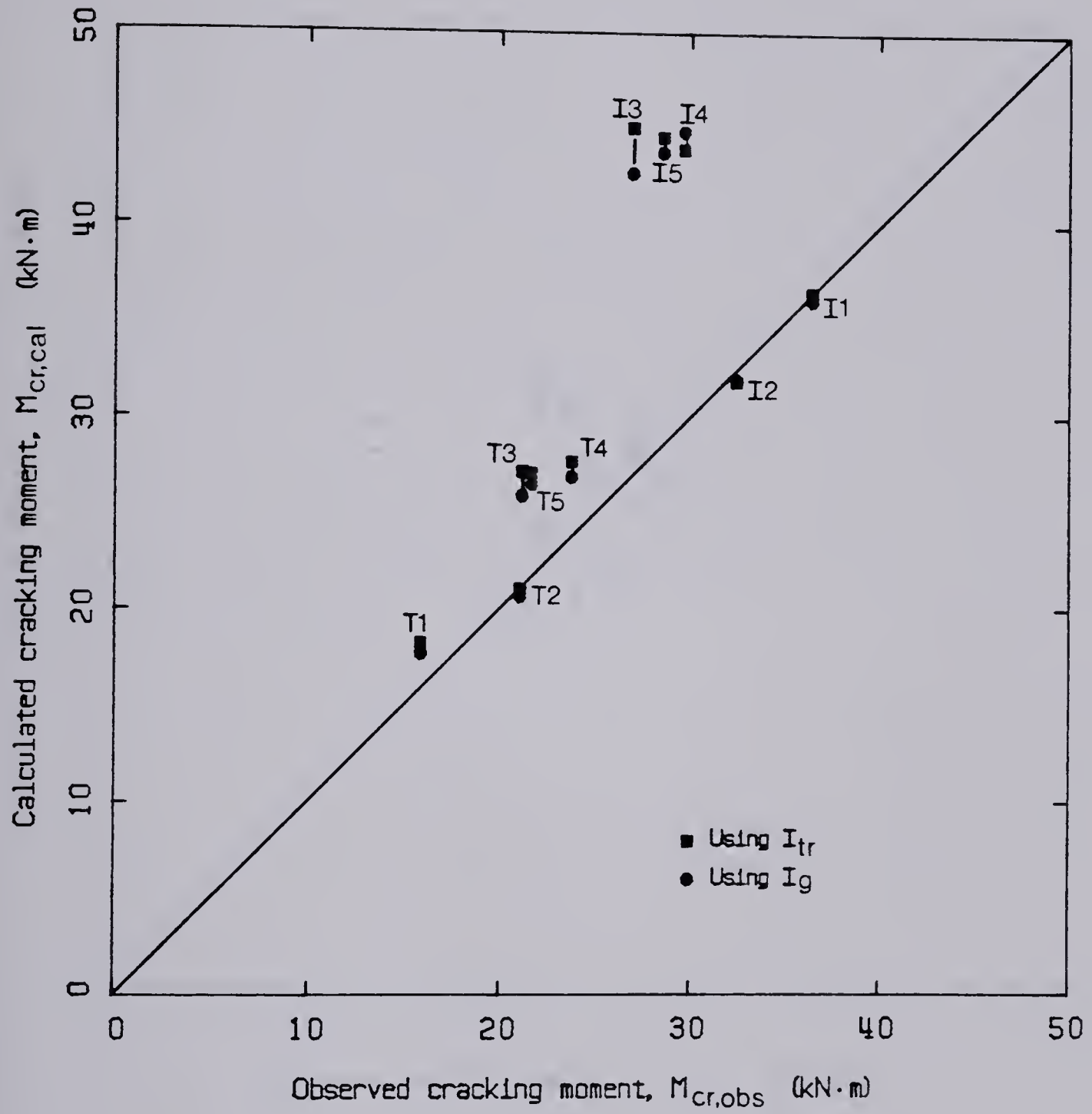

Figure 5.11 — Graphical comparison of calculated and observed cracking moments for T series and I series beams.

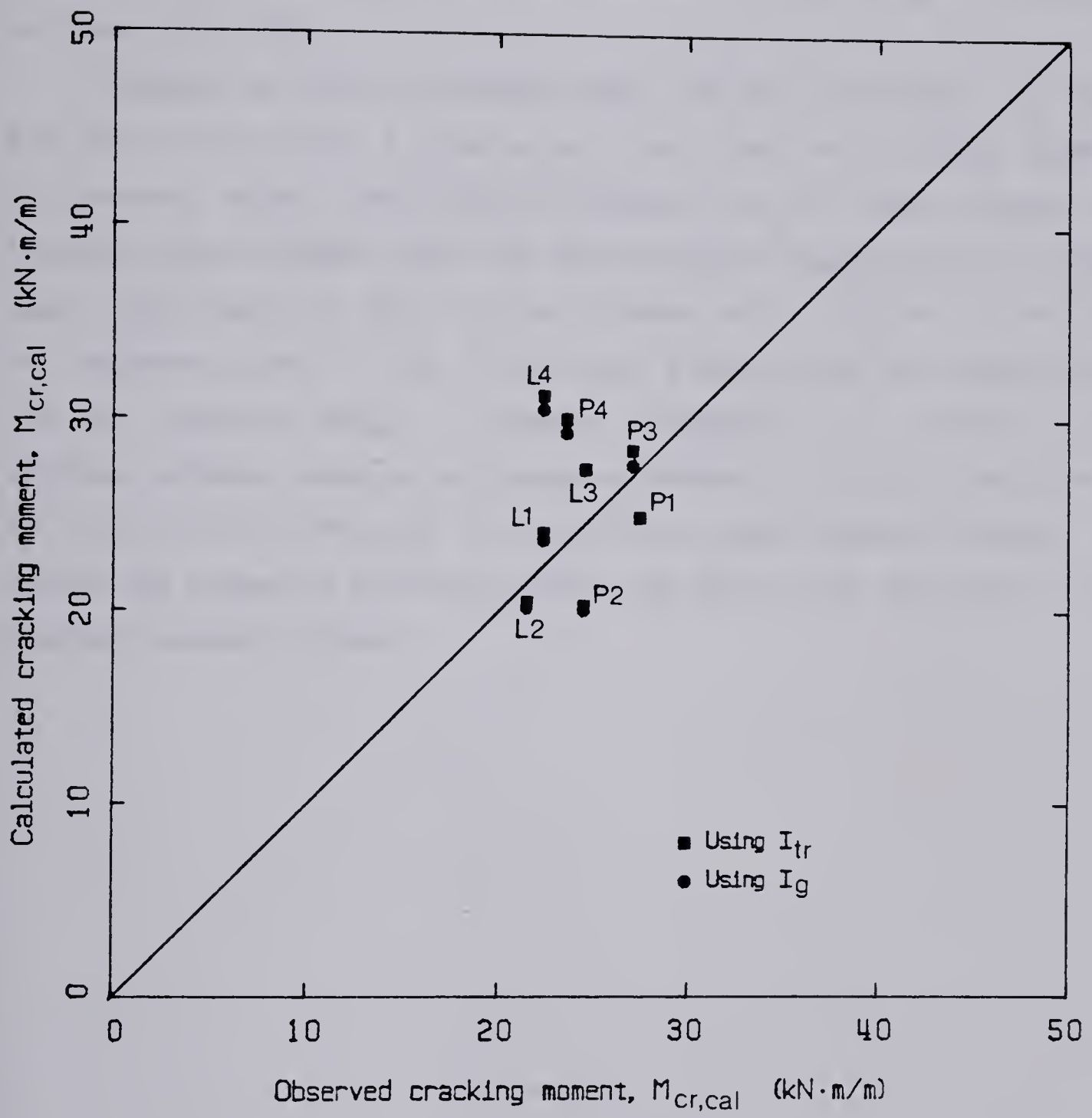

Figure 5.12 — Graphical comparison of calculated and observed cracking moments for slabs.

5.2.2 Comparison of calculated and observed yielding moments

The calculated yielding moment capacities for the R-beams given in Table 5.12 are compared graphically to the observed values in Fig. 5.13. Similar comparison for the T-beams and the I-beams is made in Fig. 5.14, and for the slabs in Fig. 5.15.

Although the CSA-ACI equation (Eqn. 3.4) and the straight line theory (Eqn. 3.5) do not differ a great amount, the former one is always closer to the observed values. For both the R-beams and the slabs, however, the observed moment capacity was in all cases noticeably greater than the calculated values, approximately 3 kN·m for the R-beams and 7 kN·m/m for the slabs. The calculated values for the T-beams and I-beams seem to compare better with the observed values. A possible explanation for a portion of the difference between measured and computed moments is that the initial crack did not always occur at the point of maximum dead load moment at midspan. As a result the moment at the crack could be as much as 0.5 kN·m less than the maximum calculated moment.

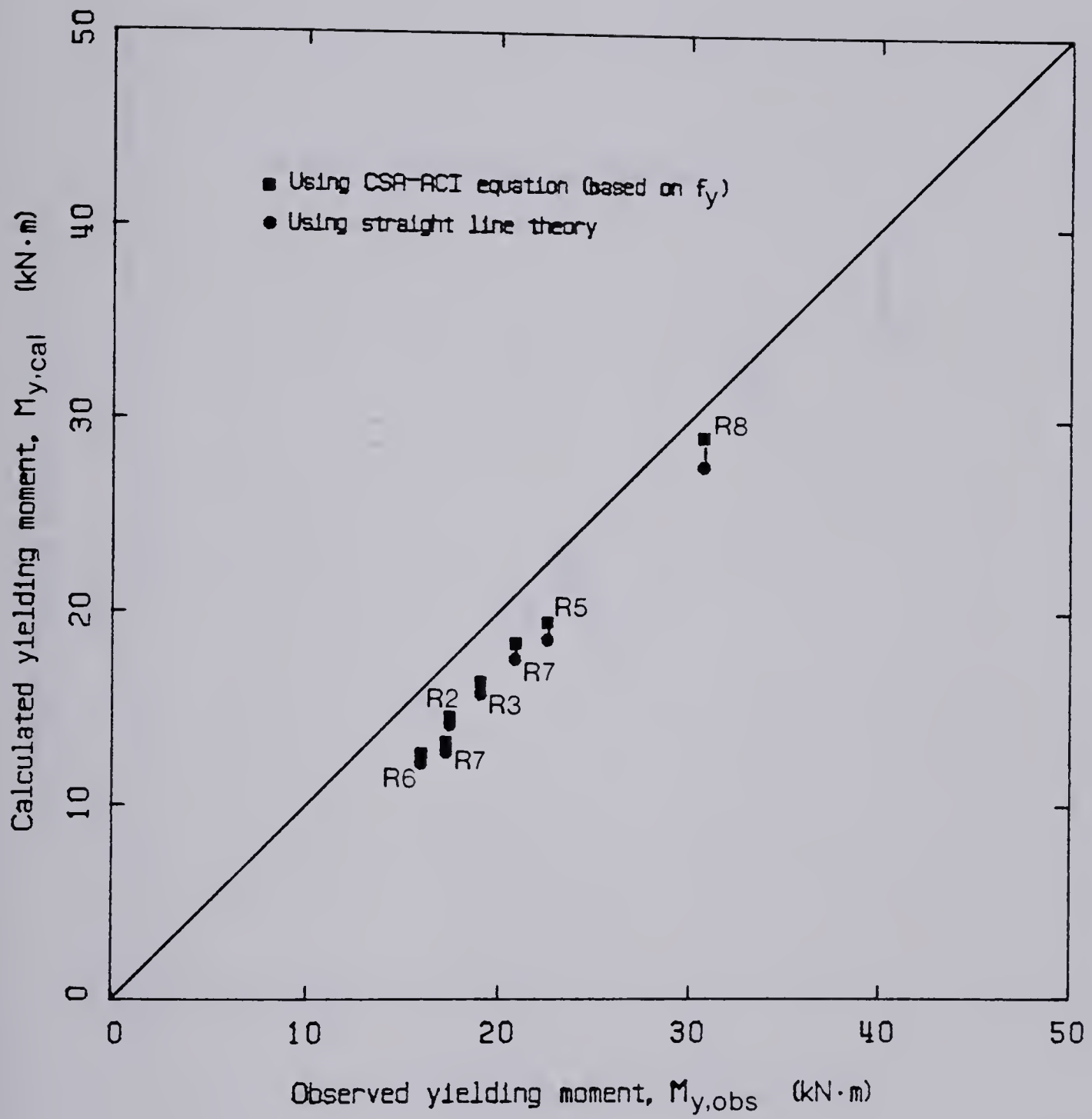

Figure 5.13 — Graphical comparison of calculated and observed yielding moments for R series beams.

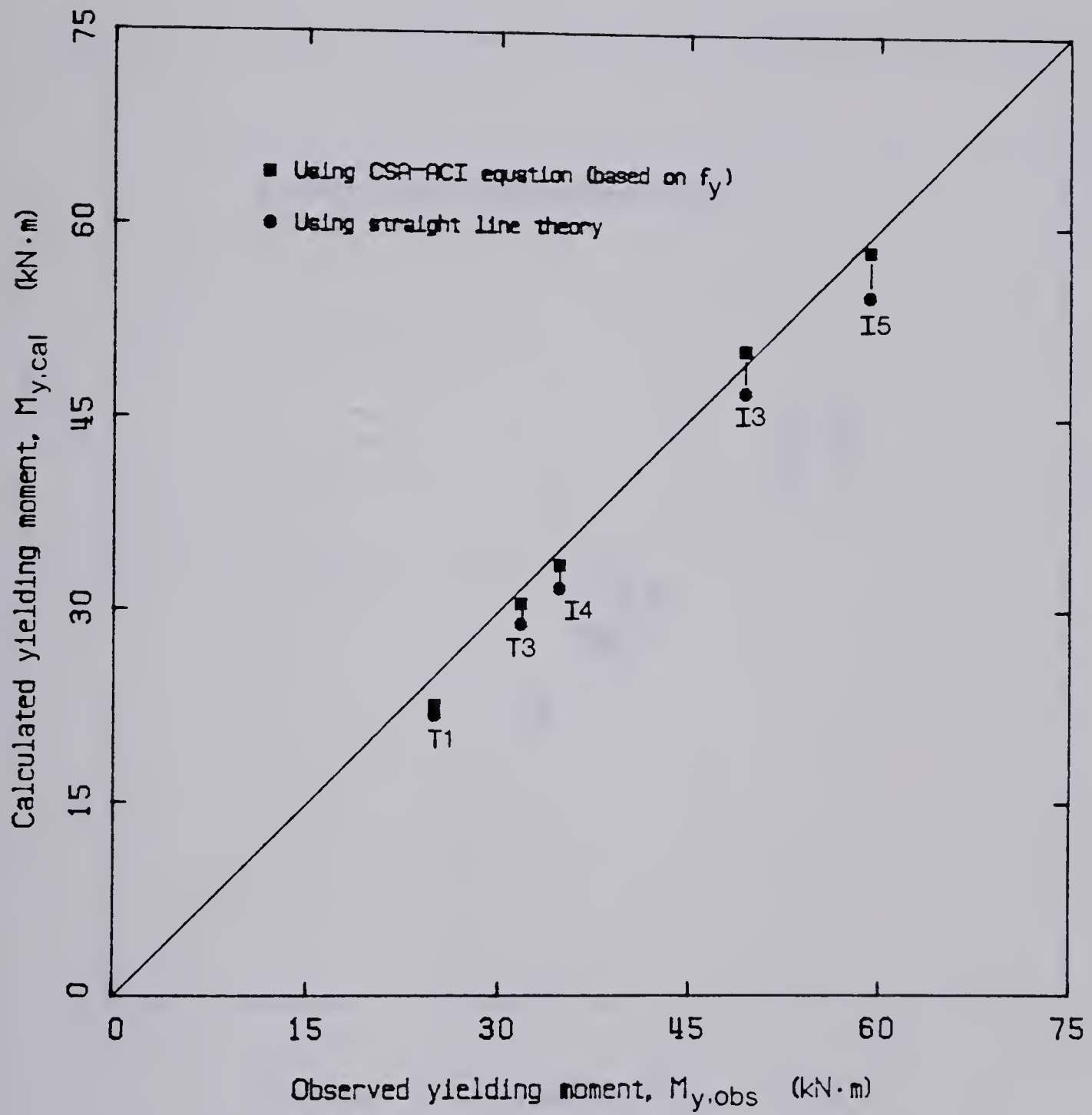

Figure 5.14 — Graphical comparison of calculated and observed yielding moments for T series and I series beams.

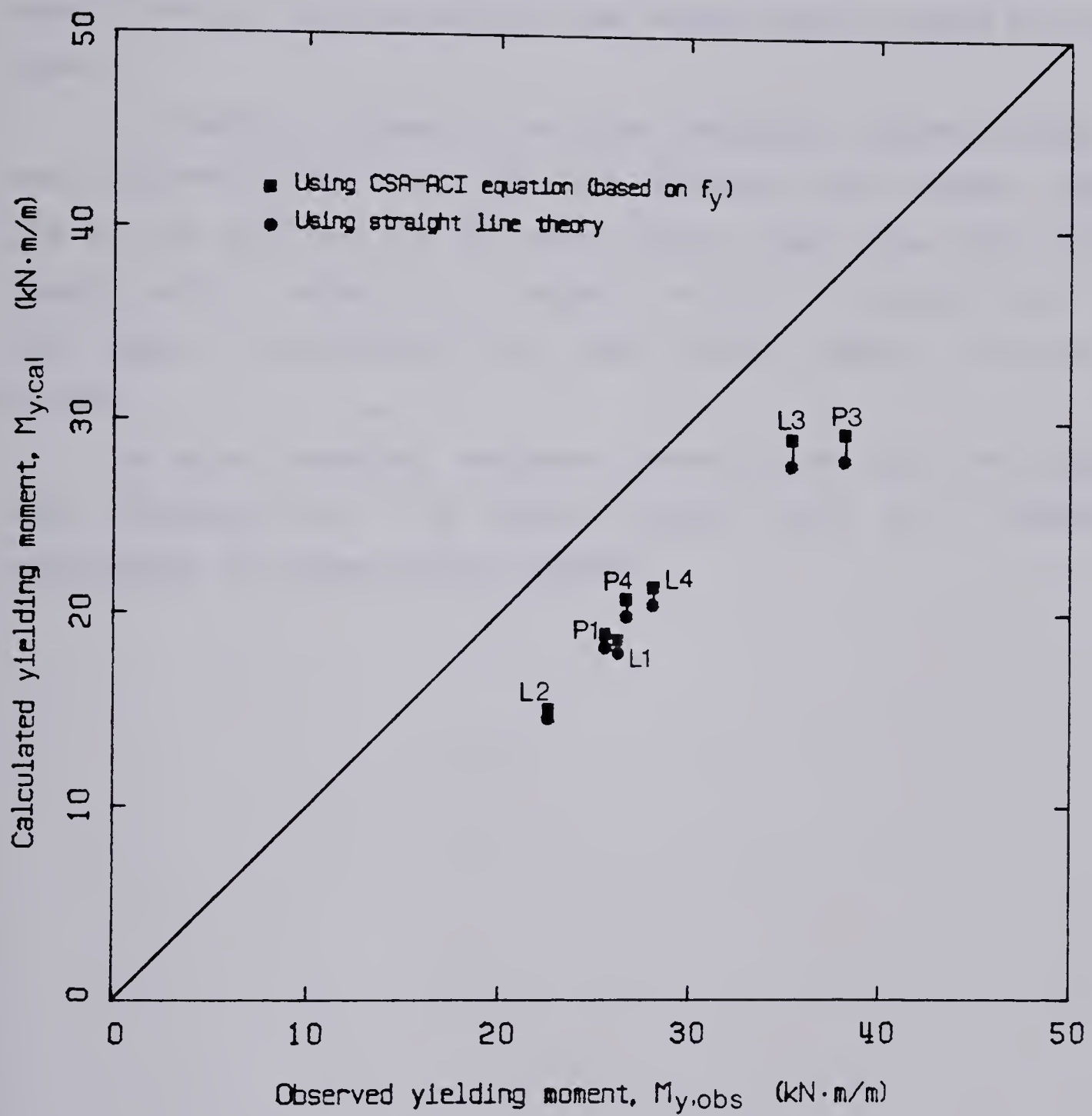

Figure 5.15 — Graphical comparison of calculated and observed yielding moments for slabs.

5.2.3 Comparison of calculated and observed ultimate moments

The calculated and observed ultimate moment capaties are compared in Fig. 5.16 for the rectangular beams, in Fig. 5.17 for the T- and I-beams and in Fig. 5.18 for the slabs. Also included in the figures is the yielding moment capacity found by using the CSA-ACI code equation (Eqn. 3.4), called M_n in the codes.

As expained in Chapter 3, the strain compatibility calculations have not been performed in the cases where the reinforcing bars fractured. Figures 5.16 to 5.18 show that for the cases when the rebars broke, the CSA-ACI equation, using f_{su} instead of f_y, compares well with the observed values. In other cases, it overestimates the ultimate moment capacity as could be expected.

The strain compatibility calculations, where applied, match the observed values exceptionally well. The CSA-ACI equation based on f_y consistently underestimates the ultimate moment capacities.

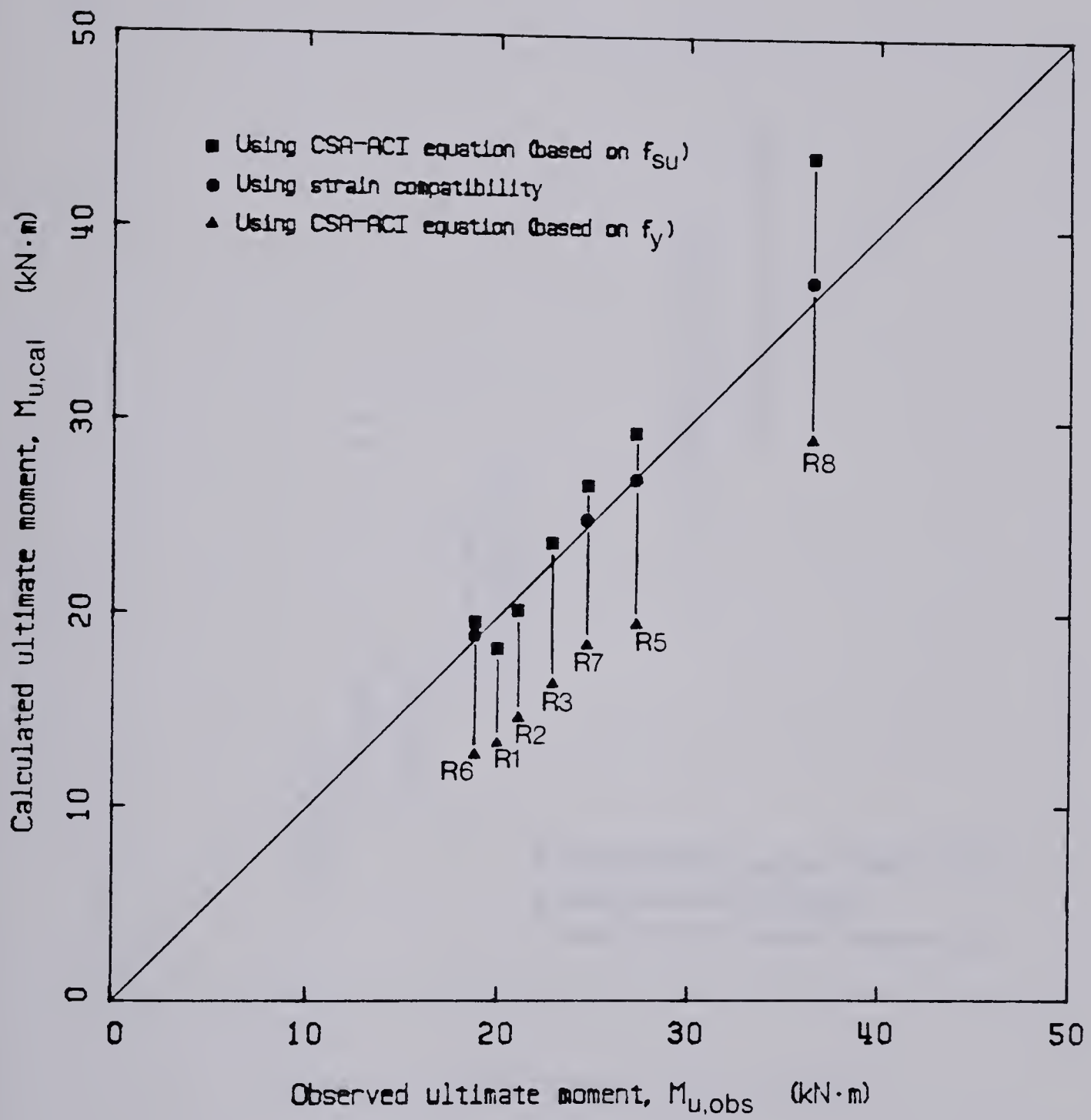

Figure 5.16 — Graphical comparison of calculated and observed ultimate moments for R series beams.

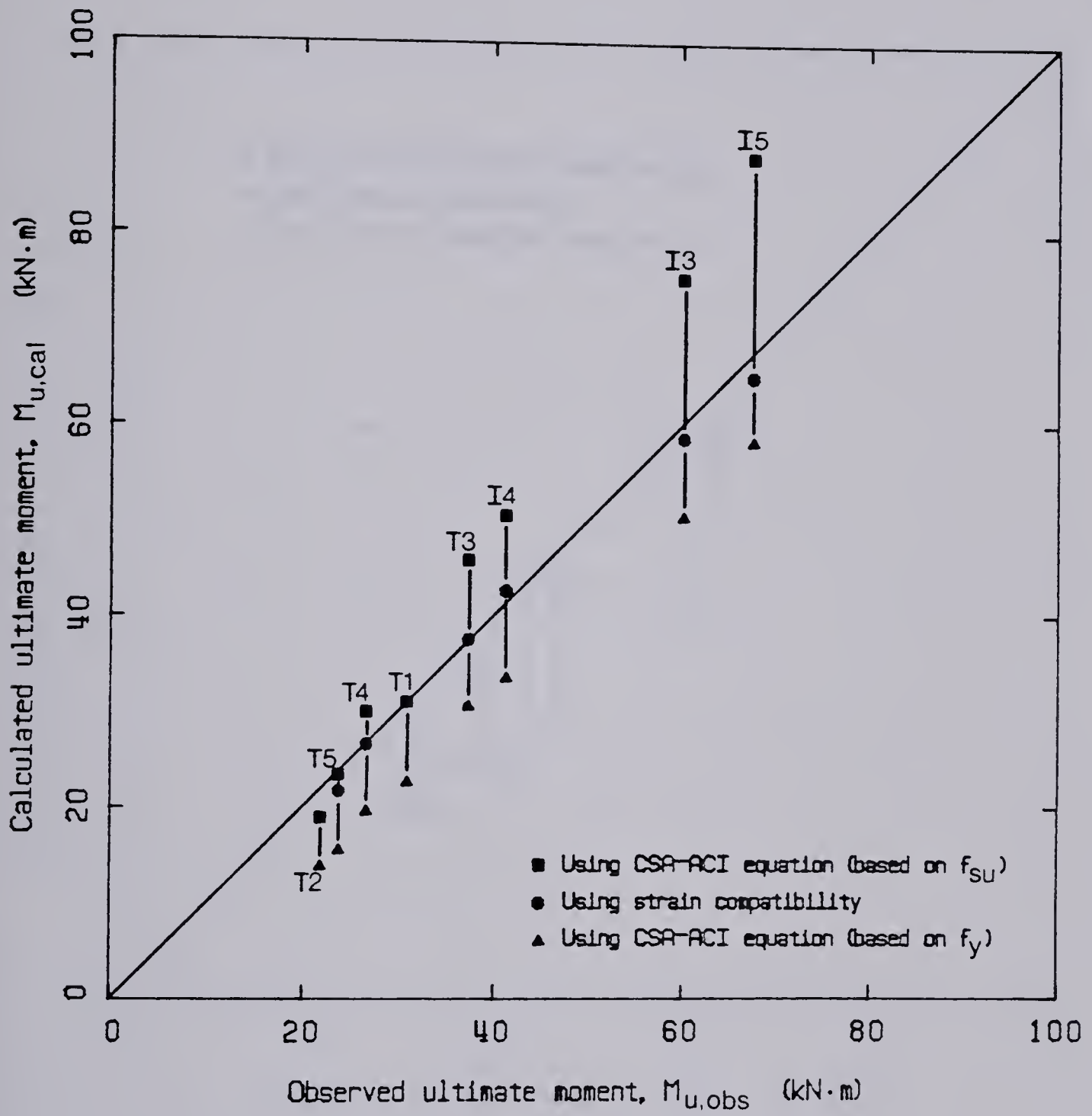

Figure 5.17 — Graphical comparison of calculated and observed ultimate moments for T series and I series beams.

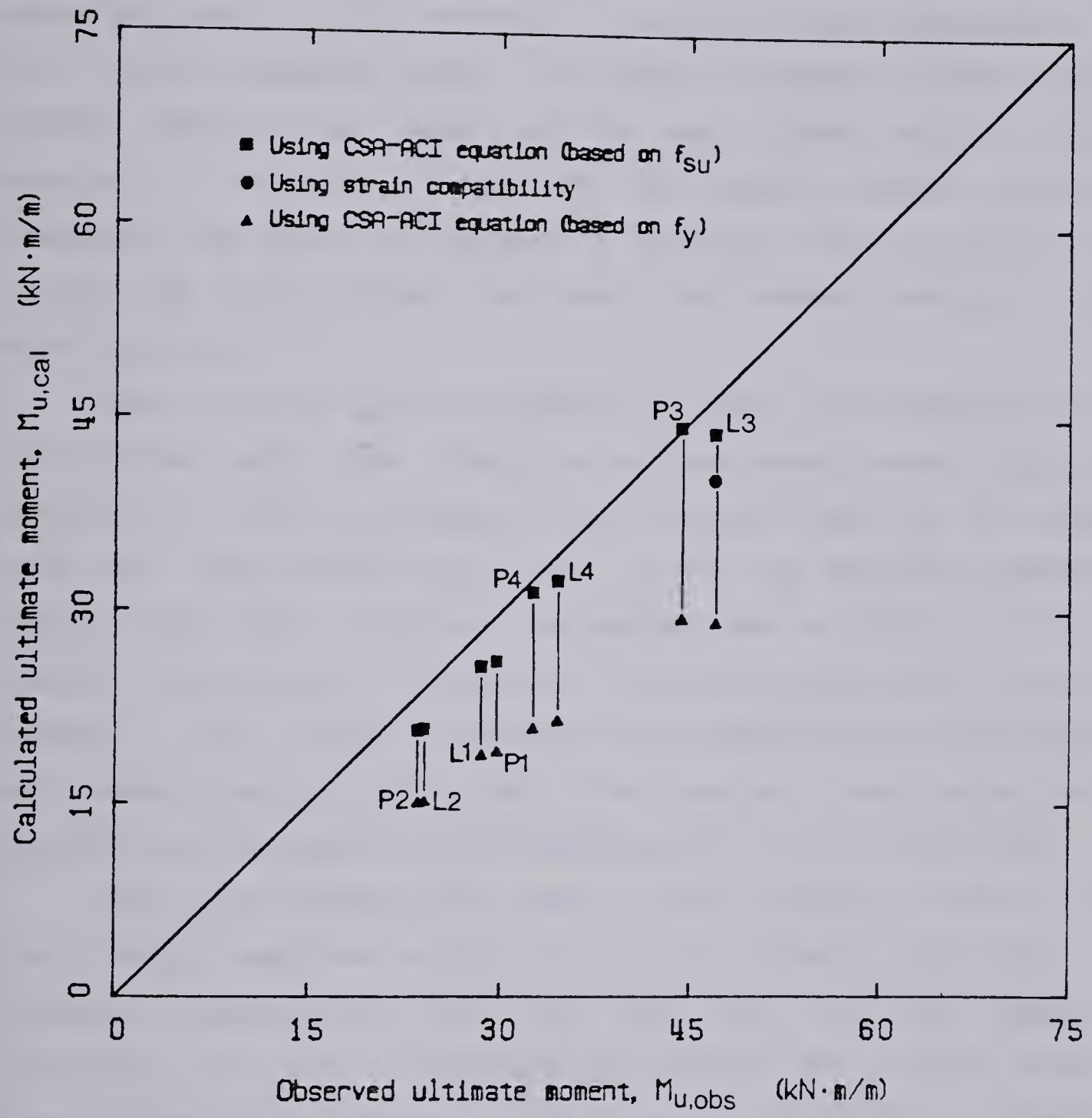

Figure 5.18 — Graphical comparison of calculated and observed ultimate moments for slabs.

5.2.4 Boundary between ductile and brittle behaviour

The definition of a ductile behaviour will be the same as Leonhardt used in his 1961 paper (see section 2.1). That is, a beam will be said to be ductile if M_u was greater than $1.05 \cdot M_{cr}$. The reinforcement ratio is plotted against the ratio f_c / f_{su} (as determined by tests on control specimens) in Fig. 5.19 for the rectangular beams. The filled in symbols indicate that the *observed* behaviour was ductile, and the open symbols indicate a brittle behaviour. In the case of beam R6, the expected behaviour based on calculations was brittle, but because of shrinkage stresses induced in the concrete the cracking moment was lower than expected, bringing the ratio M_u / M_{cr} up above 1.0.

Using the points given it is difficult to select a line dividing the points into brittle and ductile cases. Taking the observed ultimate moment, $M_{u,obs}$, for the beams as a basis, the necessary tensile concrete strength can be calculated (using Eqn. (3.3)), so that $M_{cr} = M_u$. To find the respective compressive strength, Eqn. (5.5) is used, with the average value of 0.69 for K (for all batches). This will give for each beam a new value of the ratio f_c / f_{su} (for a constant ρ), which can help in selecting a more definite position of a boundary line between brittle and ductile cases. This procedure is only carried out for the beams that are expected to be reasonably close to this boundary line.

Such a line intersects the y-axis at 0.042 and has a slope of 1.32. The correlation coefficient is 0.98. This line is included in Fig. 5.19. Also included is Leonhardt's test line from 1961 (Eqn. 2.5), which appears to overestimate the amount of reinforcement necessary for a ductile behaviour. Similar procedures are followed for the T-beams in Fig. 5.20, for I-beams in Fig. 5.21 and for the slabs in Fig. 5.22. The boundary line for the T-beams intersects the y-axis at 0.047 and has a slope of 2.40. The correlation coefficient for this line is 0.99. Leonhardt's line (which was based on rectangular shapes only) is lower than the calculated line in this case, and would underestimate the reinforcement ratio necessary for a ductile behaviour. The line for I-beams intersects the y-axis at 0.137 and has a slope of 3.38 and

a correlation coefficient of 0.98. Leonhardt's line is in this case Eqn. (2.5) modified by Eqn. (2.12). The calculated line gives in this case higher values than Leonhardt's line. The boundary line for the slabs is only based on the line loaded slabs, since a calculation for the other ones becomes more approximate. This should not cause any errors since the behaviour of the line loaded and point loaded slabs was very similar. This line intersects the y-axis at 0.051 and have a slope of 1.18. Correlation coefficient is 0.98. As is the case for the rectangular beams, the calculated boundary line for the slabs is somewhat lower than Leonhardt's line. These lines are all shown in the figures mentioned.

The ratio d/h does not vary much in practise and usually is about 0.9. In this test series, the rectangular shapes (beams and slabs) and the I-beams all had this ratio close to 0.9. For the T-beams on the other hand, the ratio was closer to 0.8, which means that the reinforcement was farther away from the bottom of the beams than usual. If the rebars were moved down to get a comparable ratio of d/h, one would have to reduce the amount of the steel in order to get the same behaviour as in the tests. Since A_S would become a little smaller and d a little larger, the reinforcement ratio would decrease somewhat. This means that if the ratio d/h = 0.9 is taken as a reference value, the calculated line in Fig. 5.20 overestimates by some amount the reinforcement ratio necessary for a ductile behaviour.

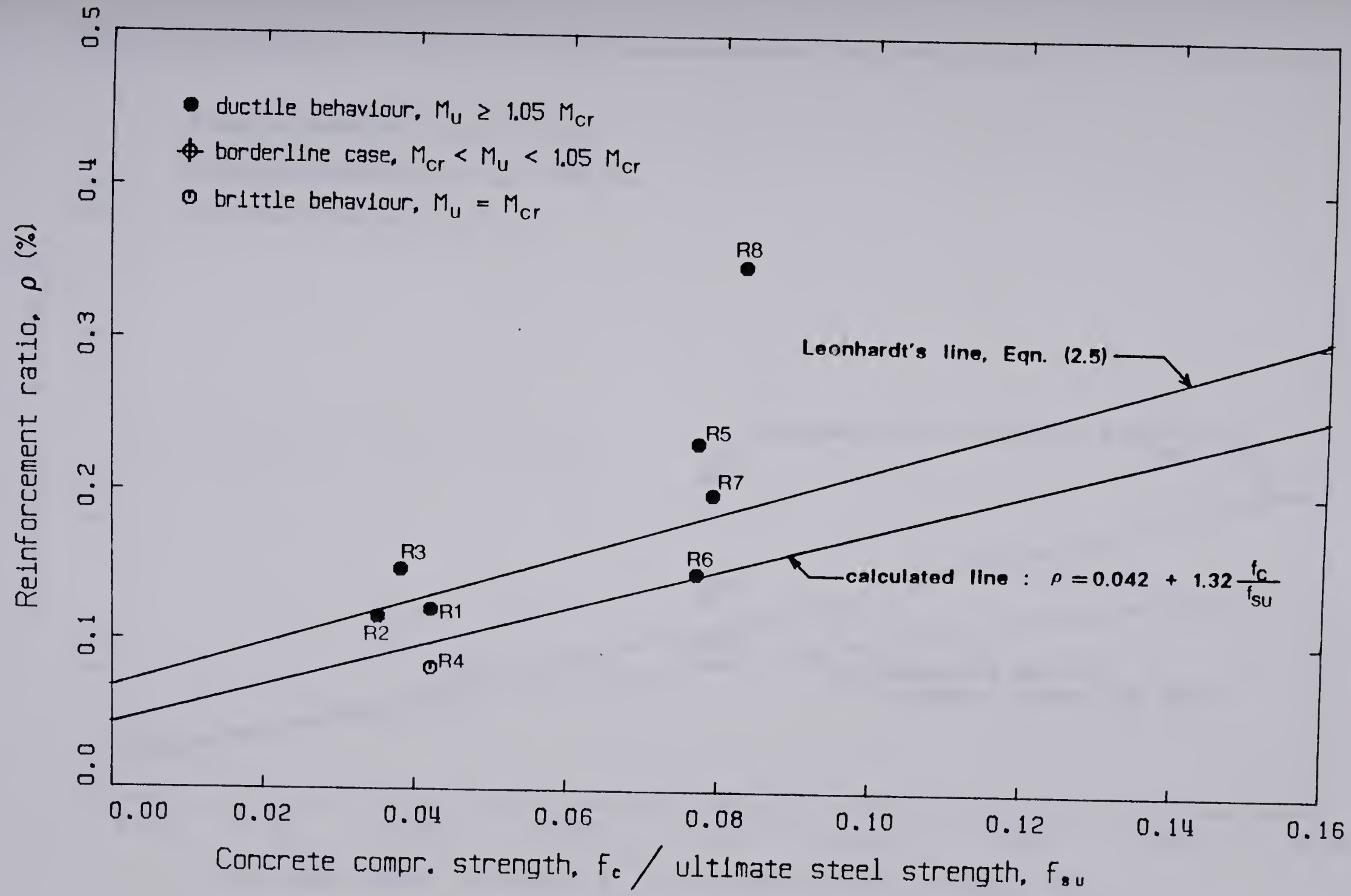

Figure 5.19 — Failure mode of R series beams.

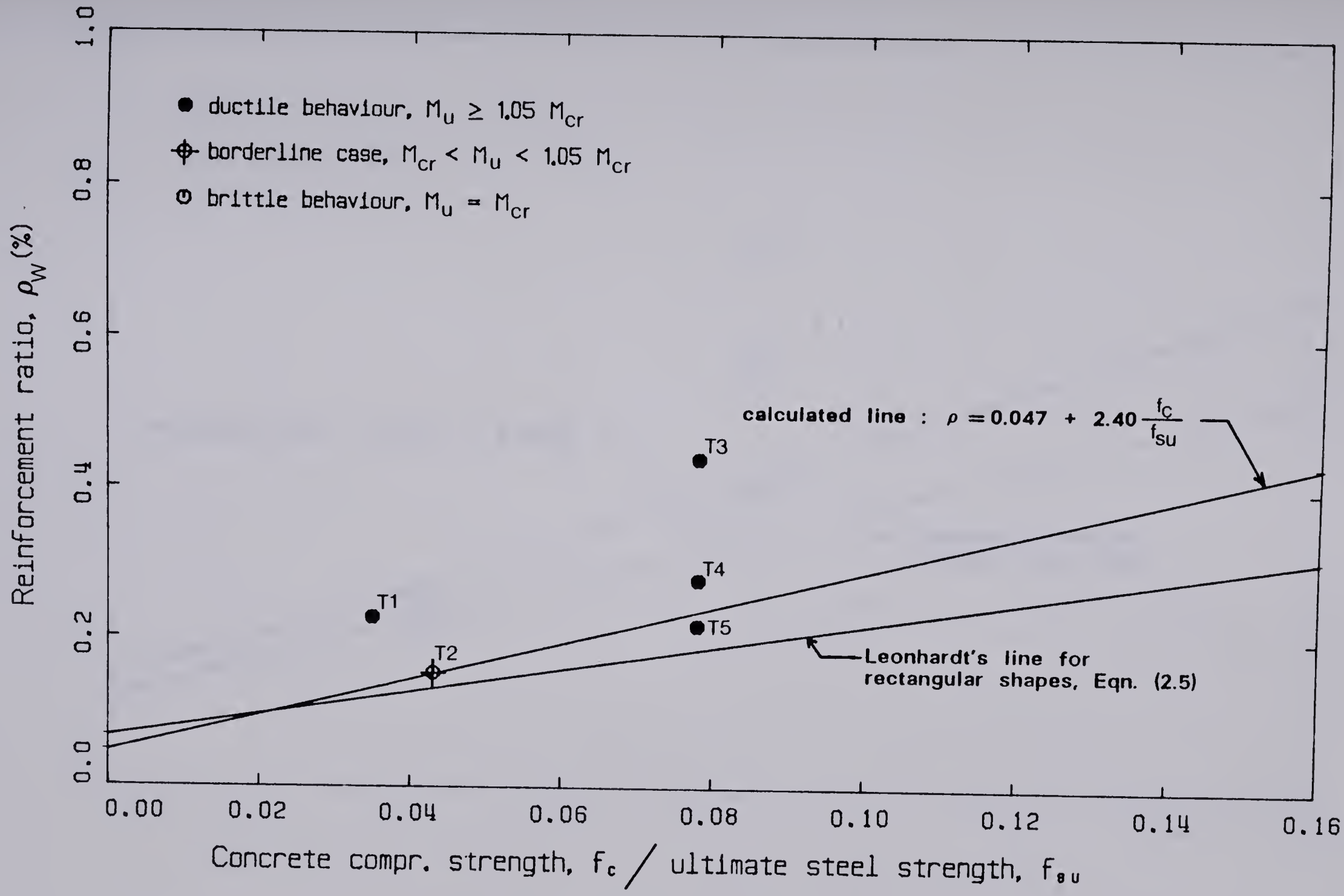

Figure 5.20 — Failure mode of T series beams.

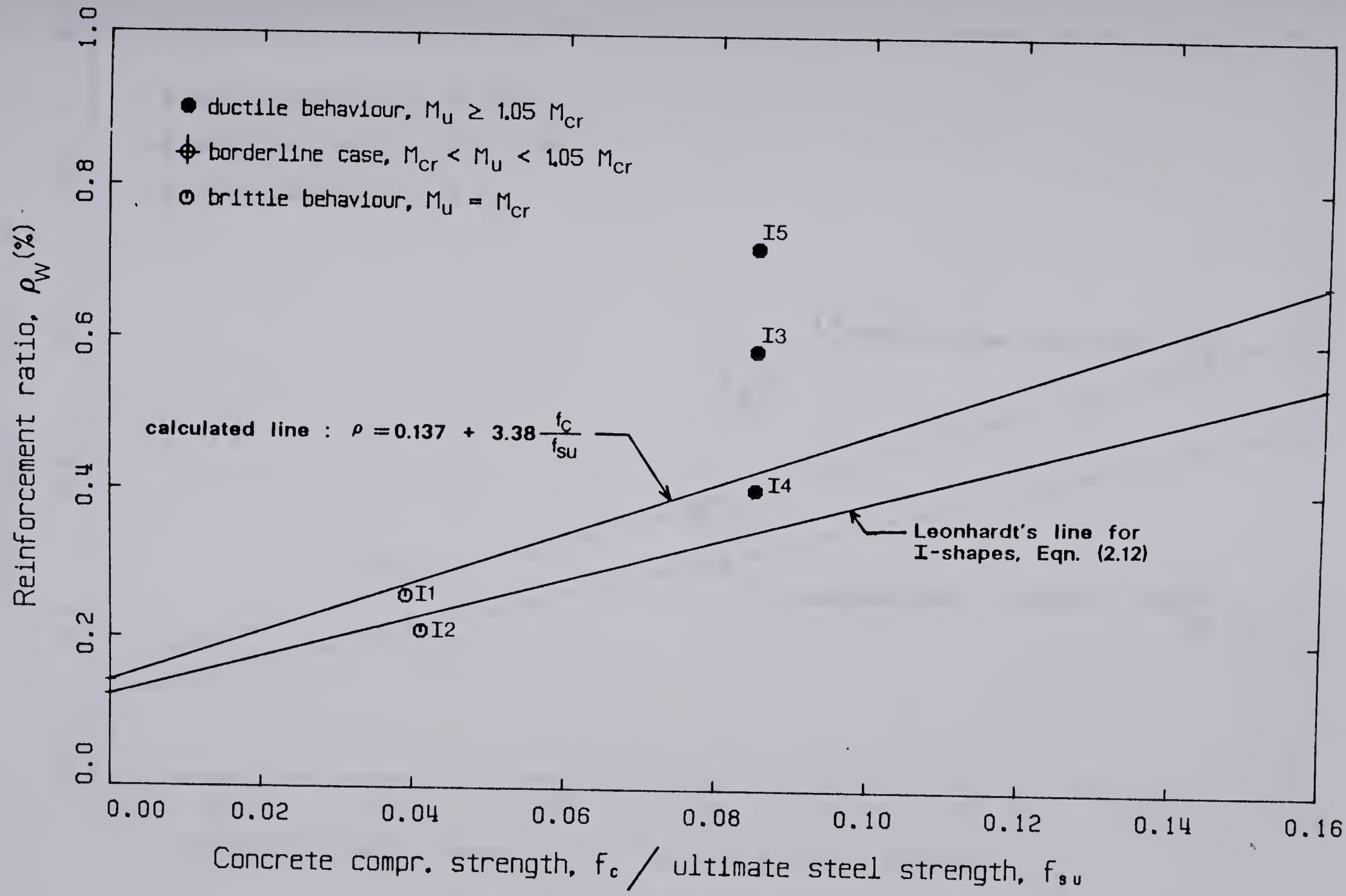

Figure 5.21 — Failure mode of I series beams.

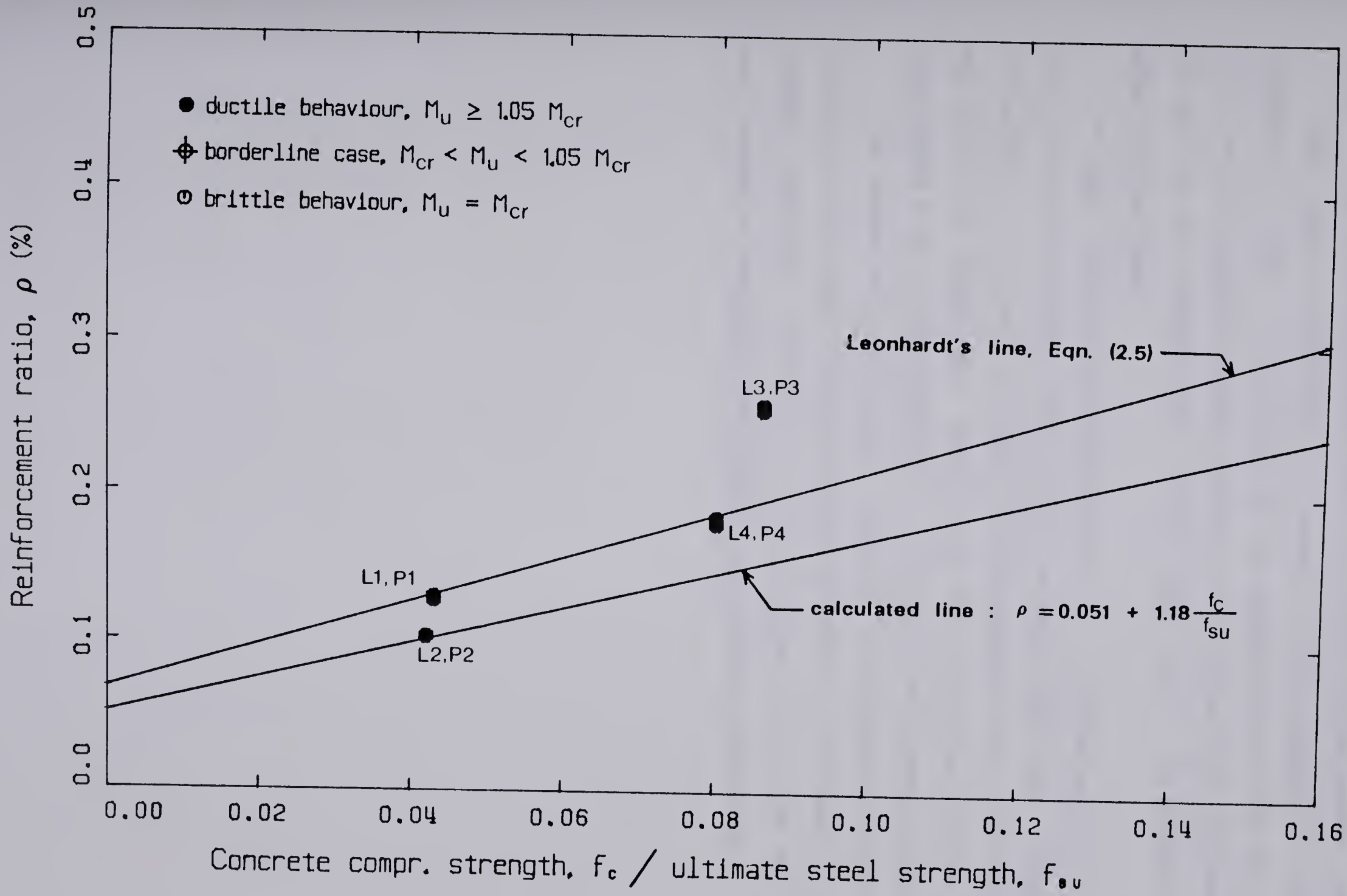

Figure 5.22 — Failure mode of slabs.

5.2.5 Reinforcement ratio based on the area of the concrete tension zone

One way of expressing the amount of reinforcement in concrete members is to base it on the area of the concrete tension zone only, Eqn. (2.1). For the rectangular shapes, this new ratio would be about 1.8 times the old one, for the T-beams about 1.3 times larger and for the I-beams only about 1.2 times larger.

In Figure 5.23 this reinforcement ratio, ρ_t , is plotted against the ratio f_c / f_{su} for all the members tested except the point loaded slabs. Those are not included for the sake of clarity, since their behaviour was very similar to that of the line loaded slabs. Drawn in on this plot are the calculated lines from Figures 5.18 to 5.22, converted to fit the new reinforcement ratio used.

The spread between the lines is less than that obtained by using ρ_w , but there is still a great difference between the lines for the R-beams and the I-beams, respectively. Therefore, it does not appear to be worth the extra work included in computing a reinforcement ratio based on tension area.

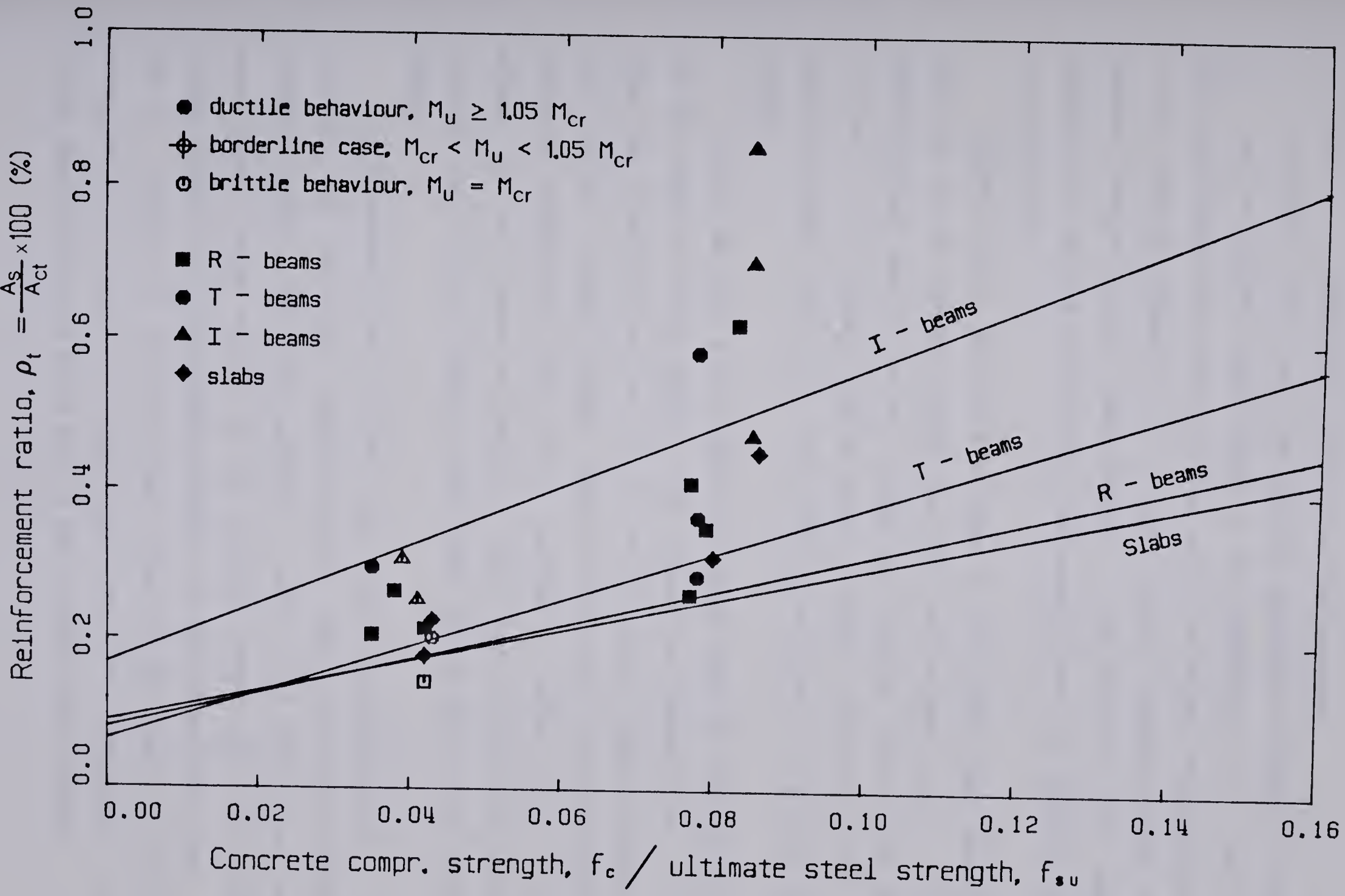

Figure 5.23 — Minimum reinforcement ratio based on the concrete tension zone only.

5.3 Selection of design rules for minimum reinforcement

In practise, usually only the specified compressive strength of concrete, f'_c , and the specified yield strength of the reinforcement, f_{yk} , are known. Since specifications may vary from one country to another, the quantities used in the following discussion will be based on the measured values of the concrete strength and the steel strength. It will be left to the reader to estimate how high the ratio of the actual strength over the specified strength is in each case.

Figures 5.19 to 5.22 were all based on the ultimate steel strength, f_{su} . The ratio of the ultimate strength over the yield strength, f_{su}/f_y , of the reinforcing bars used in the tests ranged form 1.38 to 1.55 with an average of 1.46. If this factor (1.46) is used to convert the plots to the more commonly known ratio f_c/f_y , the results are as shown in Fig. 5.24 (for all shapes).

As can be seen in this figure, the derived lines for the R-beams and for the slabs are almost identical. The T-beam line intersects the y-axis at about the same point as the line for the rectangular shapes (R-beams and slabs), but has a steeper gradient. One of the reasons for this difference in slopes is probably the ratio d/h as explained in section 5.2.4. The line obtained for the I-beams is considerably higher than the others, as would be expected, and is close to being 3 times higher than the line for the rectangular shapes.

As mentioned before, the tests were done on specimens cured at about 50% R.H., and the tensile strength therefore reduced by some amount by shrinkage stresses. The lines calculated in section 5.2.4 were based on the actual needed tensile strength of the concrete, derived from the observed ultimate moment. The compressive strength was then derived using Eqn. (5.5) with K = 0.69. The effect of moist curing will thus have the effect of moving the line upwards by some amount since the compressive concrete strength does not have to be as high to get the same tensile strength.

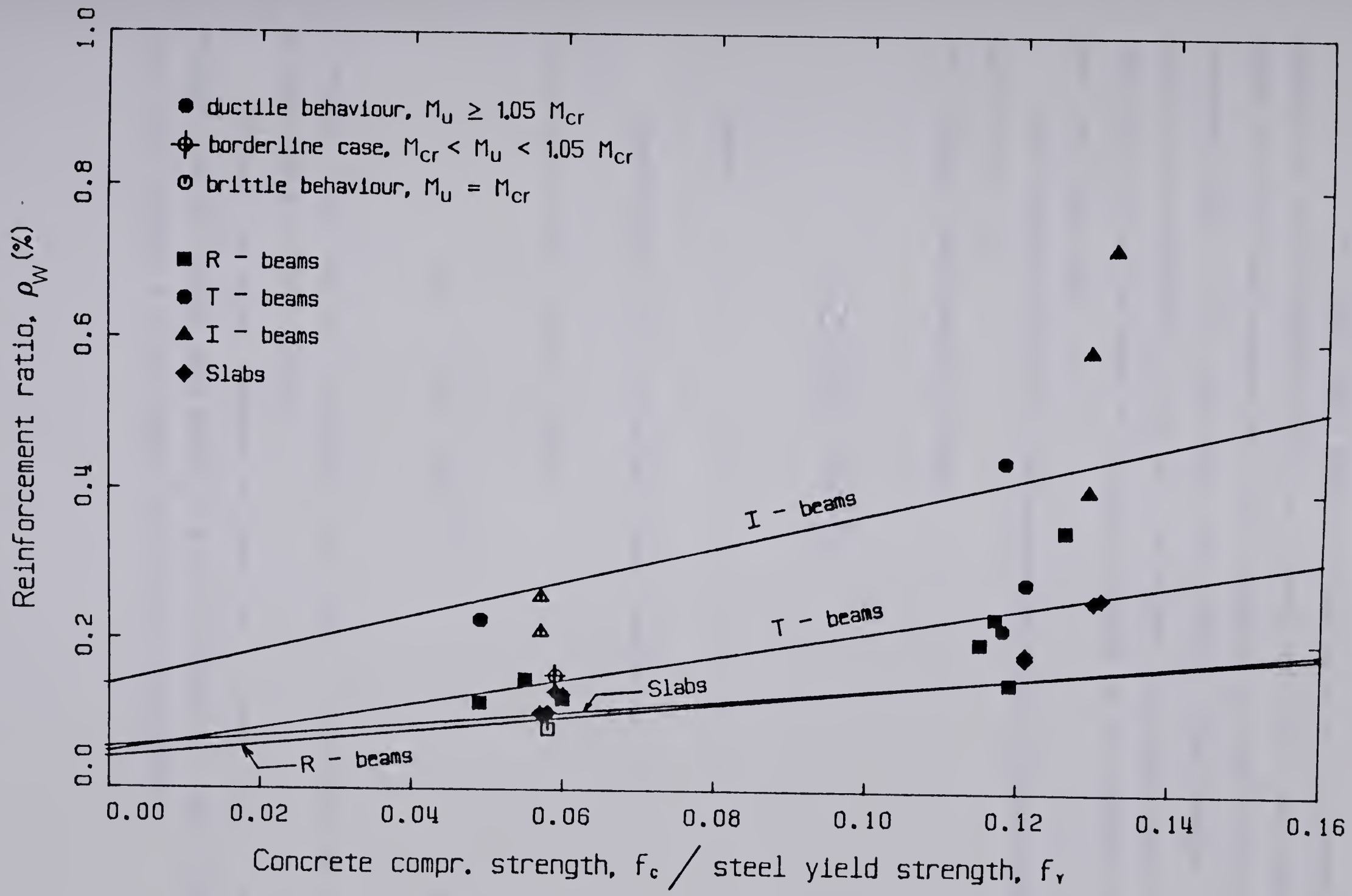

Figure 5.24 — Minimum reinforcement ratio in terms of concrete strength over steel yield strength.

It is not very likely that a beam or a slab, as parts of a building, are subjected to a 100% relative humidity at all times, and also if the humidity is higher than 50% these members are often restrained at the ends, allowing some shrinkage cracks to form and reduce the effective tensile strength. The following recommendations will not take into account the possible cases of a 100% R.H., but will be based on the same conditions as the specimens were cured and tested under.

The following equations are recommended for concrete members having a ratio of d/h = 0.9:

For rectangular shapes (beams and slabs):

$$\rho_{min} = 0.050 + 0.90 \cdot \frac{f_c}{f_y} \qquad (5.9)$$

For T-beams:

Same equation as for rectangular shapes, multiplied by 1.4.

For inverted T-beams (flange in tension):

$$\rho_{min} = 0.140 + 2.30 \cdot \frac{f_c}{f_y} \qquad (5.10)$$

It must be noted here that the equations given above do not include any kind of performance or safety factors.

Although the above equations are valid for a large range of steel strengths, the low strength steel should be preferred (because of higher ultimate strain) when designing a ductile member using minimum reinforcement.

6. CONCLUSIONS

As indicated in Figure 2.4, there is at present a great discrepancy between various rules and recommendations for minimum reinforcement ratio in concrete flexural members.

The minimum reinforcement ratio was selected to ensure a ductile failure in which the ultimate moment capacity after cracking was at least 1.05 times the cracking moment.

The results obtained in this test series indicate that the minimum reinforcement ratio is basically a function of 4 variables: f_c , f_y , d/h and cross-section shape. T-beams and inverted T-beams required 1.4 and 2.8, respectively, as much reinforcement as rectangular beams and slabs to develop a ductile failure.

No major advantage was found in basing the reinforcement ratio on the tension zone area of the concrete.

The recommendations given in Eqn. (5.9) for both beams and slabs suggest that the 1977 CSA-ACI rules are grossly conservative for rectangular beams.

References

ACI Committee 224, 1980 : *"Control of Cracking in Concrete Structures"*, Concrete International, Vol. 2, No. 10, Oct. 1980, Detroit.

ACI Committee 439, 1969 : *"Effect of Steel Strength and of Reinforcement Ratio on the Mode of Failure and Strain Energy Capacity of Reinforced Concrete Beams"*, ACI Journal Proceedings, Vol. 66, No. 3, March 1969, pp. 165-173.

American Concrete Institute (ACI), 1977 : *"Building Code Requirements for Reinforced Concrete (ACI 318-77)"*, Detroit, 1977.

American Concrete Institute (ACI), 1977 : *"Commentary on Building Code Requirements for Reinforced Concrete (ACI 318-77)"*, Detroit, 1977.

Bolotin, V.V., 1969 : *"Statistical Methods in Structural Mechanics"*, Translated by Samuel Aroni, Holden-Day Inc., San Francisco, 1969.

Cady, P.D.; Clear, K.C. and Marshall, L.G., 1972 : *"Tensile Strength Reduction of Mortar and Concrete Due to Moisture Gradients"*, ACI Journal Proceedings, Vol. 69, No. 11, Nov. 1972, pp. 700-705.

Canadian Standards Association (CSA), 1977 : *"Code for the Design of Concrete Structures for Buildings (CAN3-A23.3-M77)"*, Rexdale, Ontario, 1977.

Canadian Standards Association (CSA), 1977 : *"Methods of Test for Concrete (CAN3-A23.2-M77)"*, Rexdale, Ontario, 1977.

Carlson, R.W., 1937 : *"Drying shrinkage of Large Concrete Members"*, ACI Journal Proceedings, Vol. 33, No. 3, Jan-Feb. 1937, pp. 327-336.

Comite Euro-International du Beton (CEB), 1978 : *"CEB-FIP Model Code for Concrete Structures"*, Bulletin d'Information, No. 124/125 E, Paris, 1978.

Hrabok, M., 1981 : An elastic finite element program for slabs, unpublished.

International Organization for Standardization (ISO), 1976 : *"Bases for design of structures - Notation - General symbols (ISO 3898-1976(E))"*, Paris, 1976.

Leonhardt, F., 1961 : *"Die Mindestbewehrung im Stahlbetonbau"*, 56. Jahrgang, Heft 9, Sept. 1961, Verlag von Wilhelm Ernst und Sohn, Berlin, 1961.

Leonhardt, F., 1977 : *"Crack Control in Concrete Structures"*, International Association for Bridge and Structural Engineering (IABSE) Survey S-4/77, Zurich, 1977.

Lecnhardt, F. and Monning, E., 1973 : *"Vorlesungen uber Massivbau"*, Erster Teil, Grundlagen zur Bemessung im Stahlbetonbau, Springer-Verlag, Berlin, 1973.

Linder, C.P. and Spraque, J.C., 1955 : *"Effect of Depth of Beam Upon the Modulus of Rupture of Plain Concrete"*, ASTM Proceedings, Vol. 55, 1955, pp. 1062-1075.

McCollister, H.M.; Siess, C.P. and Newmark, N.M., 1954 : *"Load-deformation Characteristics of Simulated Beam Column Connections in Reinforced Concrete"*, Structural Research Series No. 76, University of Illinois, Urbana, 1954.

Mirza, S.A.; Hatzinikolas, M. and MacGregor, J.G., 1979 : *"Statistical Descriptions of Strength of Concrete"*, Journal of the Structural Division, ASCE, Vol. 105, No. ST6, June 1979, pp. 1021-1037.

Mirza, S.A. and MacGregor, J.G., 1981 : *"Strength and Ductility of Concrete Slabs, Reinforced with Welded Wire Fabric"*, Unpublished.

Neville, A.M., 1970 : *"Creep of Concrete : Plain, Reinforced, and Prestressed"*, North-Holland Publishing Company, Amsterdam, 1970.

Reagel, F.V. and Willis, T.F., 1931 : *"The Effect of the Dimensions of Test Specimens on Modulus of Rupture"*, Public Roads, Vol. 12, April 1931, pp. 37 - 46.

Appendix A

GRAPHICAL PRESENTATION OF TEST RESULTS

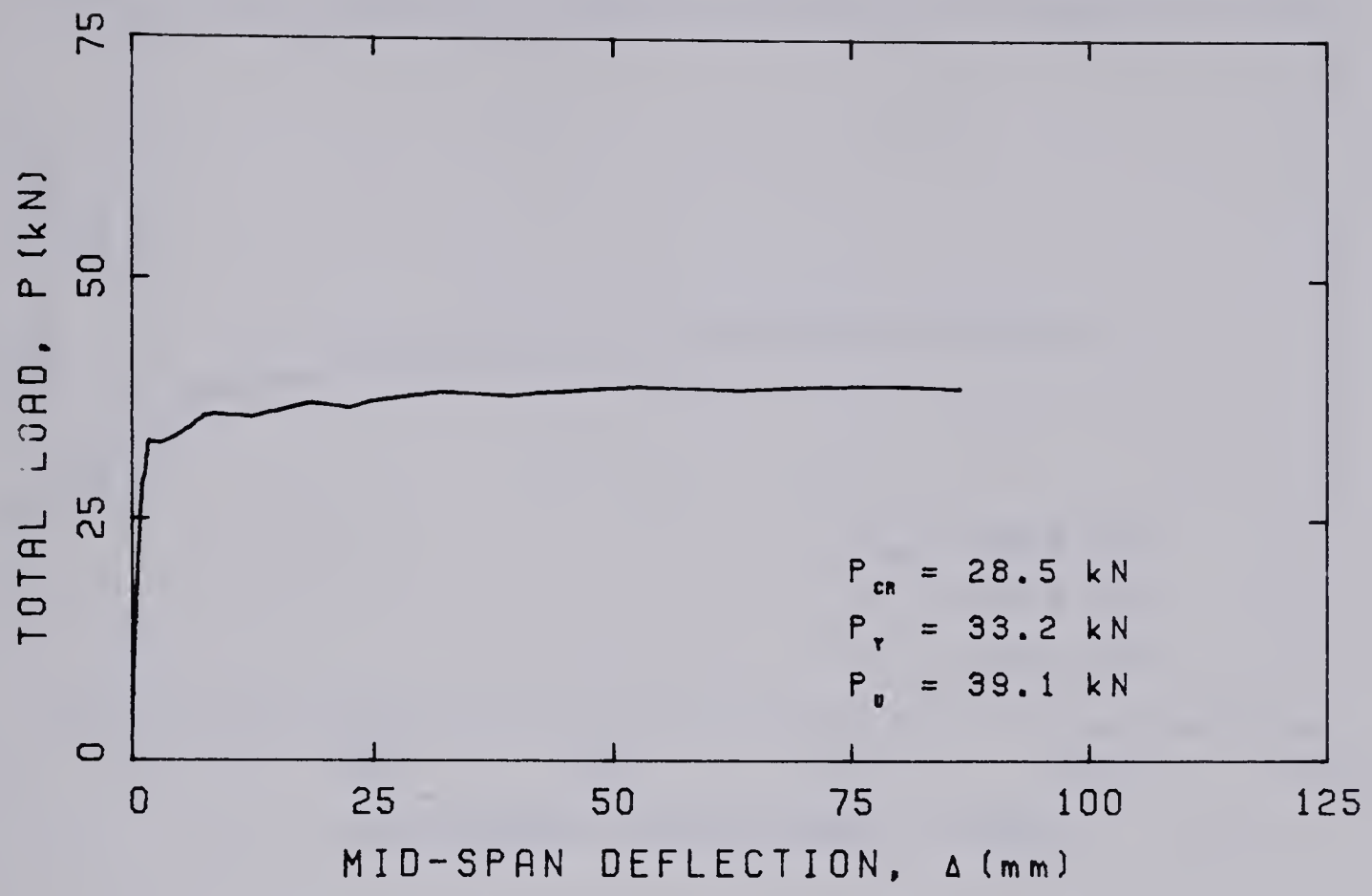

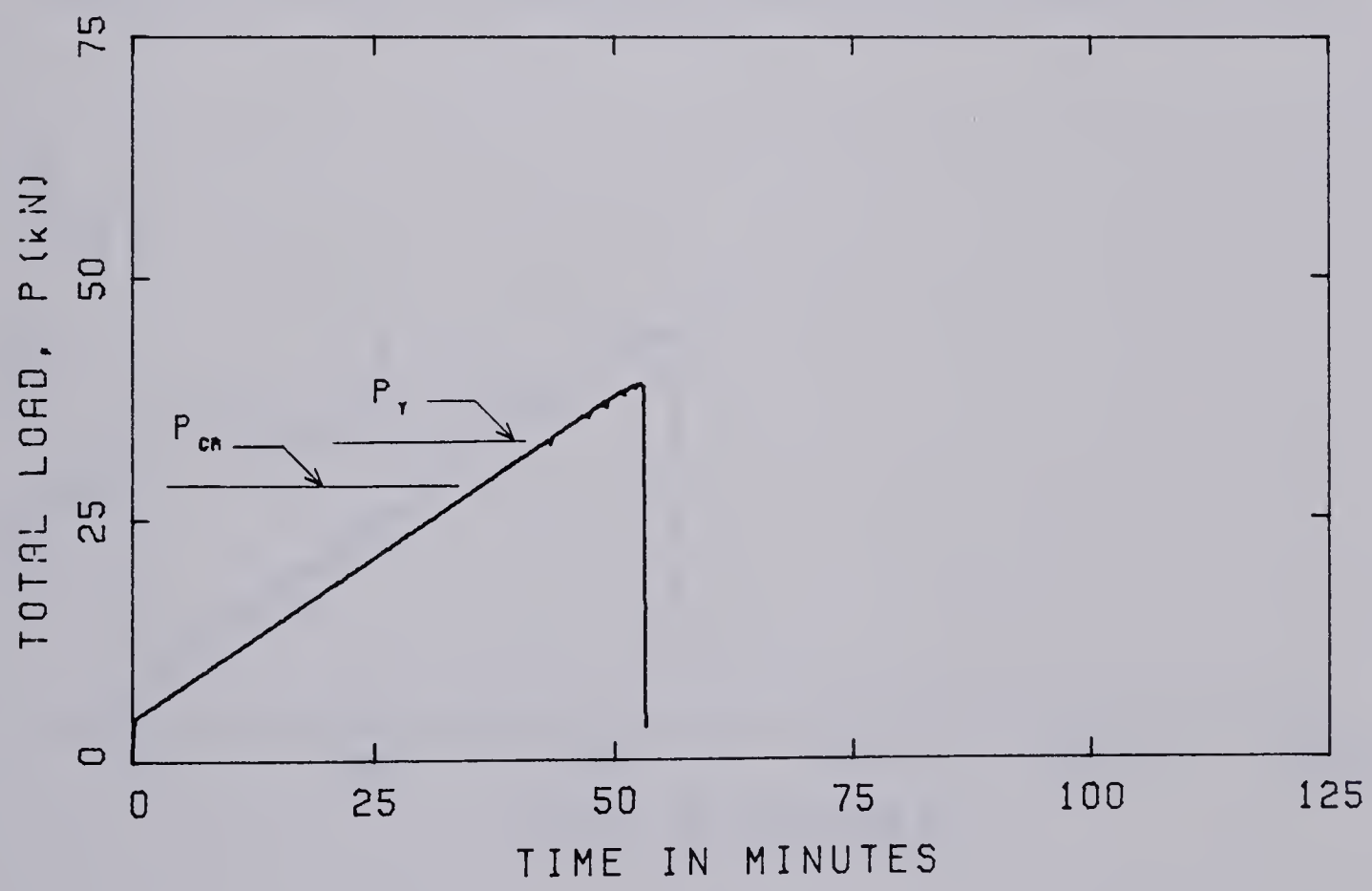

FIGURE A.1 — LOAD-DEFLECTION AND LOAD-TIME CURVES FOR BEAM R1.

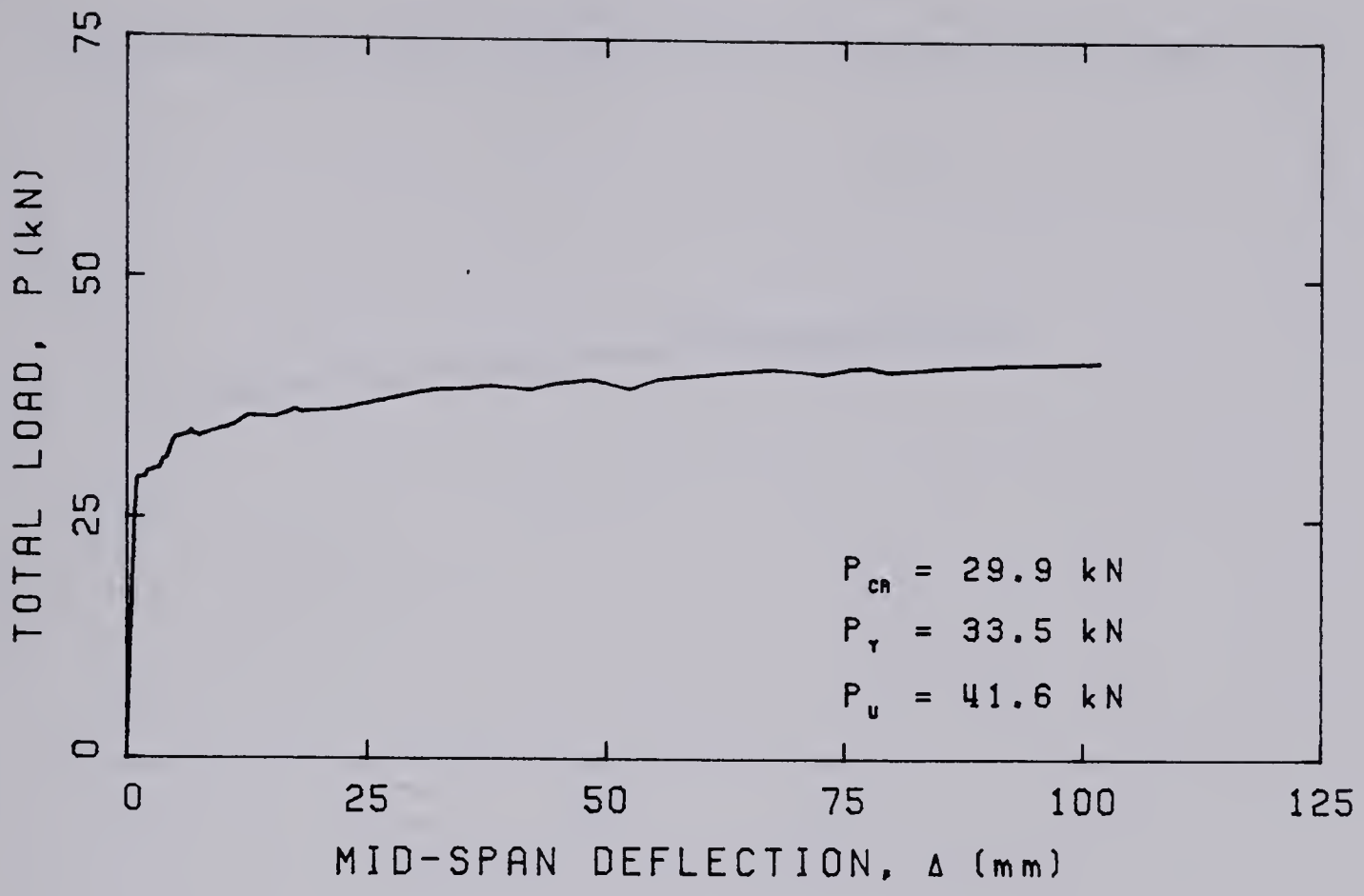

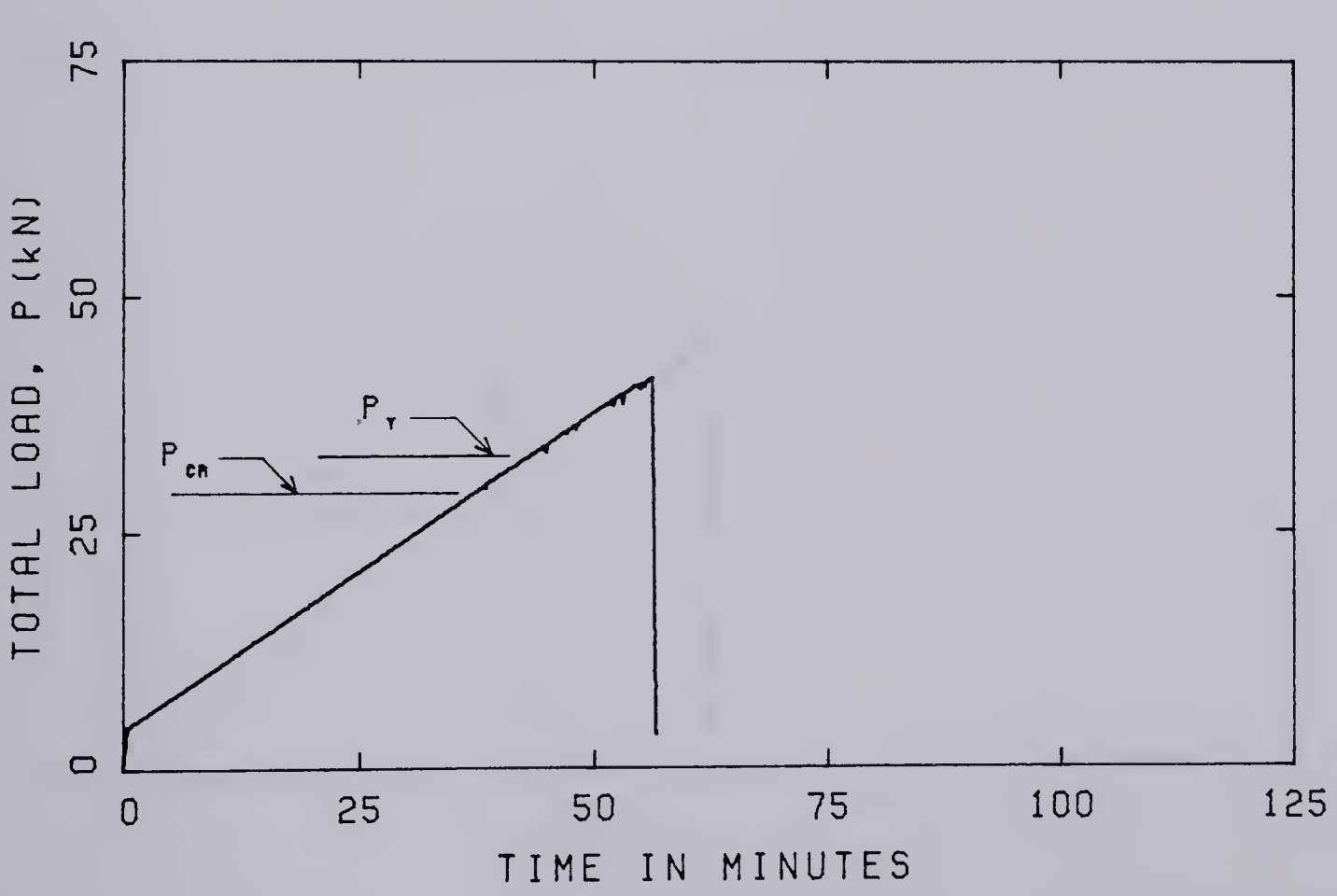

FIGURE A.2 — LOAD-DEFLECTION AND LOAD-TIME CURVES FOR BEAM R2.

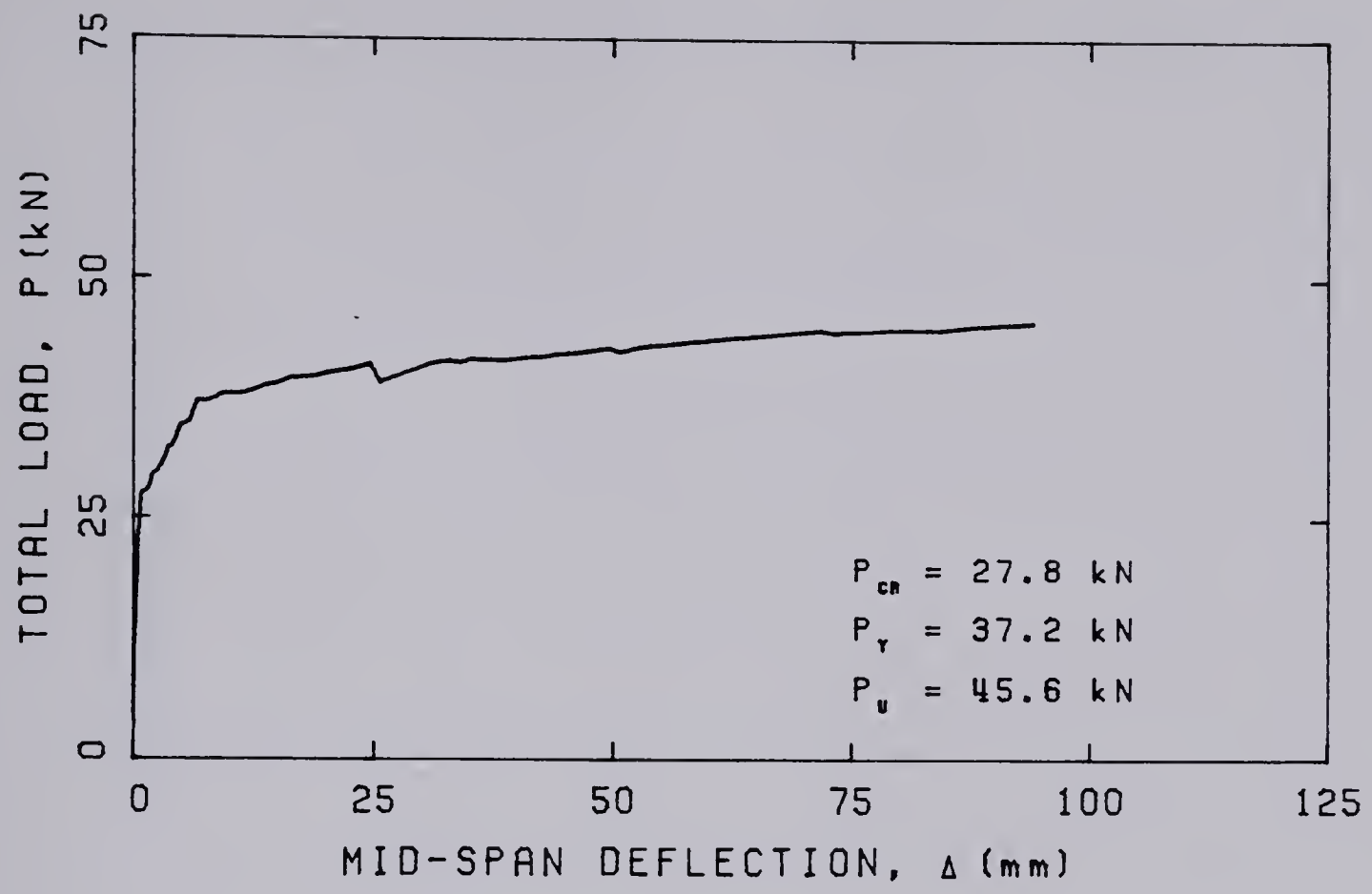

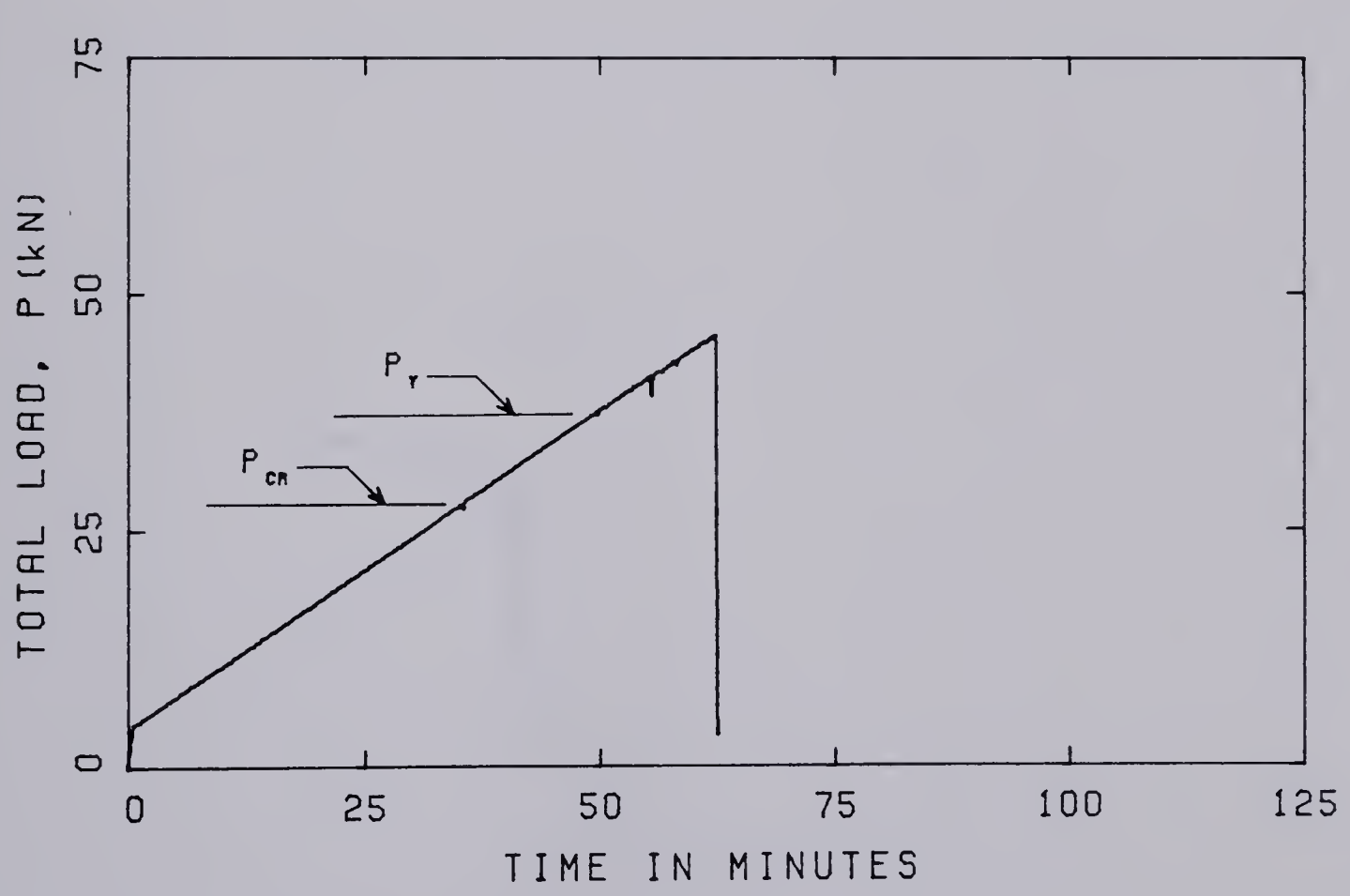

FIGURE A.3 — LOAD-DEFLECTION AND LOAD-TIME CURVES FOR BEAM R3.

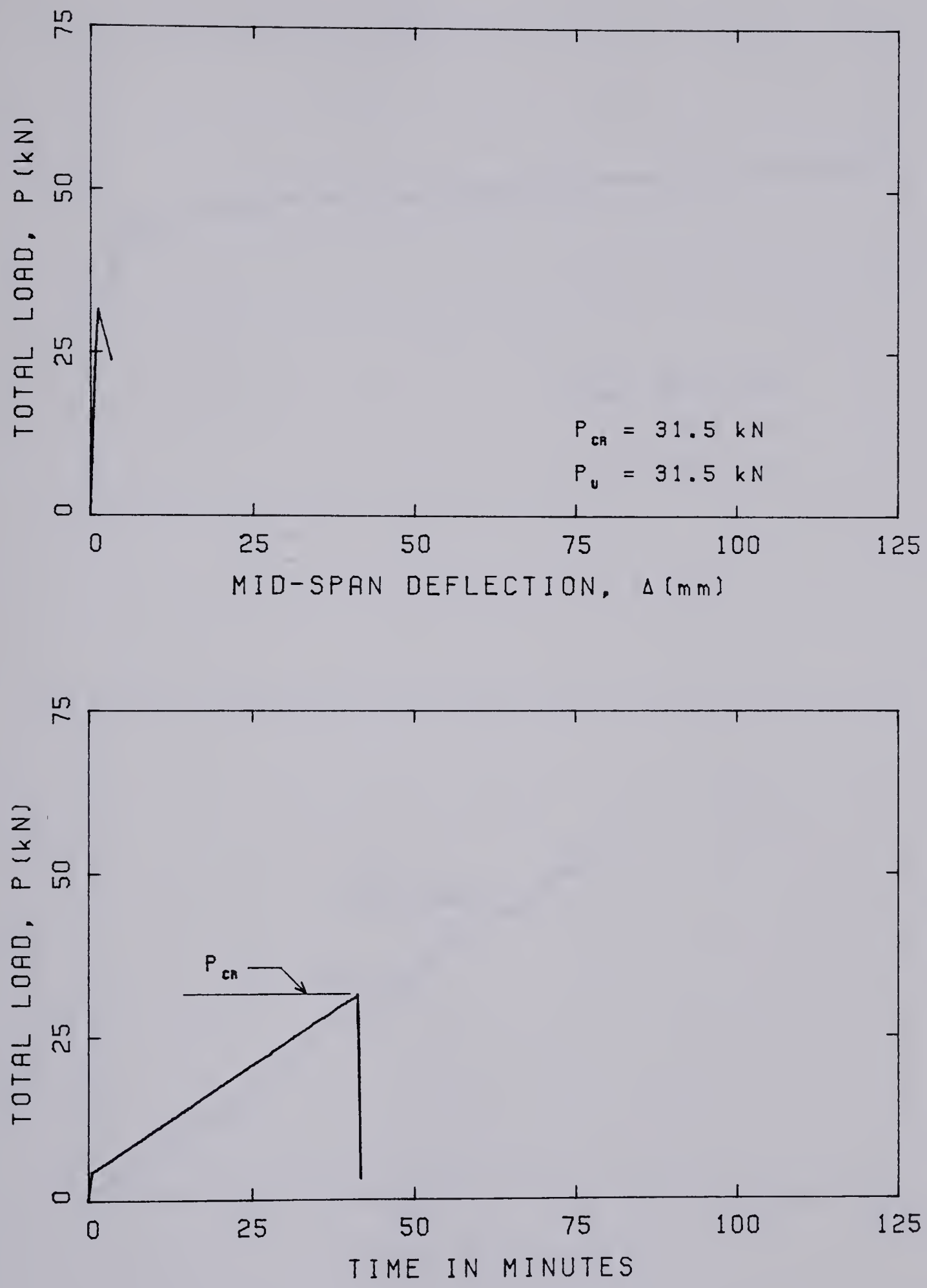

FIGURE A.4 — LOAD-DEFLECTION AND LOAD-TIME CURVES FOR BEAM R4.

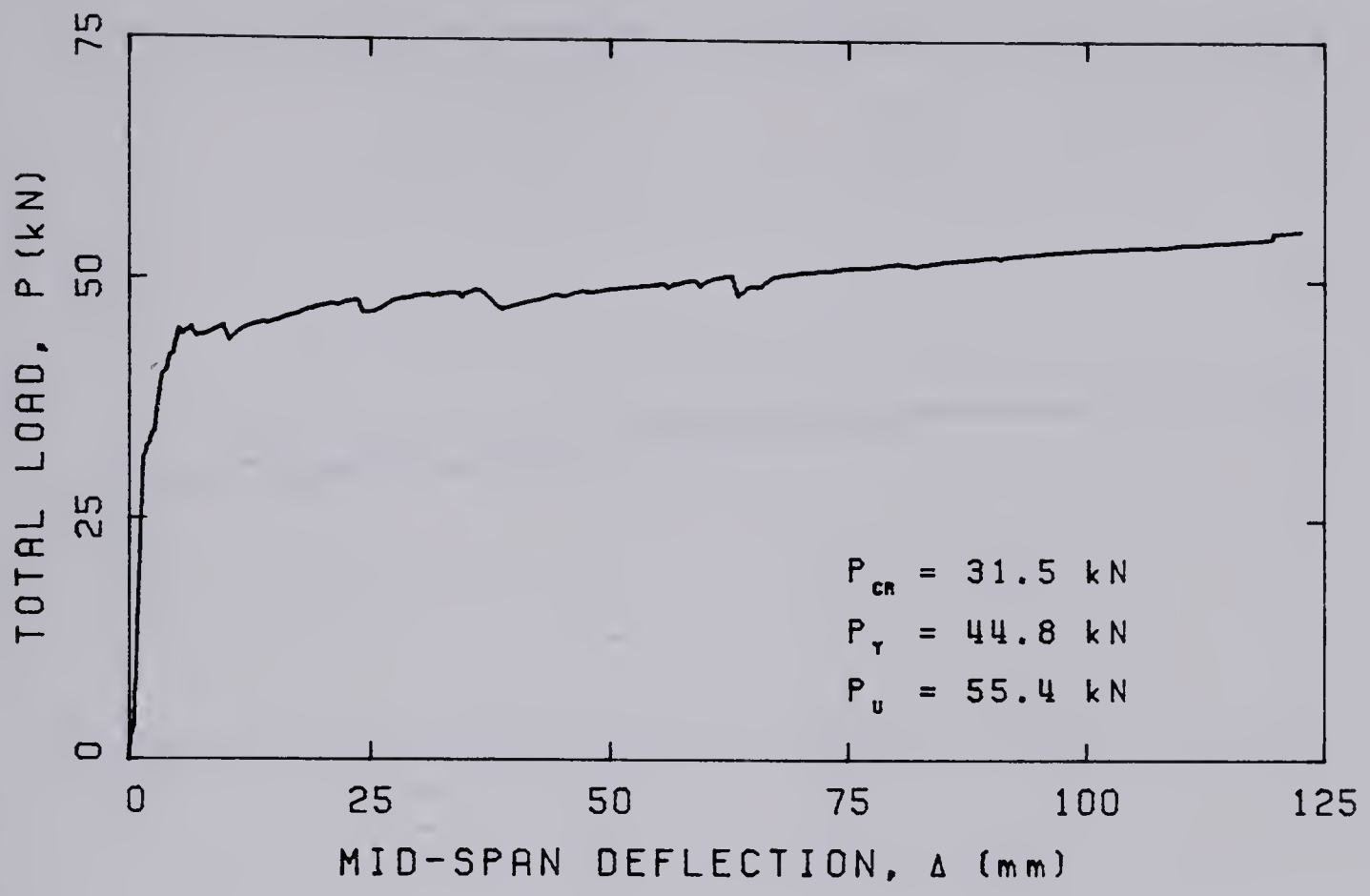

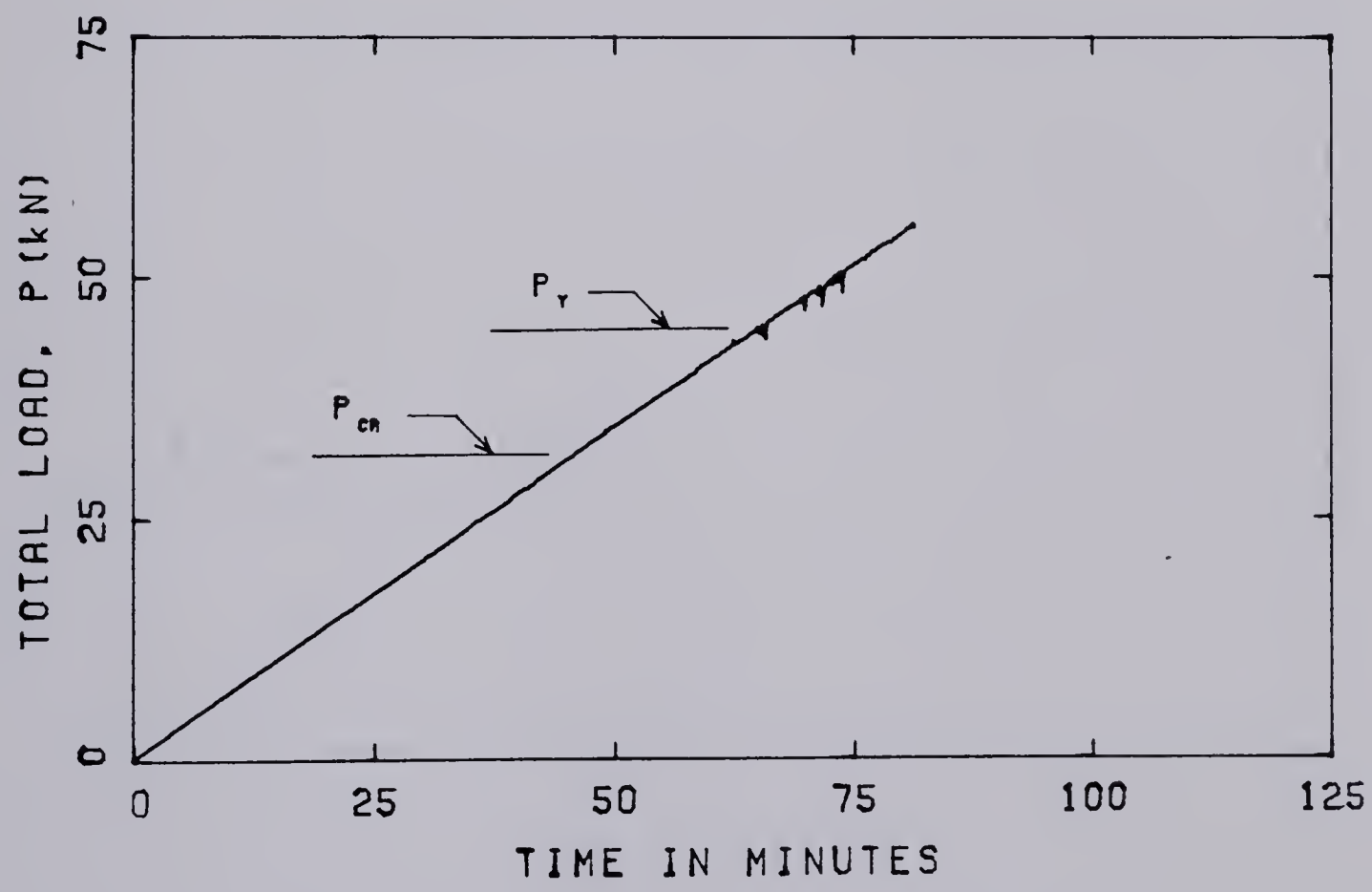

FIGURE A.5 — LOAD-DEFLECTION AND LOAD-TIME CURVES FOR BEAM R5.

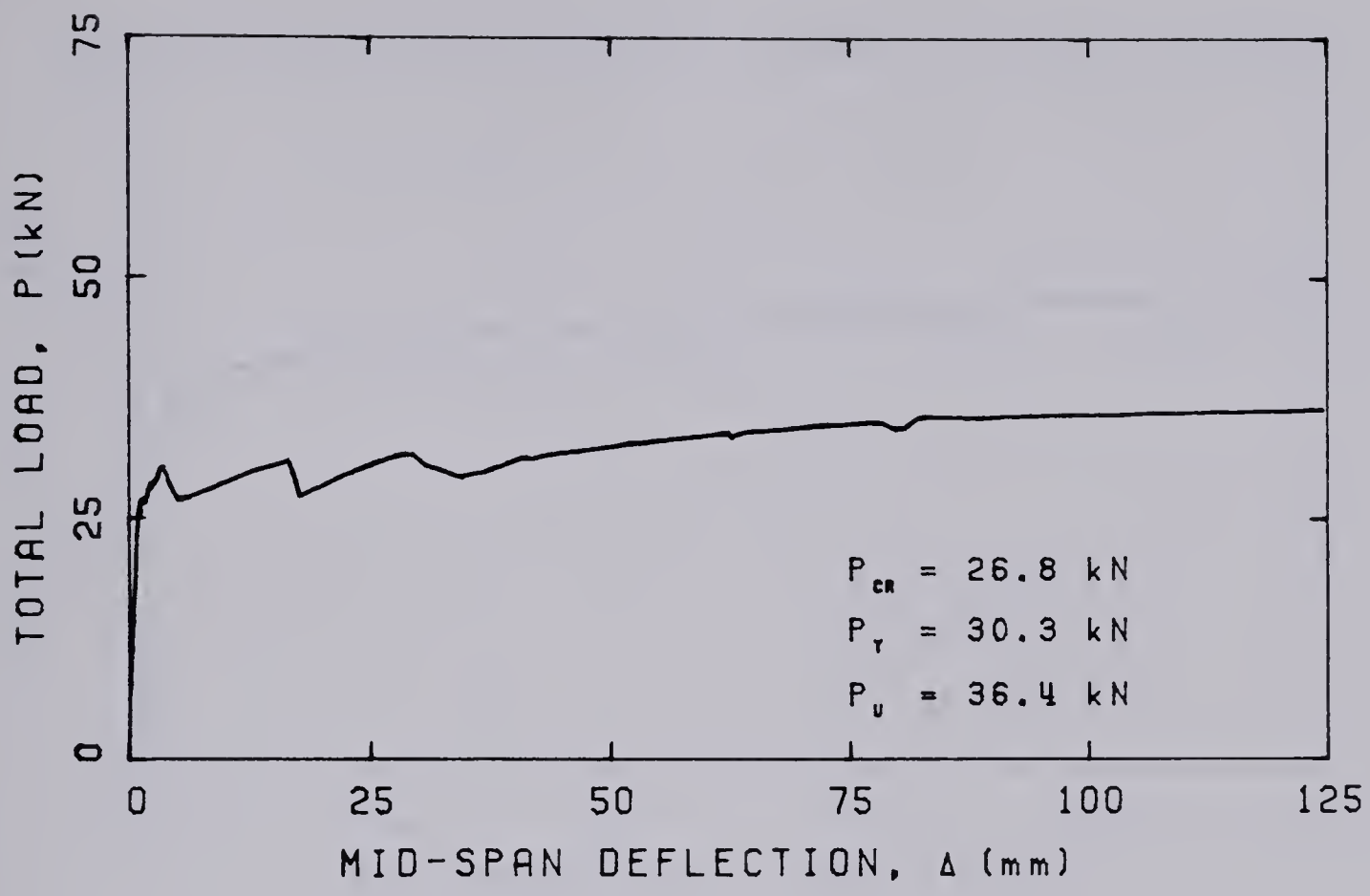

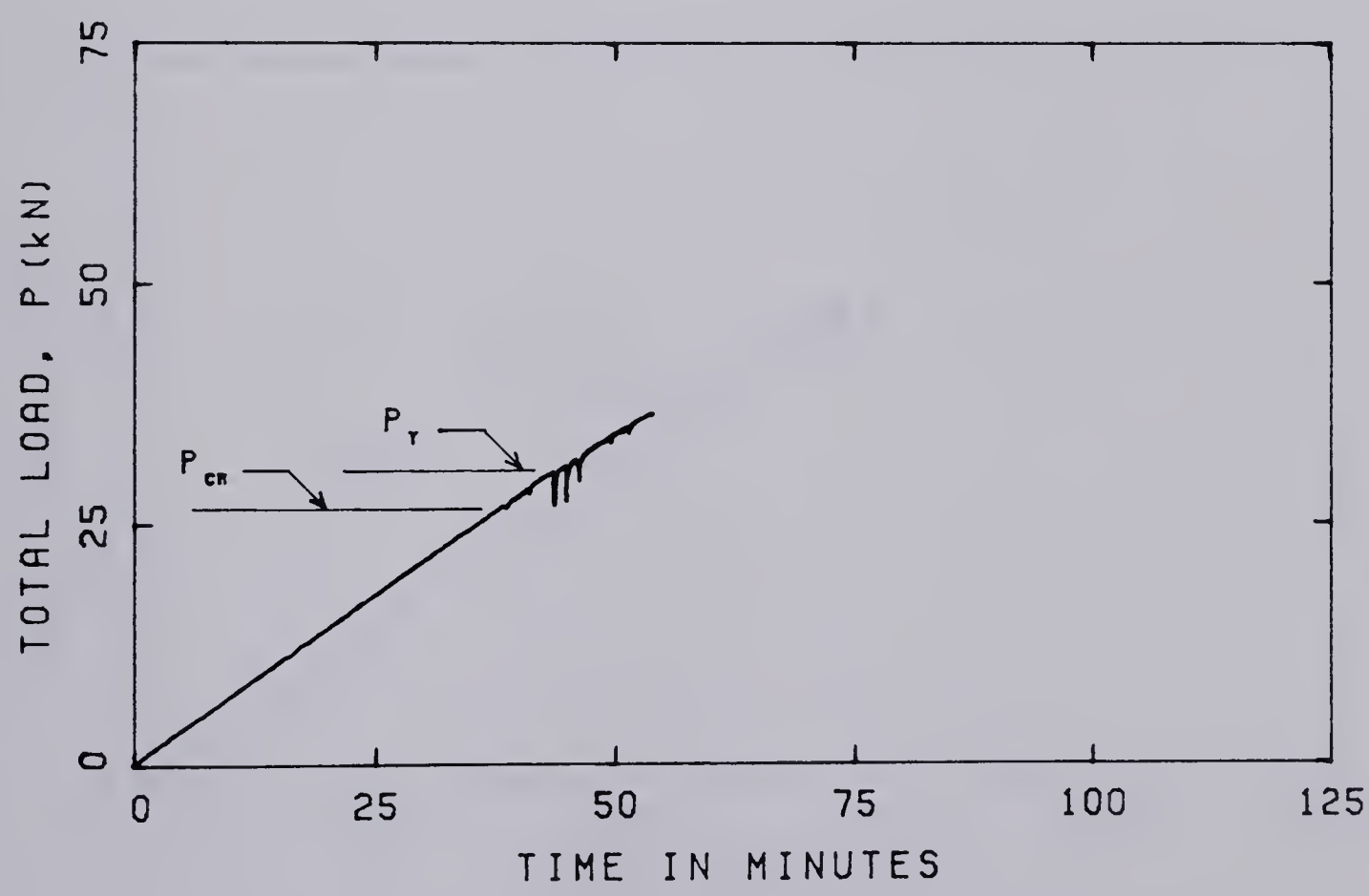

FIGURE A.6 — LOAD-DEFLECTION AND LOAD-TIME CURVES FOR BEAM R6.

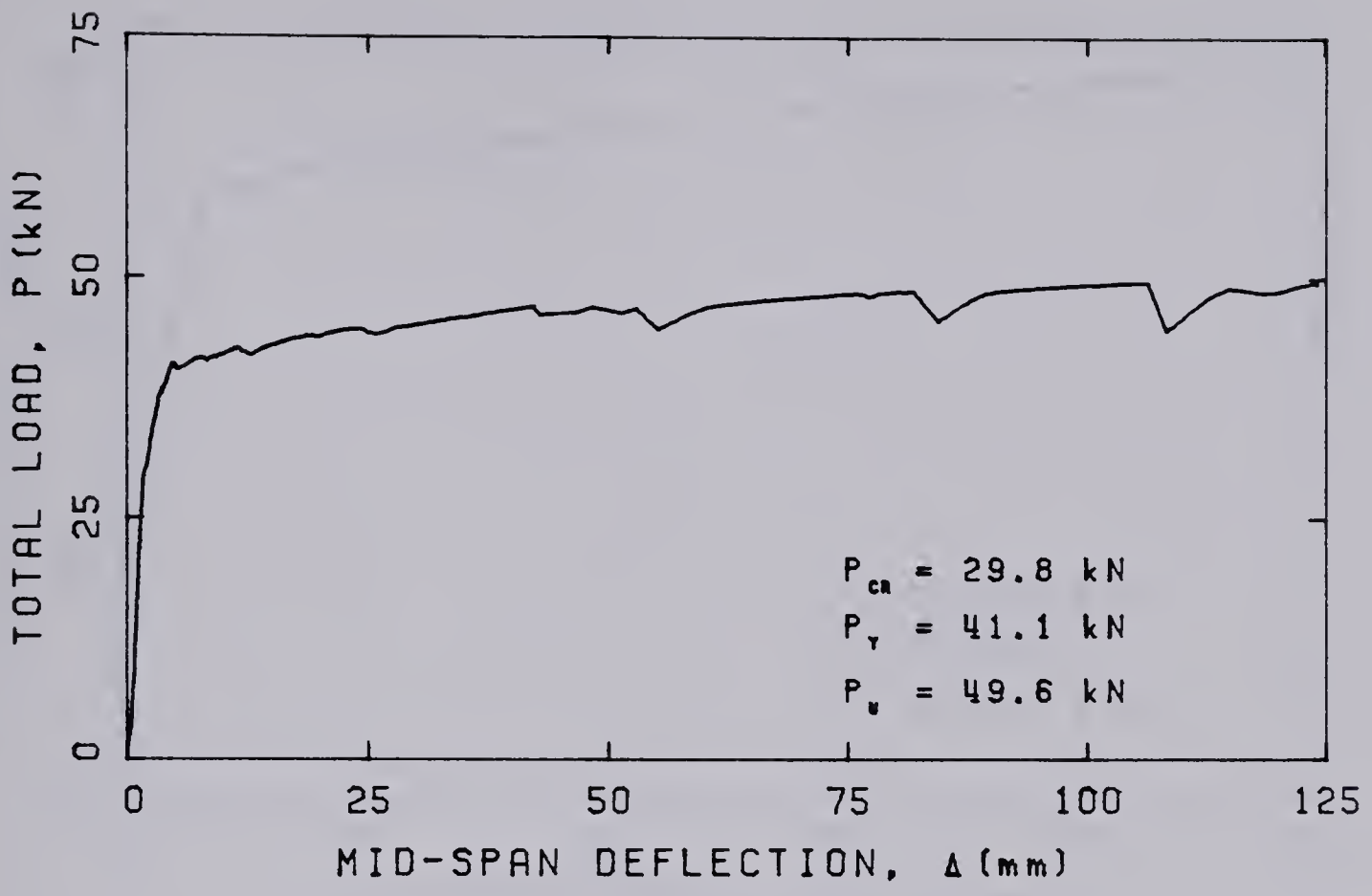

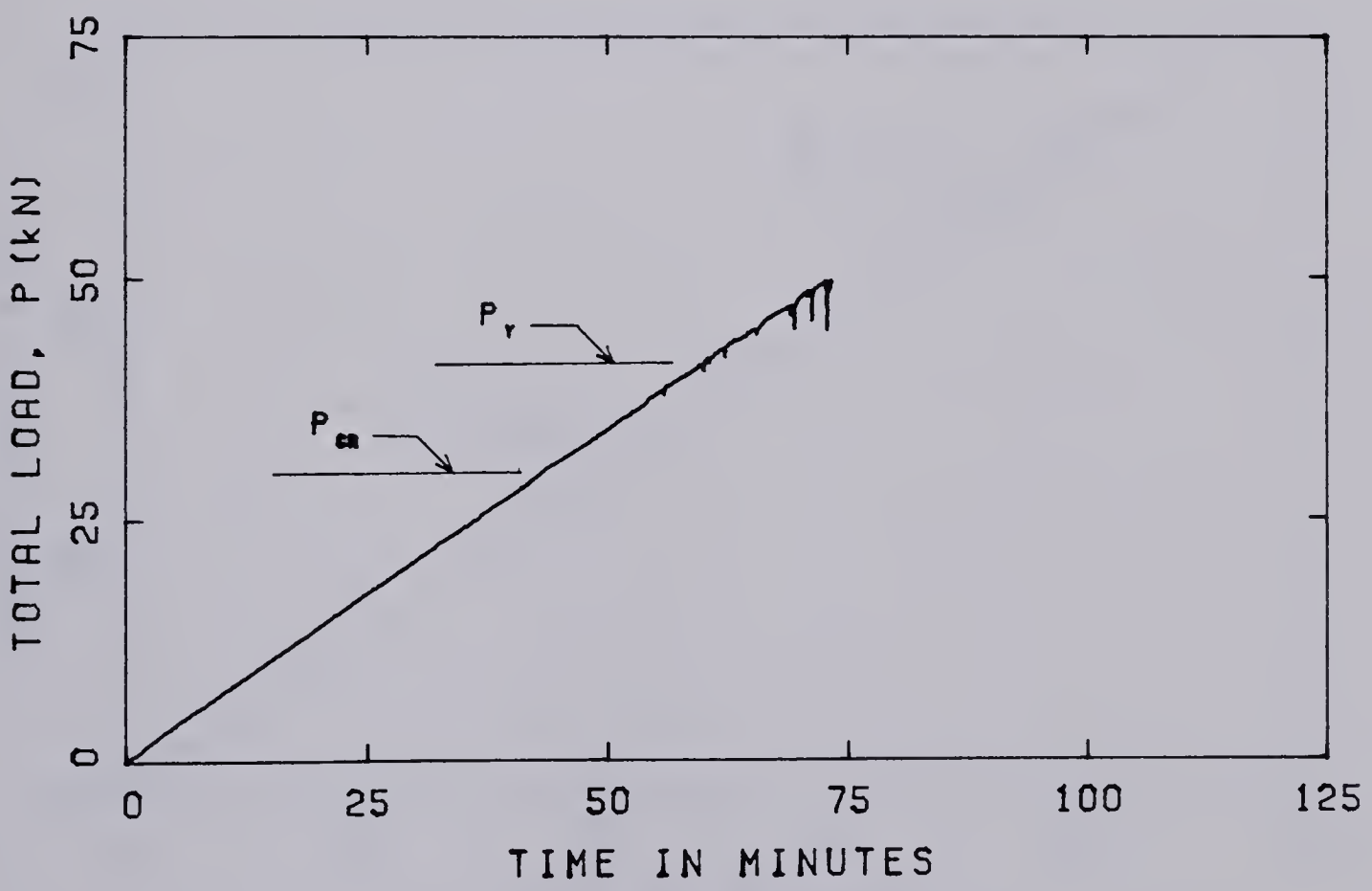

FIGURE A.7 — LOAD-DEFLECTION AND LOAD-TIME CURVES FOR BEAM R7.

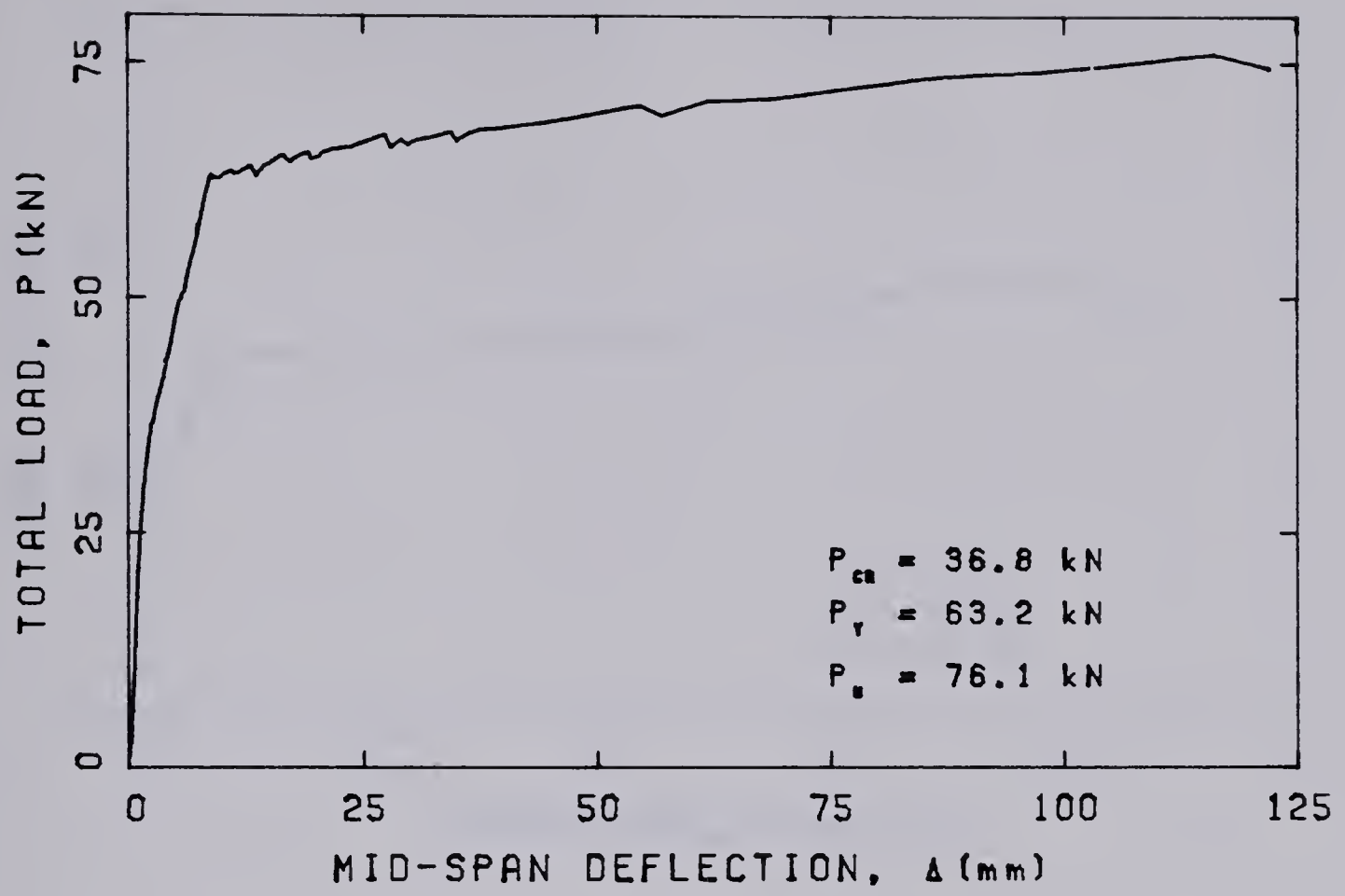

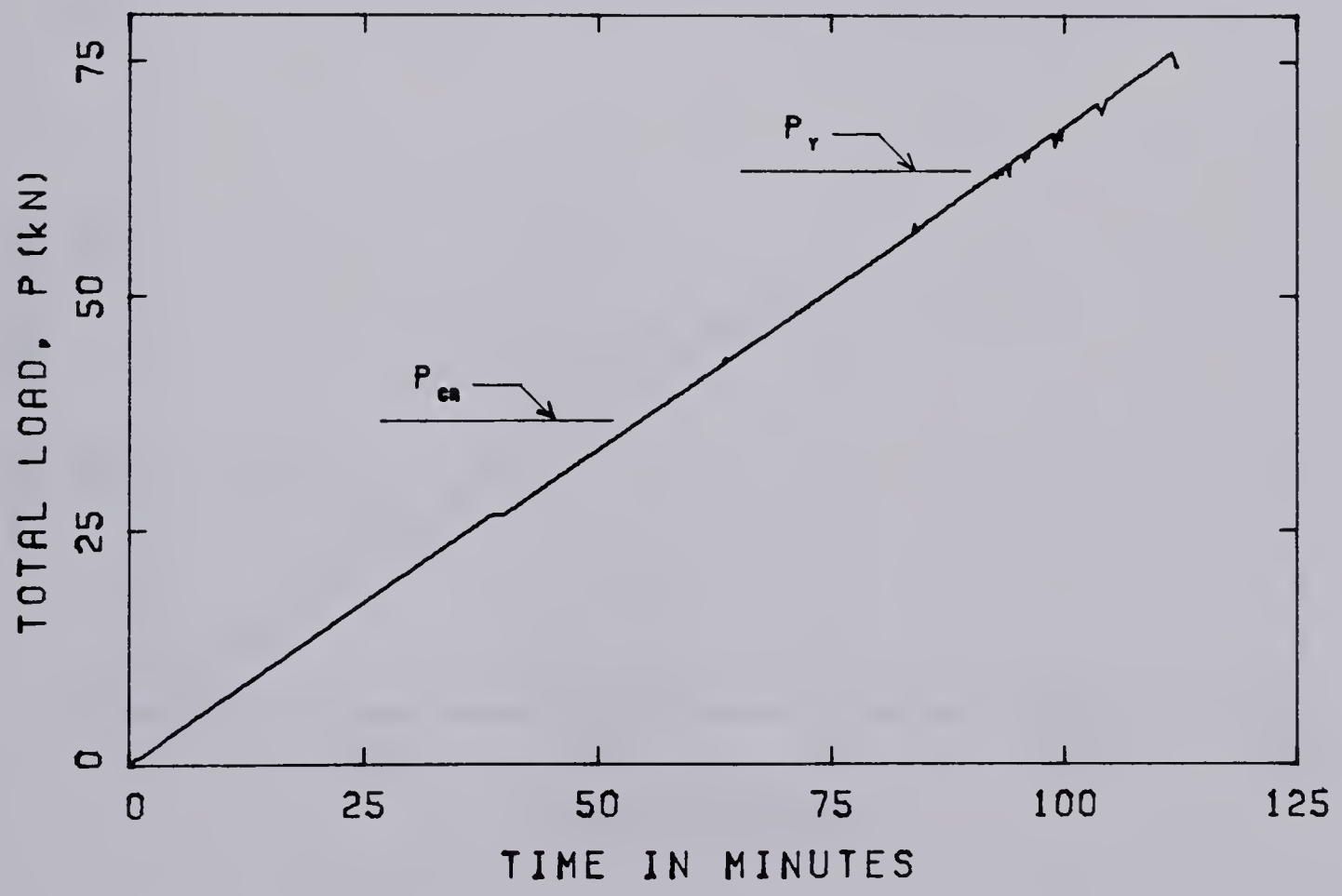

FIGURE A.8 — LOAD-DEFLECTION AND LOAD-TIME CURVES FOR BEAM R8.

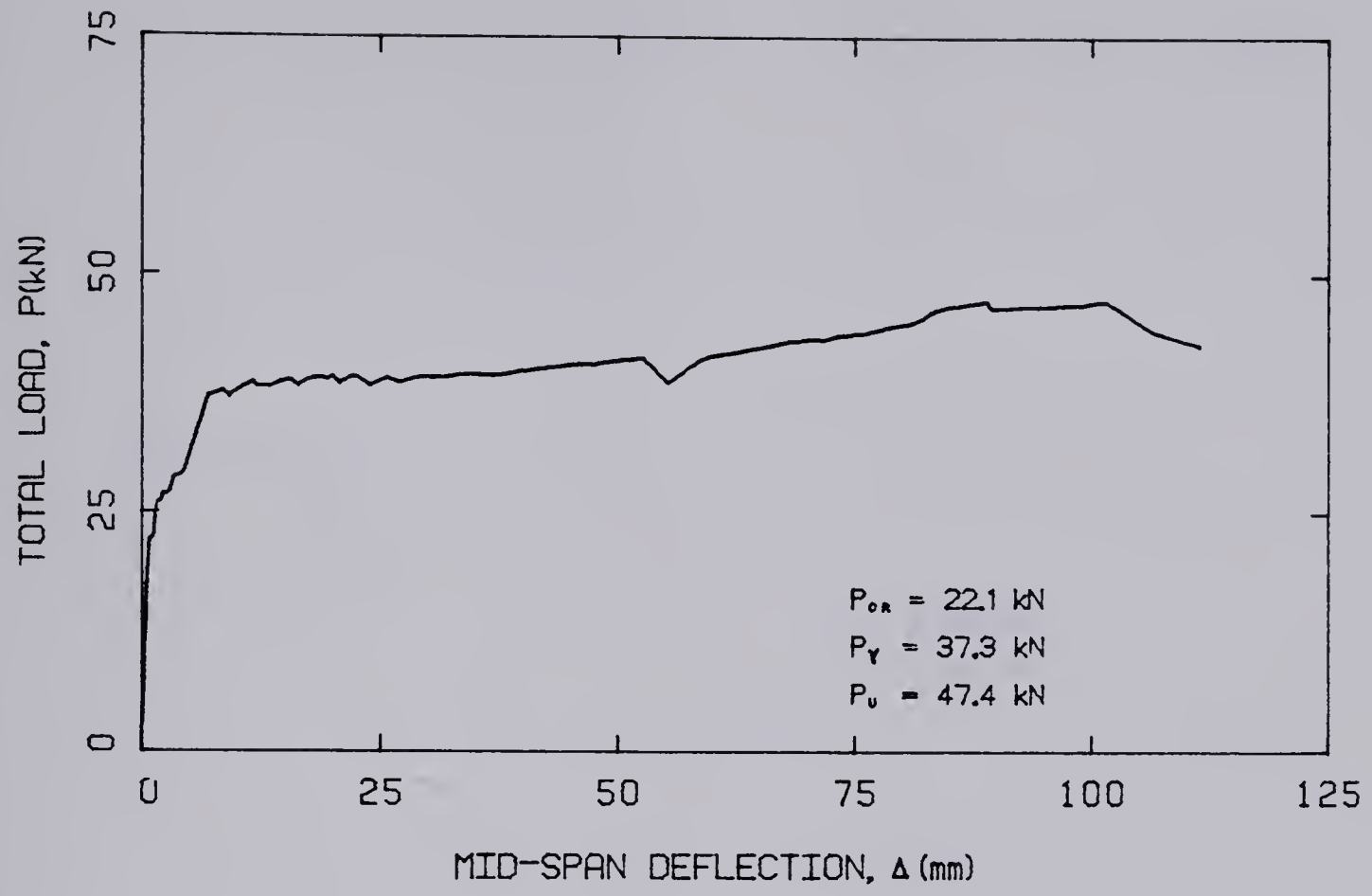

FIGURE A.9 — LOAD-DEFLECTION AND LOAD-TIME CURVES FOR BEAM T1.

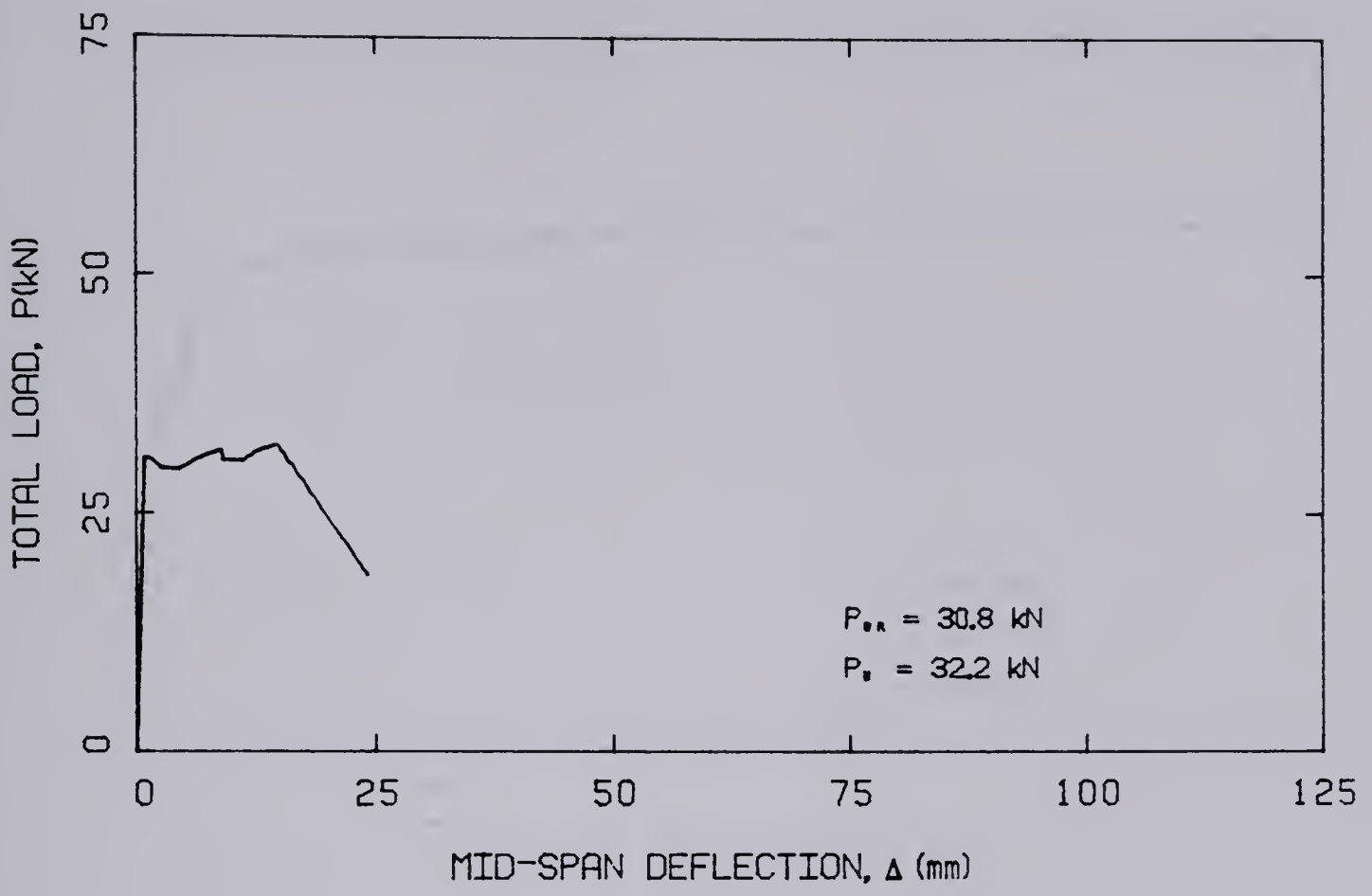

FIGURE A.10 — LOAD-DEFLECTION AND LOAD-TIME CURVES FOR BEAM T2.

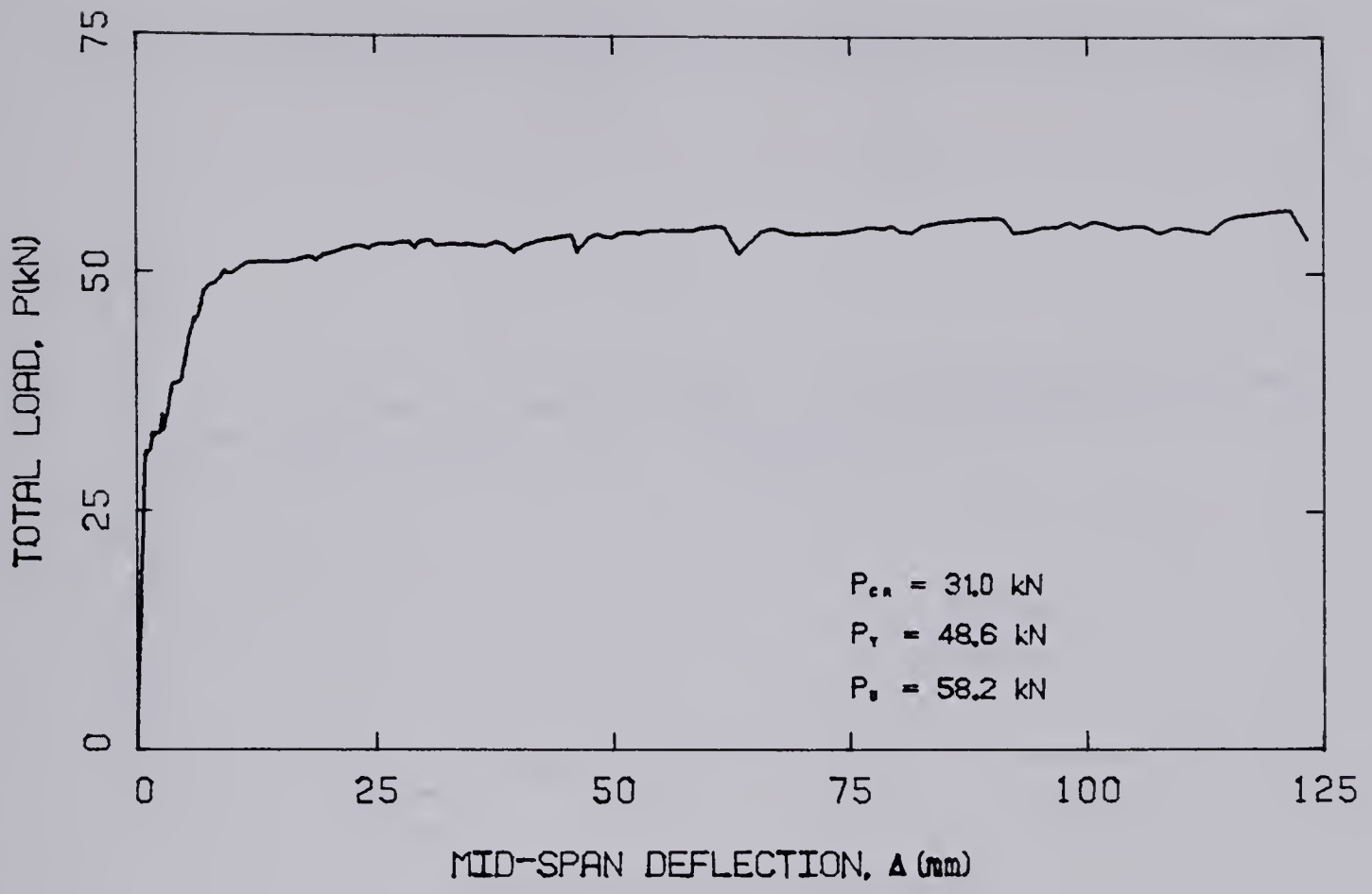

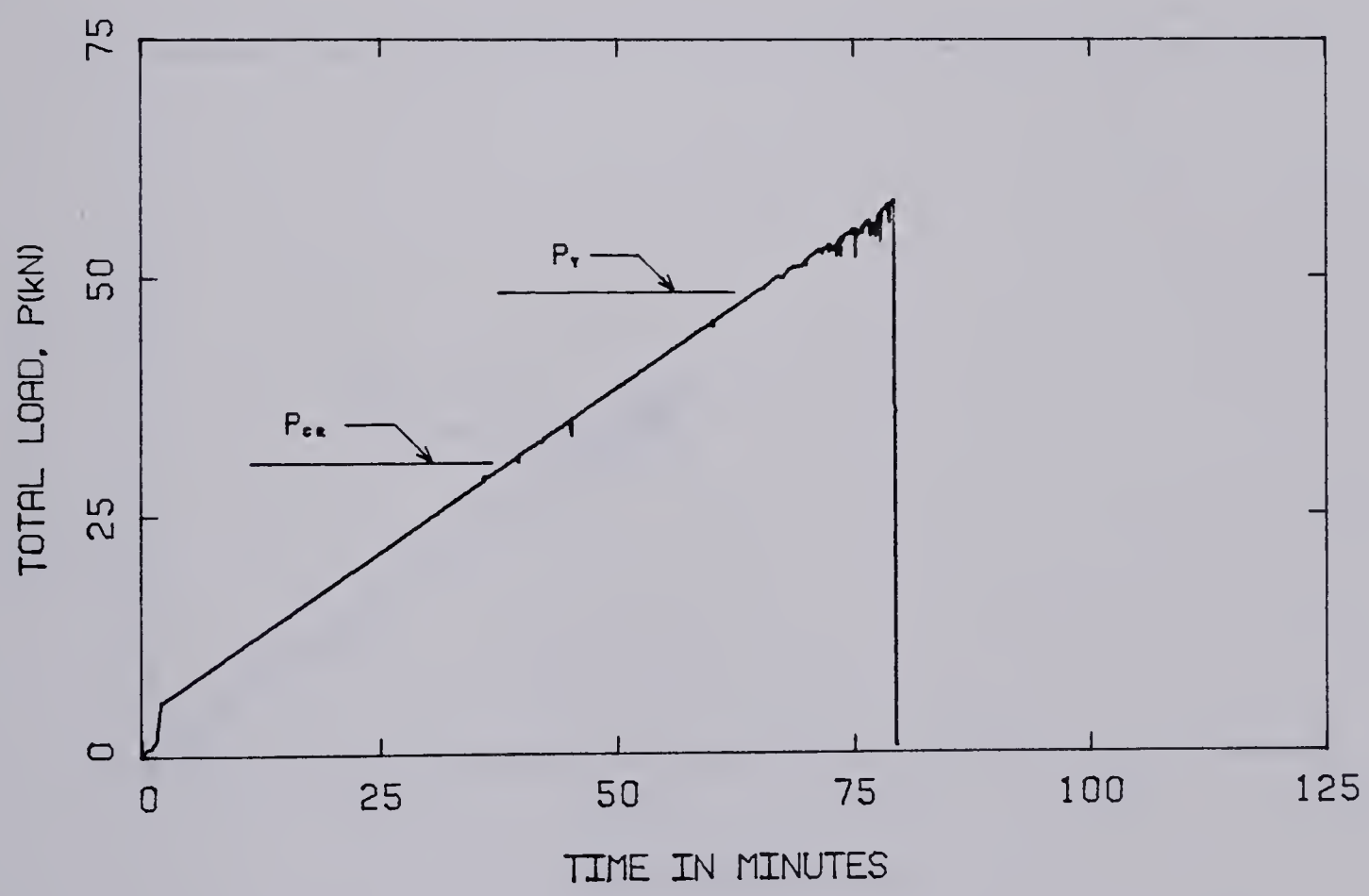

FIGURE A.11 — LOAD-DEFLECTION AND LOAD-TIME CURVES FOR BEAM T3.

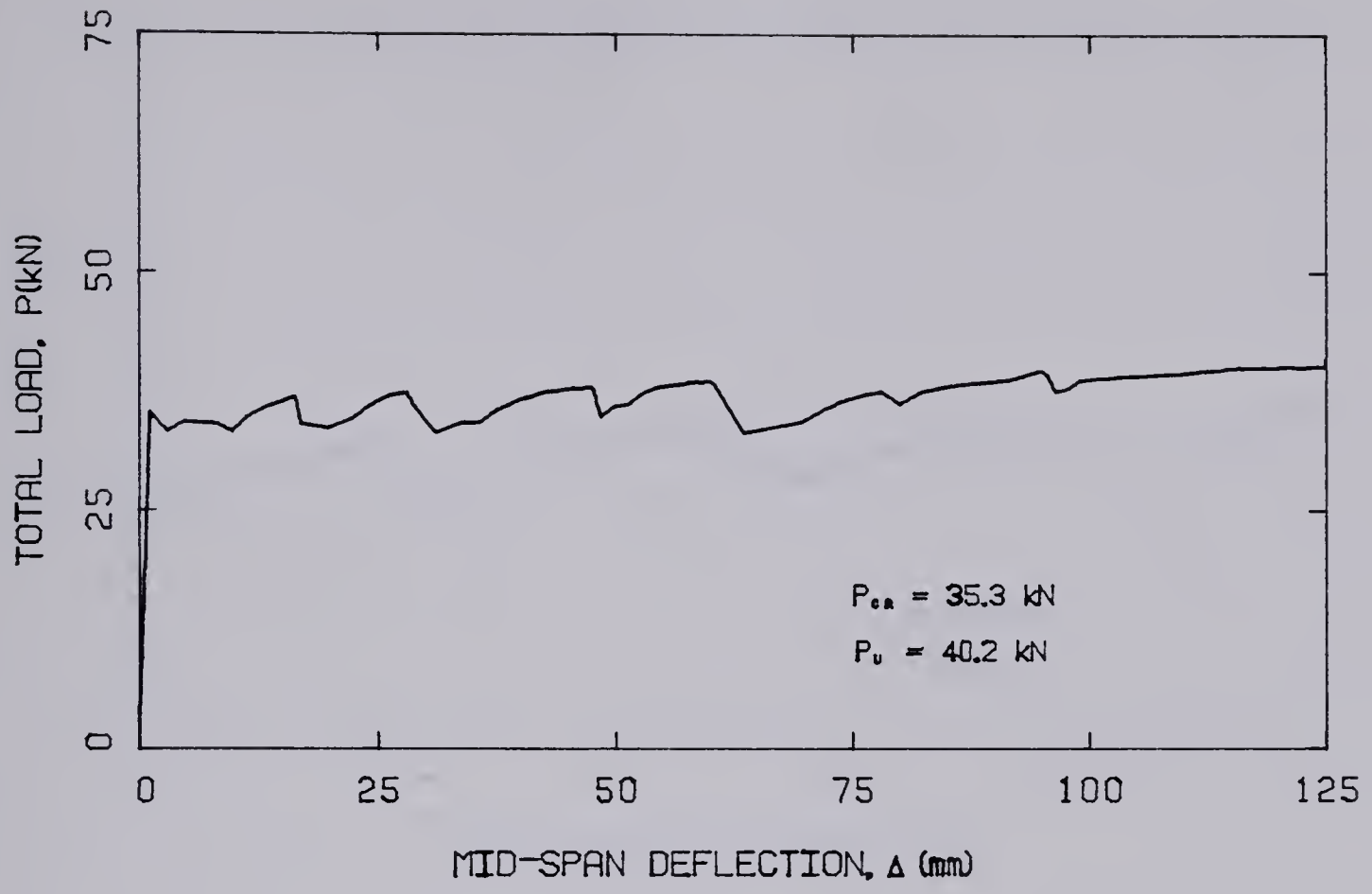

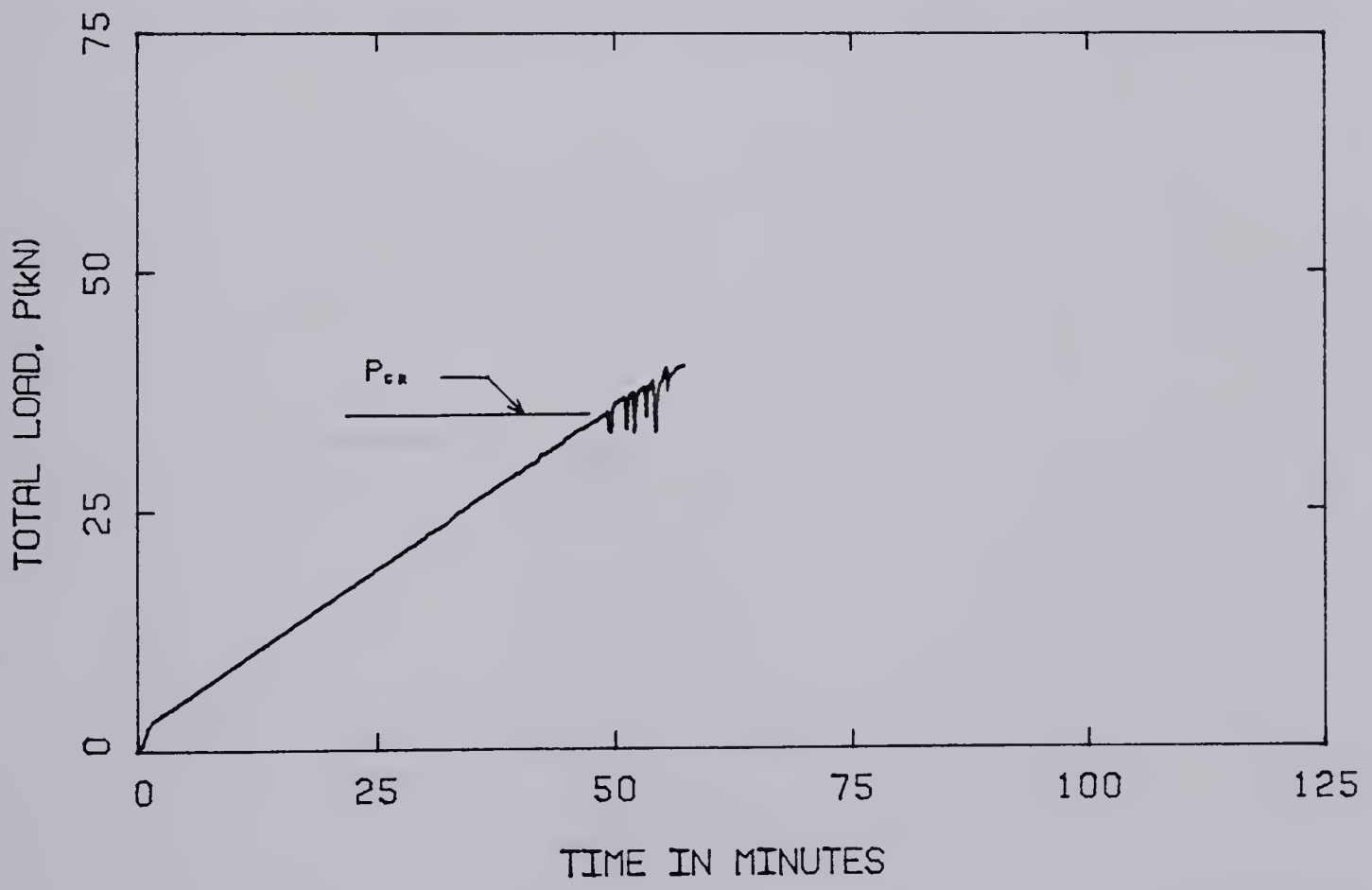

FIGURE A.12 — LOAD-DEFLECTION AND LOAD-TIME CURVES FOR BEAM T4.

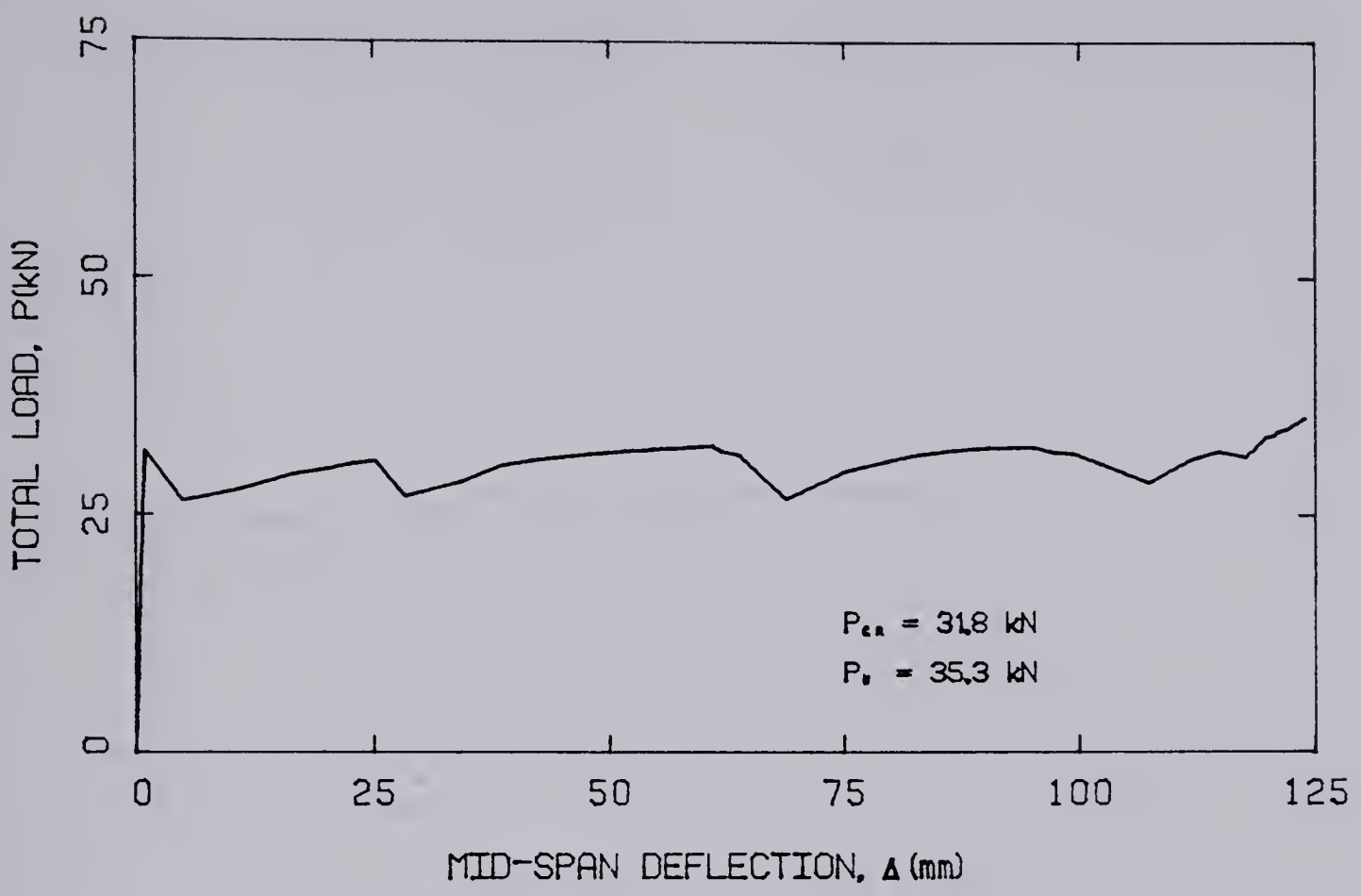

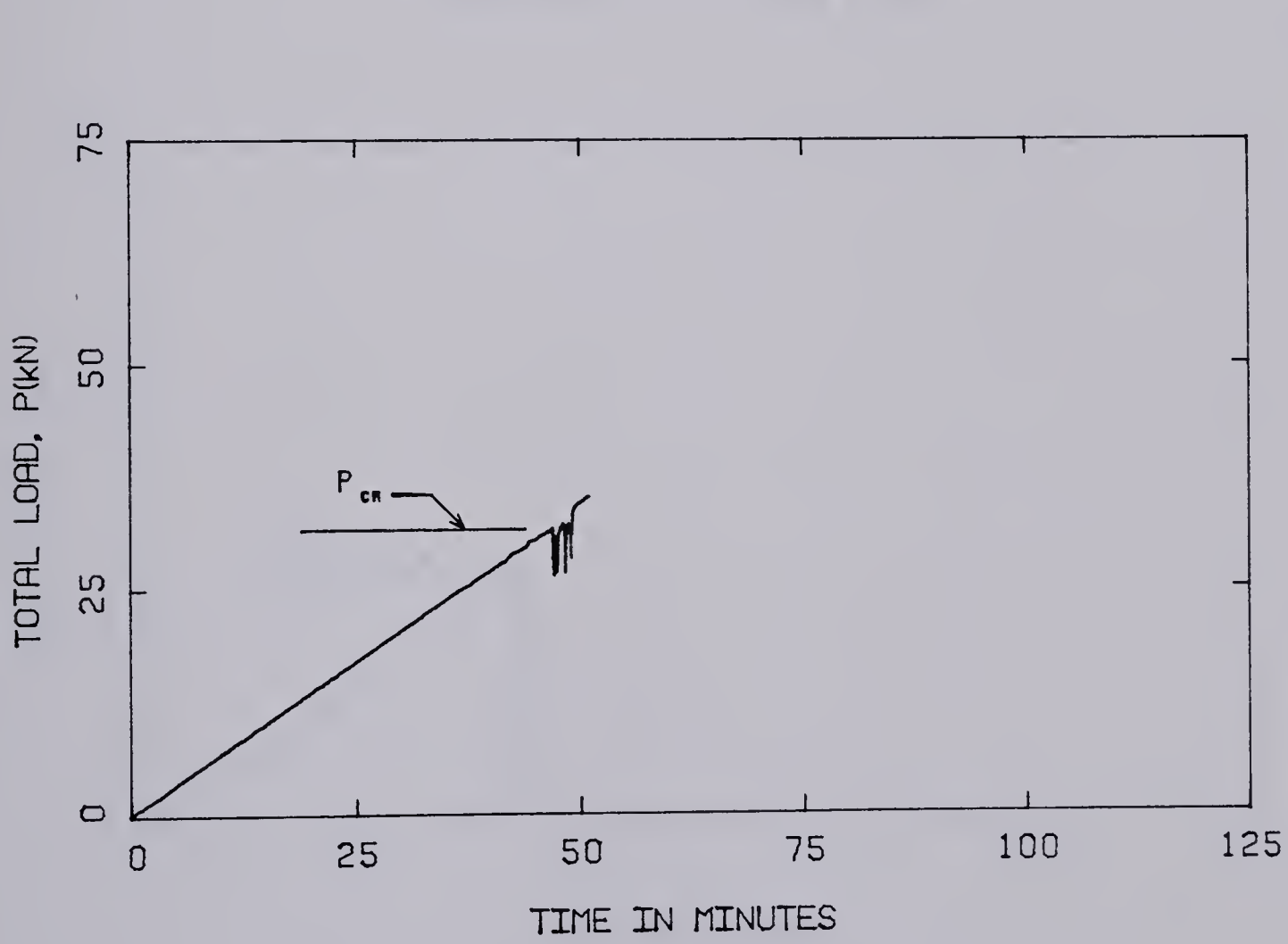

FIGURE A.13 — LOAD-DEFLECTION AND LOAD-TIME CURVES FOR BEAM T5.

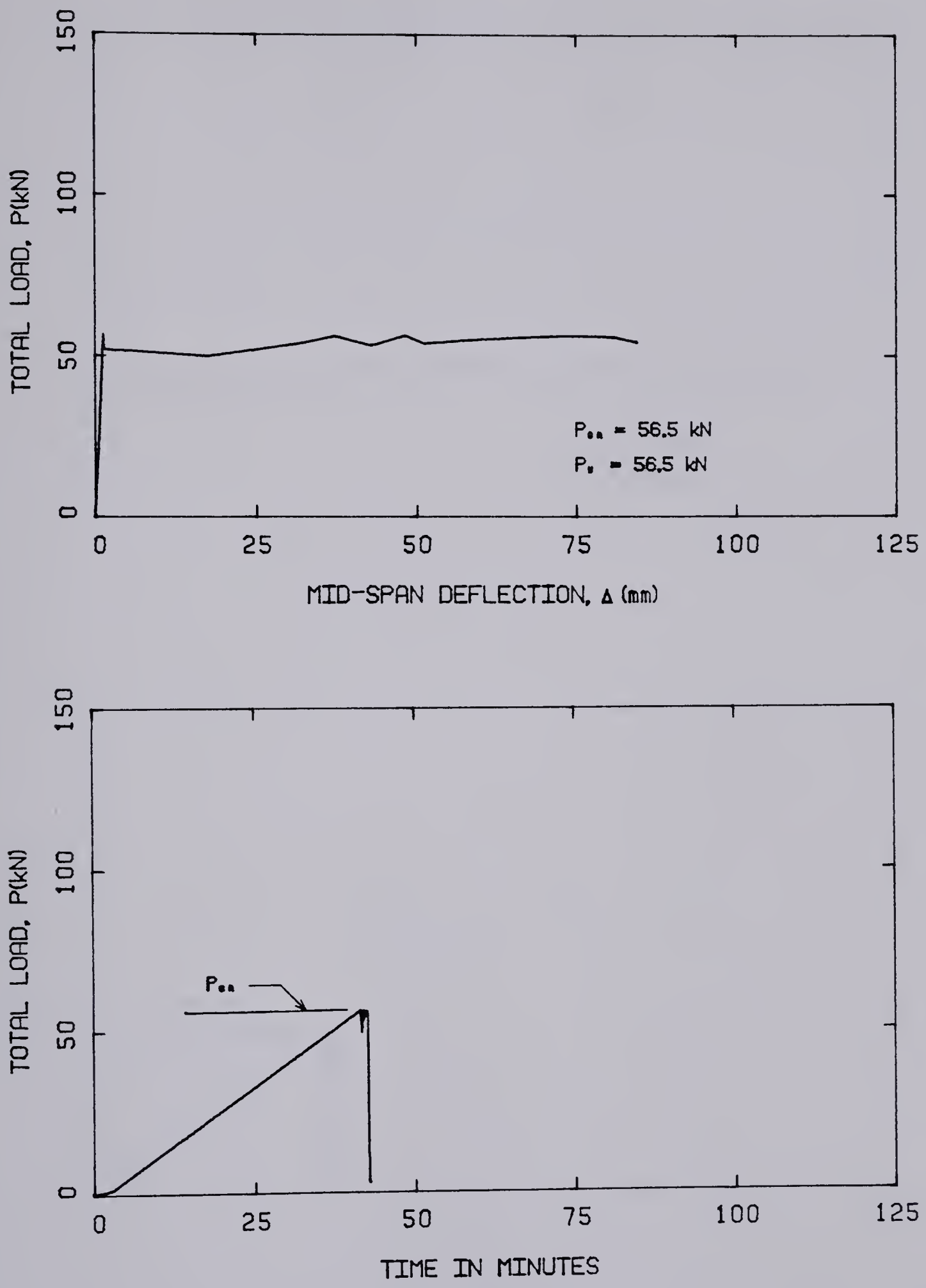

FIGURE A.14 — LOAD-DEFLECTION AND LOAD-TIME CURVES FOR BEAM I1.

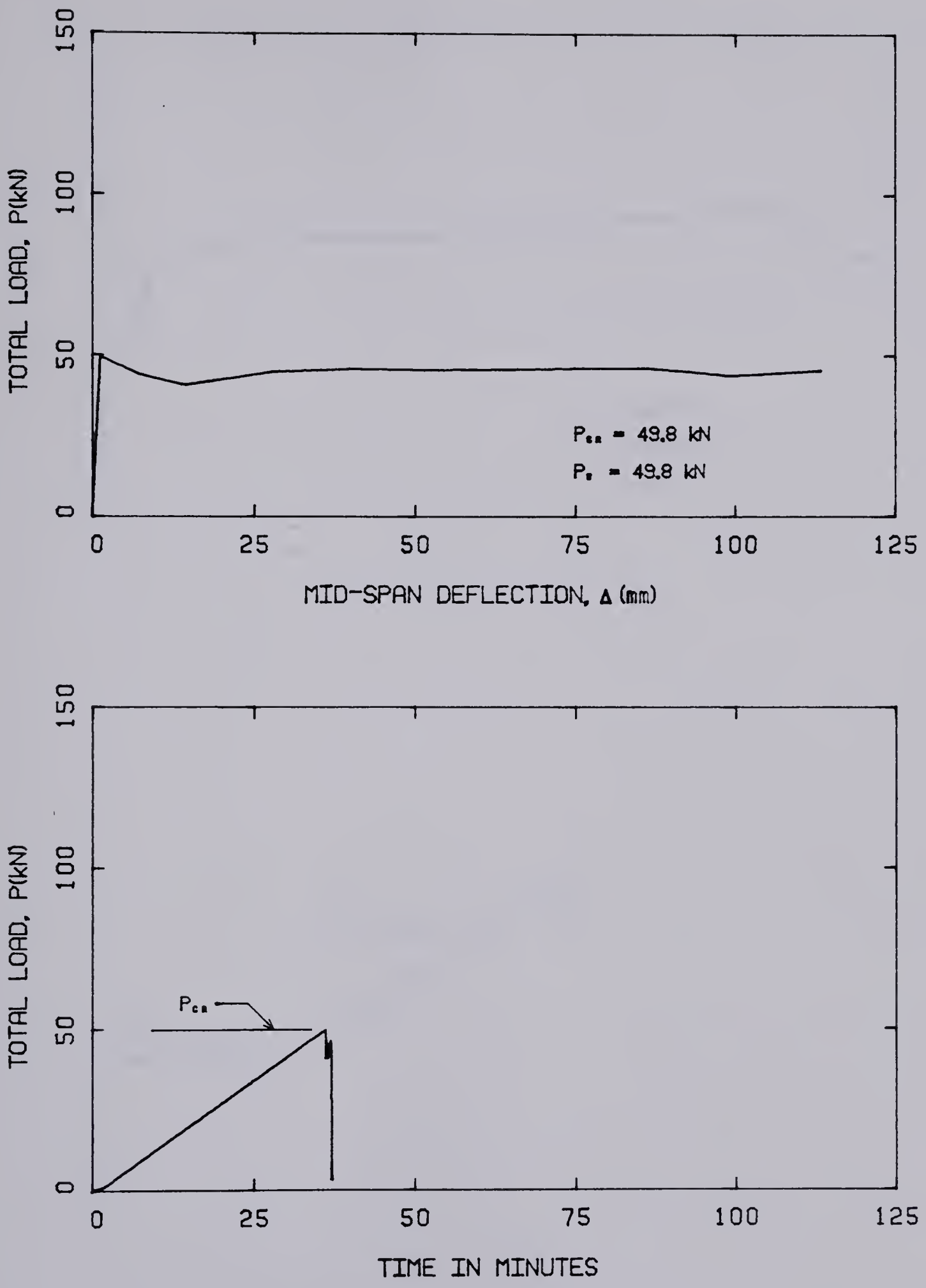

FIGURE A.15 — LOAD-DEFLECTION AND LOAD-TIME CURVES FOR BEAM I2.

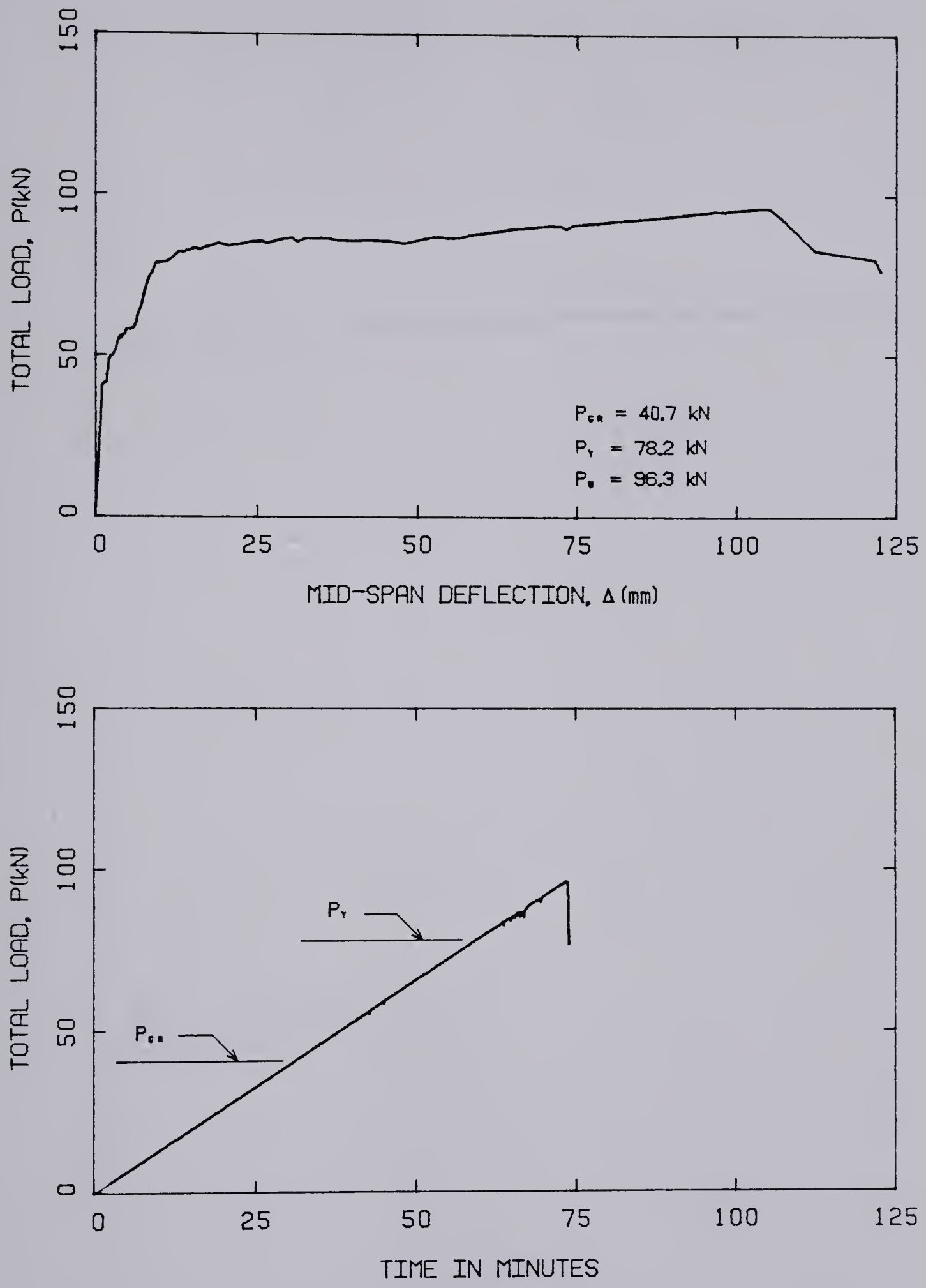

FIGURE A.16 — LOAD-DEFLECTION AND LOAD-TIME CURVES FOR BEAM I3.

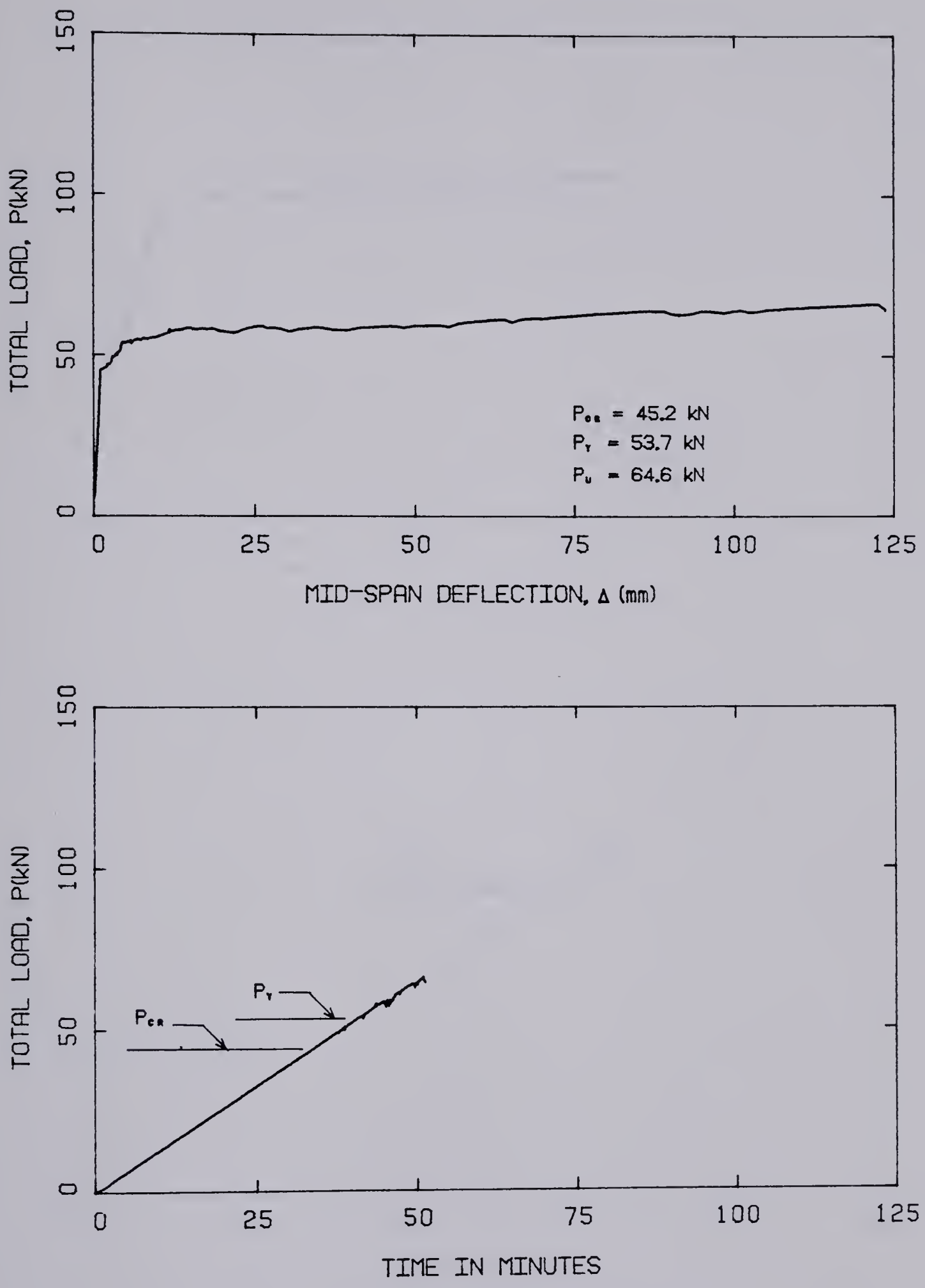

FIGURE A.17 — LOAD-DEFLECTION AND LOAD-TIME CURVES FOR BEAM I4.

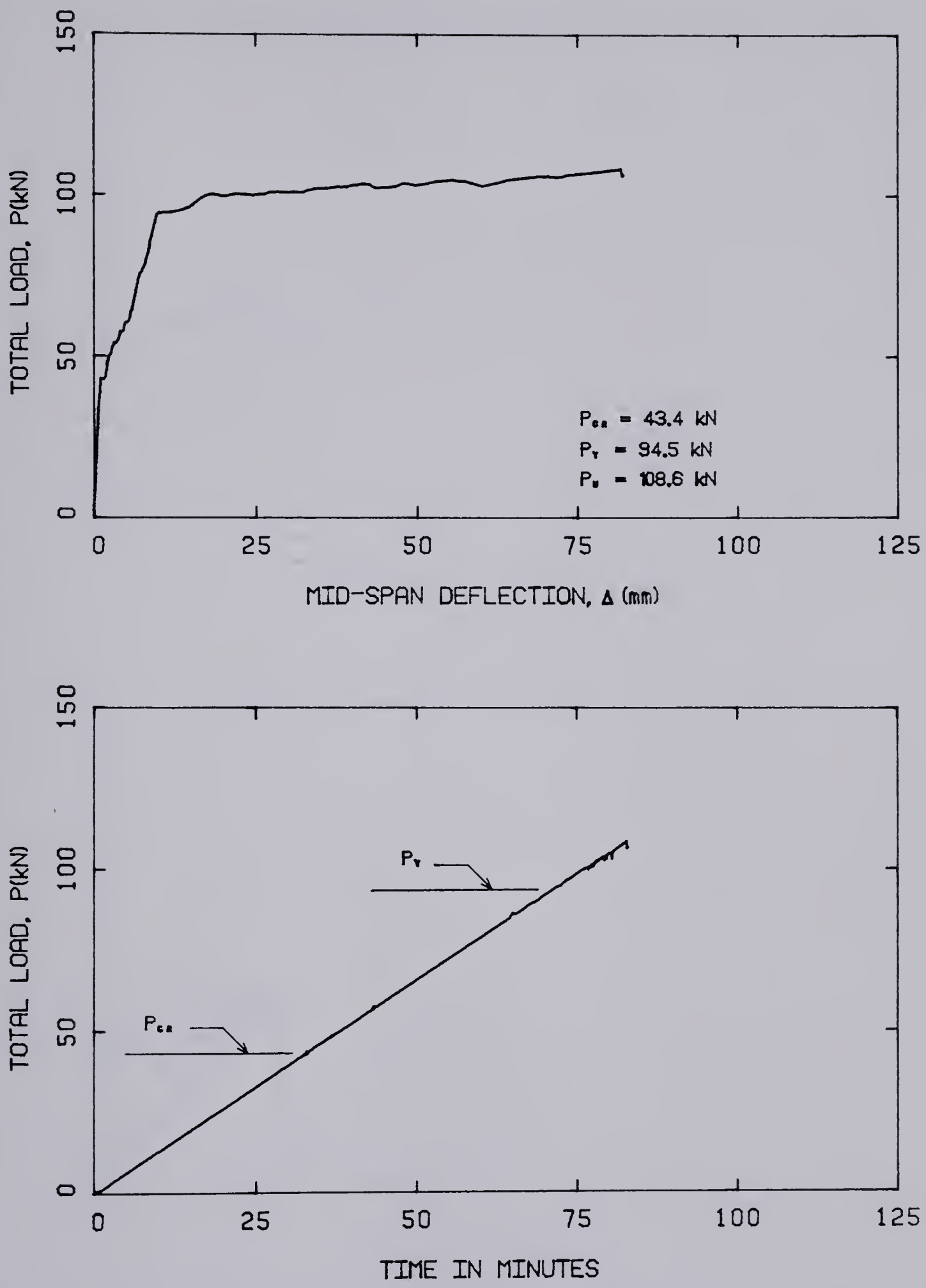

FIGURE A.18 — LOAD-DELFECTION AND LOAD-TIME CURVES FOR BEAM I5.

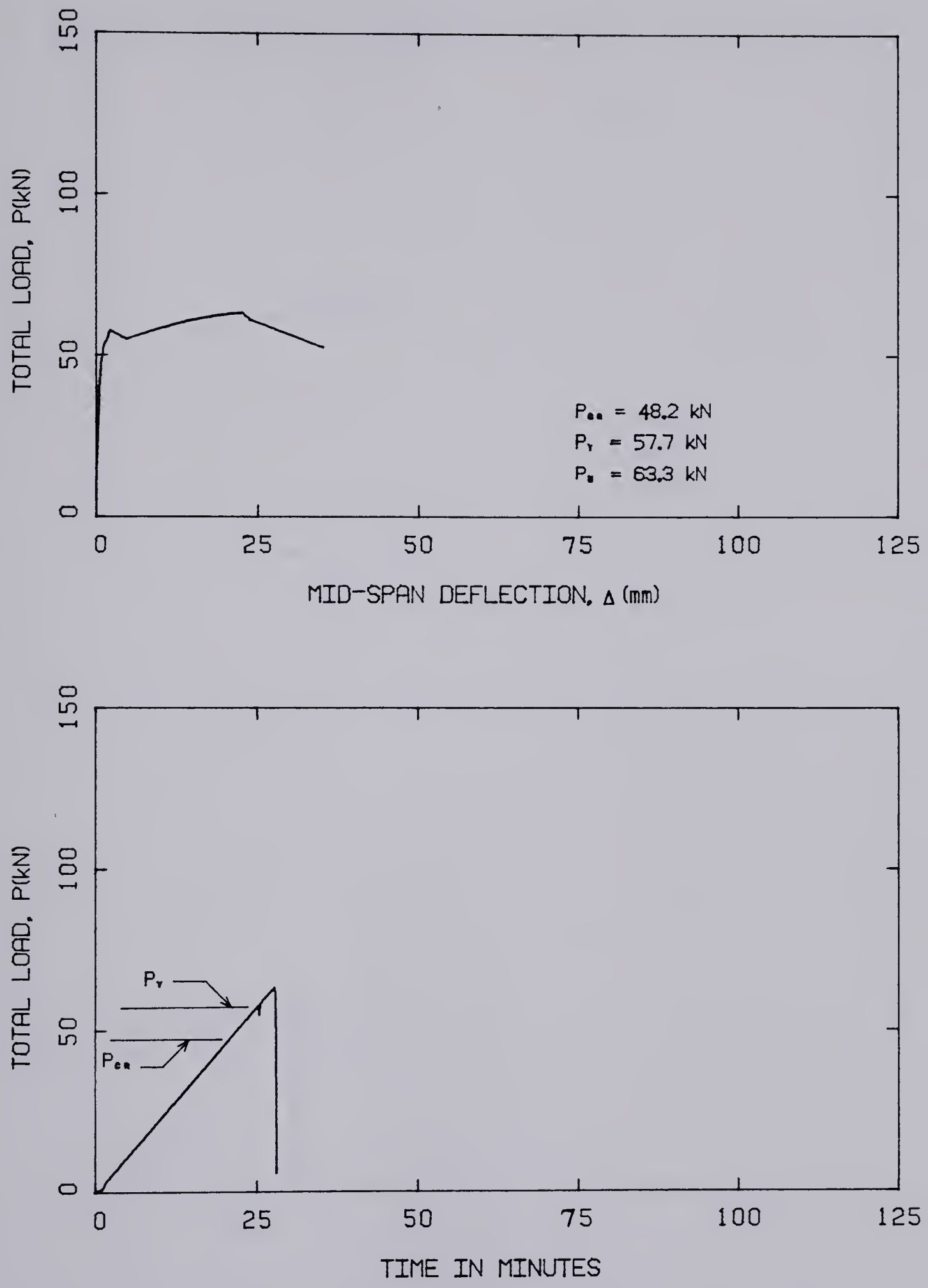

FIGURE A.19 — LOAD-DEFLECTION AND LOAD-TIME CURVES FOR SLAB L1.

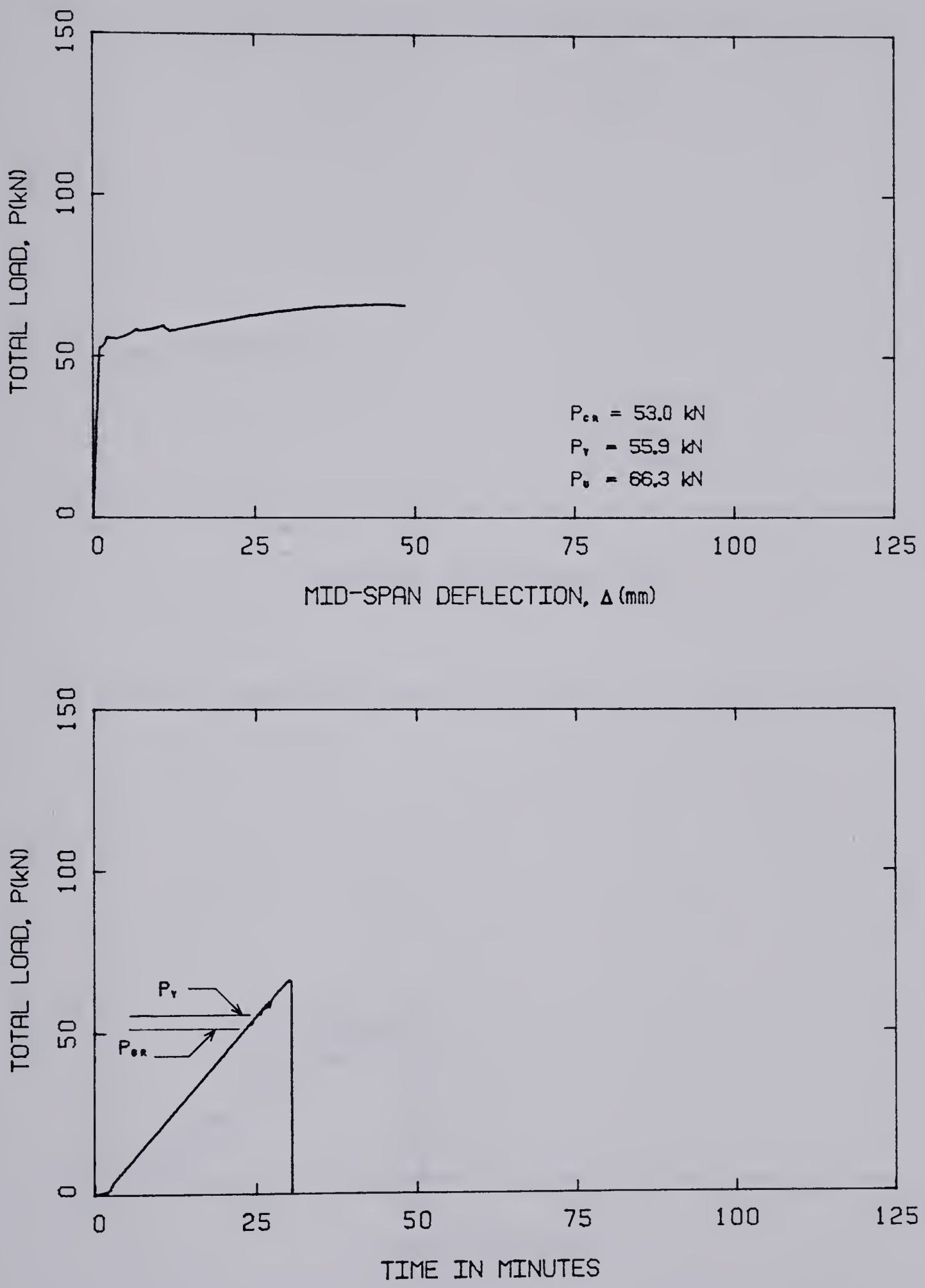

FIGURE A.20 — LOAD-DEFLECTION AND LOAD-TIME CURVES FOR SLAB P1.

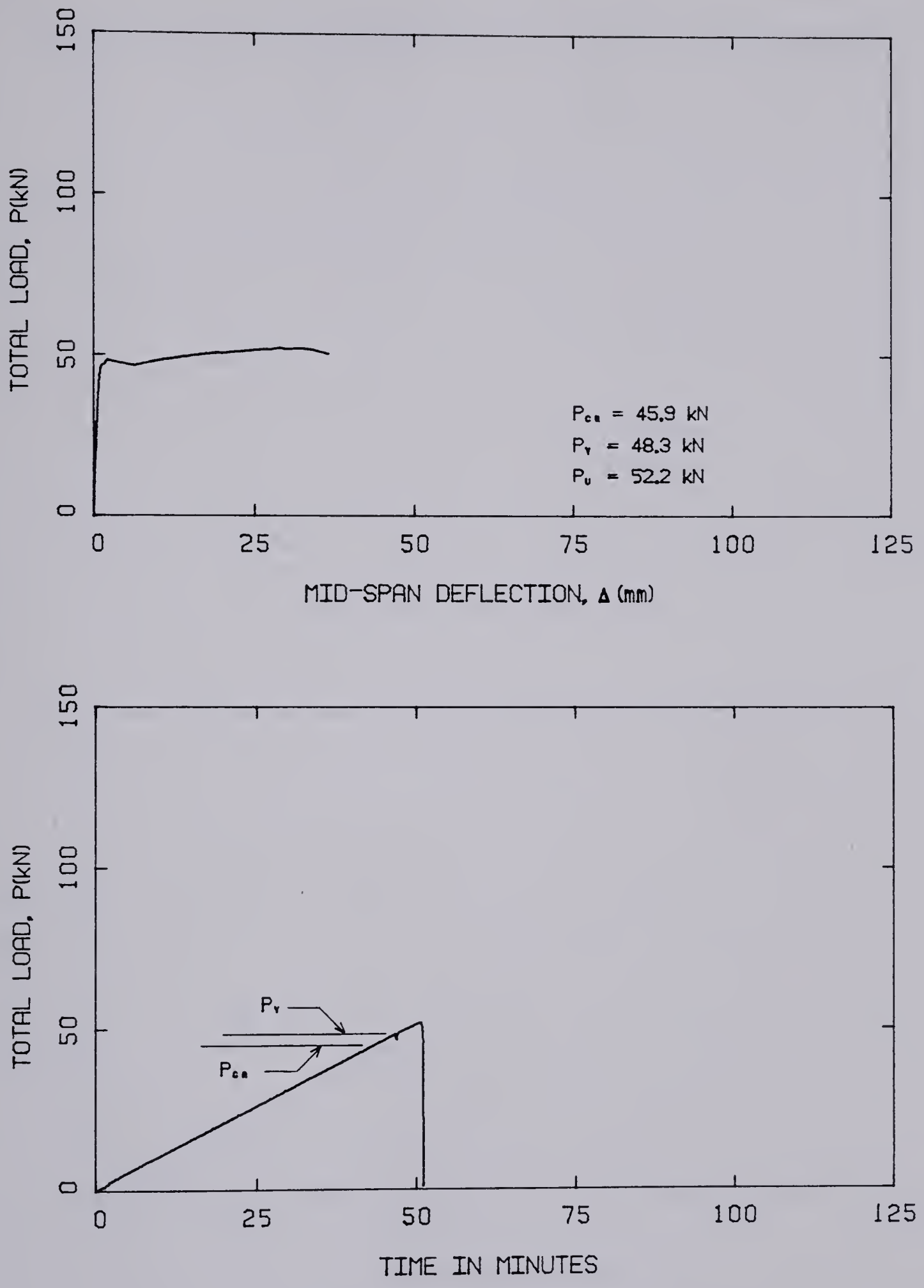

FIGURE A.21 — LOAD-DEFLECTION AND LOAD-TIME CURVES FOR SLAB L2.

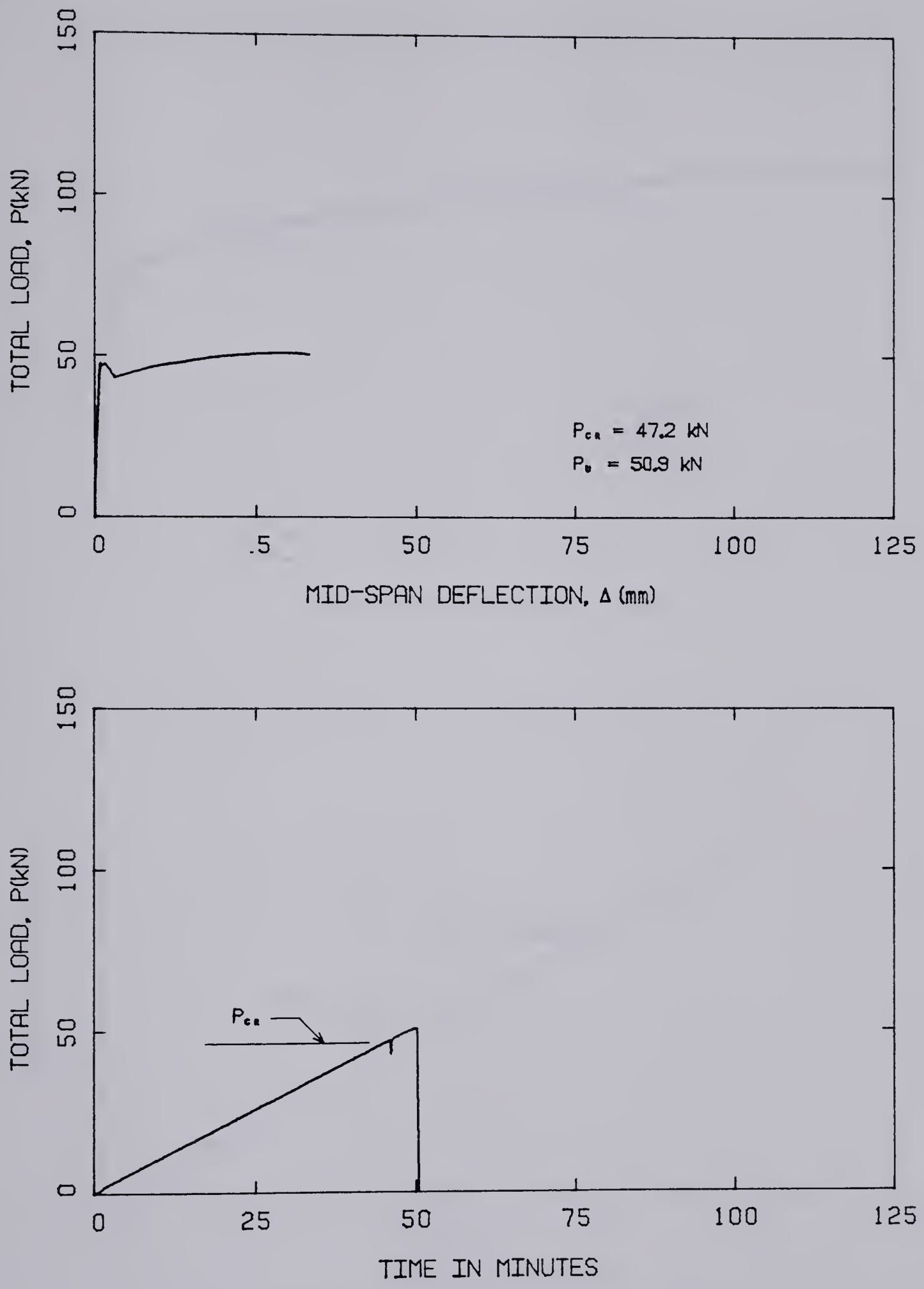

FIGURE A.22 — LOAD-DEFLECTION AND LOAD-TIME CURVES FOR SLAB P2.

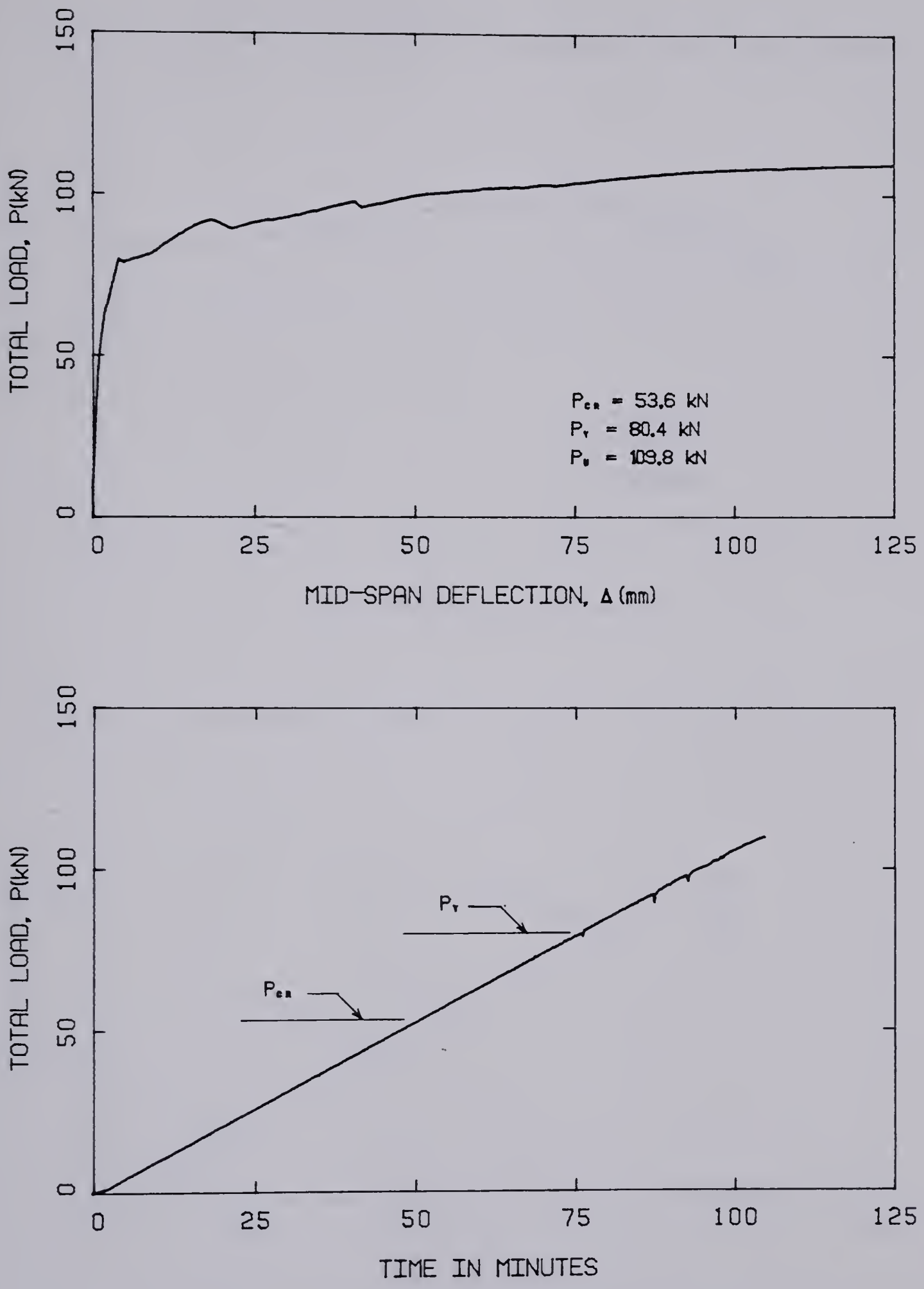

FIGURE A.23 — LOAD-DEFLECTION AND LOAD-TIME CURVES FOR SLAB L3.

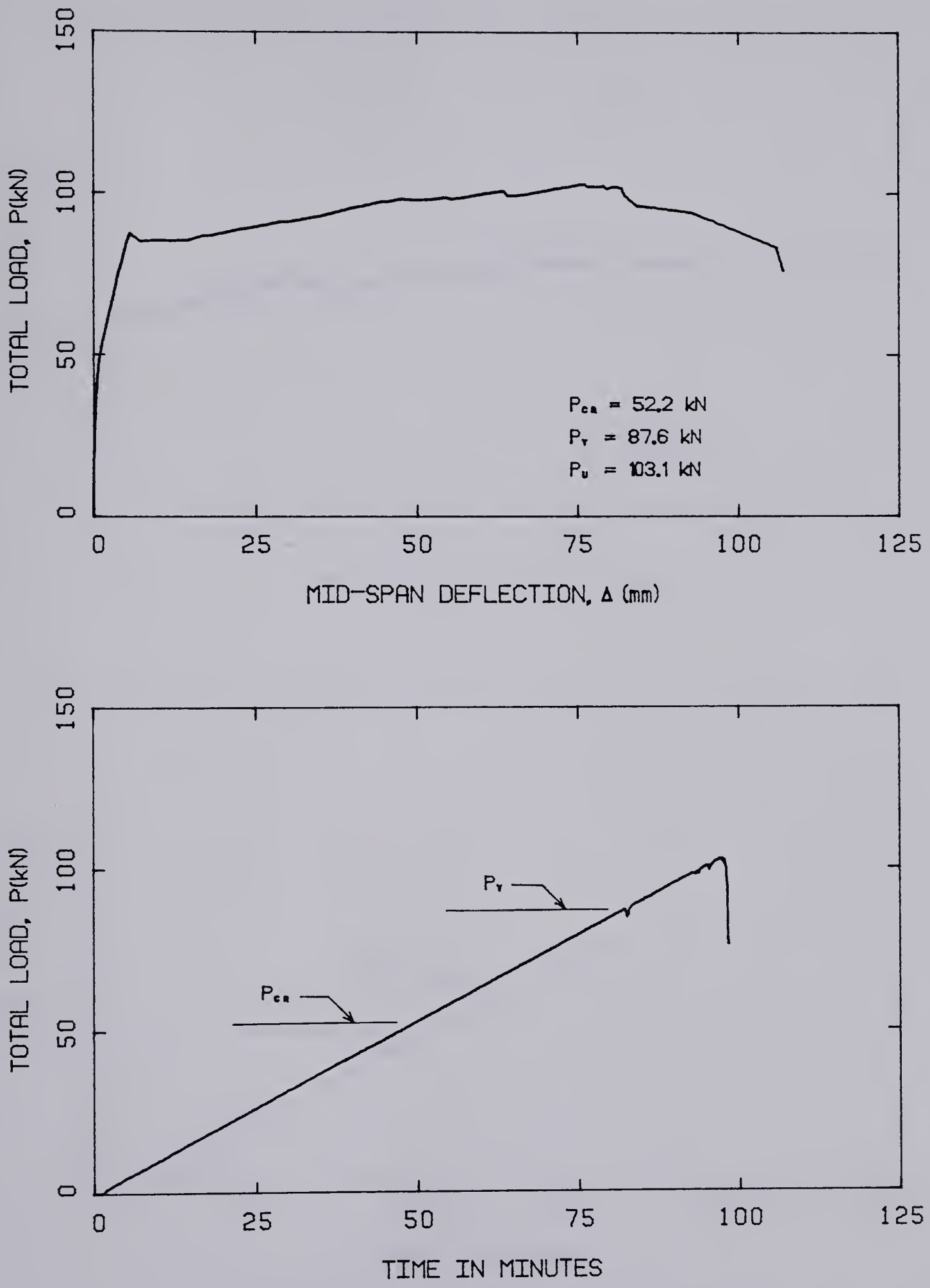

FIGURE A.24 — LOAD-DEFLECTION AND LOAD-TIME CURVES FOR SLAB P3.

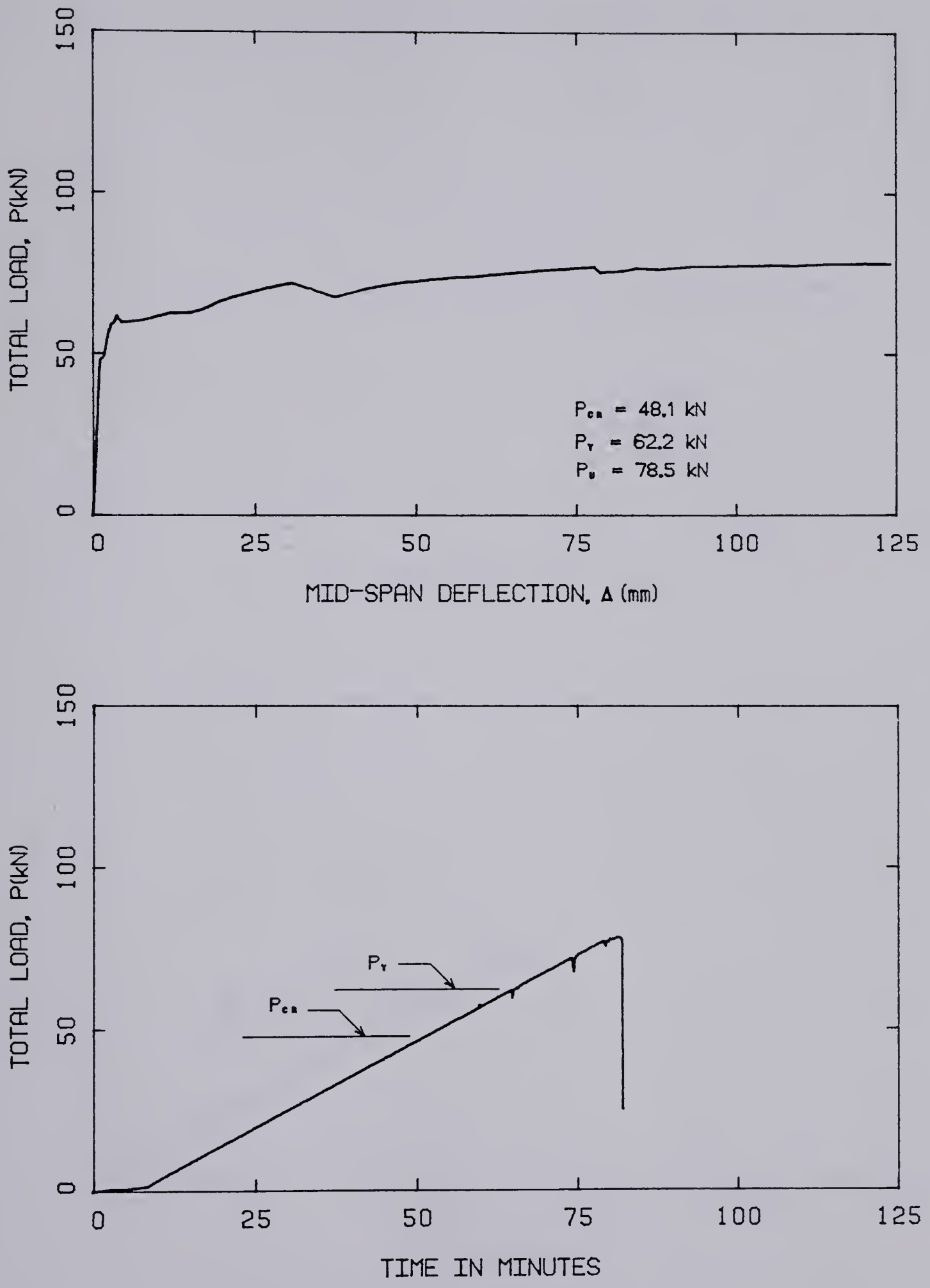

FIGURE A.25 — LOAD-DEFLECTION AND LOAD-TIME CURVES FOR SLAB L4.

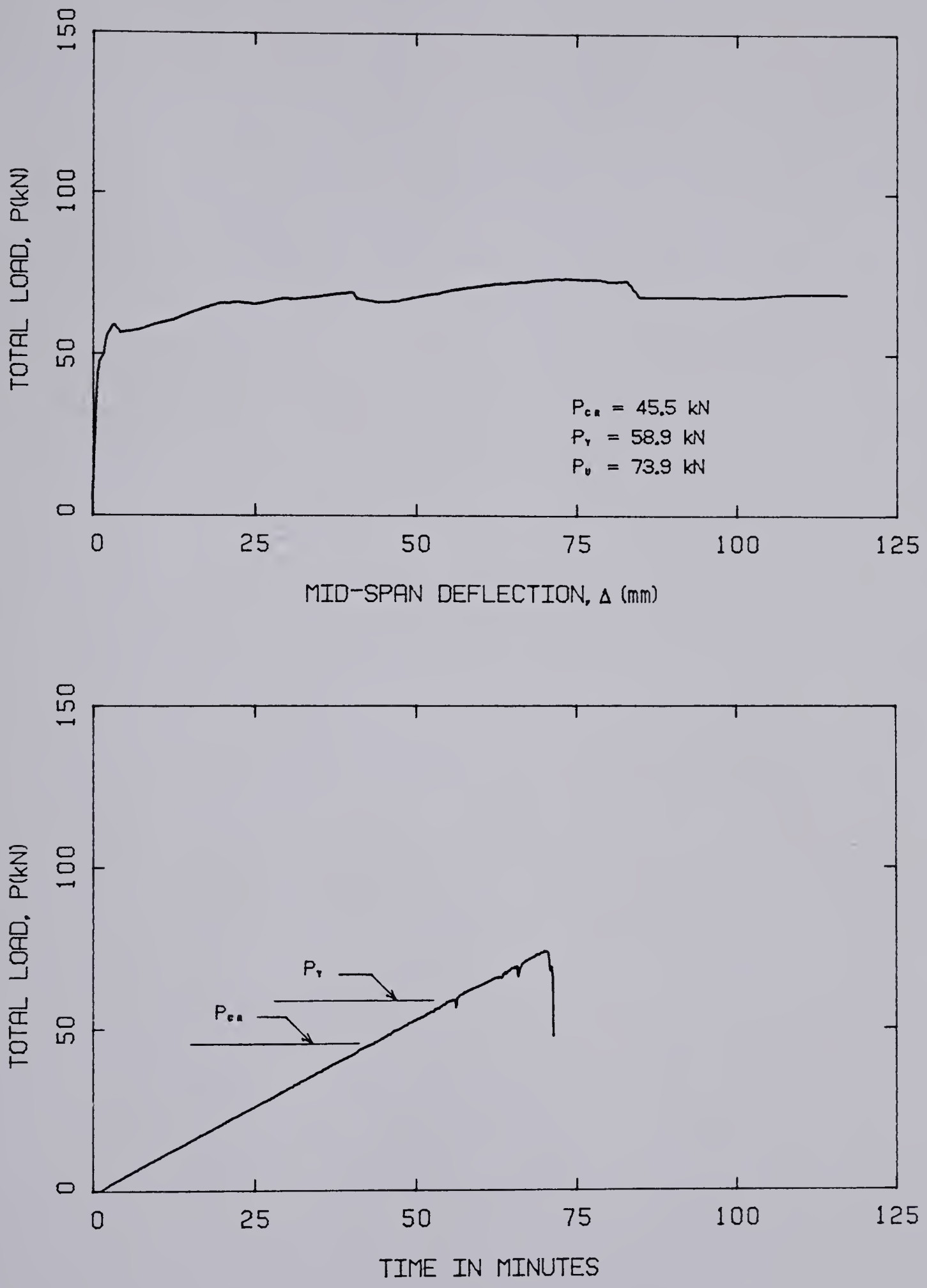

FIGURE A.26 — LOAD-DEFLECTION AND LOAD-TIME CURVES FOR SLAB P4.